

ESTIMATING UNCERTAINTIES IN INTEGRATED RESERVOIR STUDIES

A Dissertation

by

GUOHONG ZHANG

Submitted to the Office of Graduate Studies of
Texas A&M University
in partial fulfillment of the requirements for the degree of

DOCTOR OF PHILOSOPHY

December 2003

Major Subject: Petroleum Engineering

ESTIMATING UNCERTAINTIES IN INTEGRATED RESERVOIR STUDIES

A Dissertation

by

GUOHONG ZHANG

Submitted to Texas A&M University
in partial fulfillment of the requirements
for the degree of

DOCTOR OF PHILOSOPHY

Approved as to style and content by:

Duane A. McVay
(Chair of Committee)

Joel S. Watkins
(Member)

William J. Lee
(Member)

Walter B. Ayers
(Member)

Hans C. Juvkam-Wold
(Interim Head of Department)

December 2003

Major Subject: Petroleum Engineering

ABSTRACT

Estimating Uncertainties in Integrated Reservoir Studies.

(December 2003)

Guohong Zhang

B.S., Jiangnan Petroleum Institute

M.S., Research Institute of Petroleum Exploration and Development

Chair of Advisory Committee: Dr. Duane A. McVay

To make sound investment decisions, decision makers need accurate estimates of the uncertainties present in forecasts of reservoir performance. In this work I propose a method, the integrated mismatch method, that incorporates the misfit in the history match into the estimation of uncertainty in the prediction. I applied the integrated mismatch method, which overcomes some deficiencies of existing methods, to uncertainty estimation in two reservoir studies and compared results to estimations from existing methods.

The integrated mismatch method tends to generate smaller ranges of uncertainty than many existing methods. When starting from nonoptimal reservoir models, in some cases the integrated mismatch method is able to bracket the true reserves value while other methods fail to bracket it. The results show that even starting from a nonoptimal reservoir model, but as long as the experimental designs encompass the true case parameters, the integrated mismatch method brackets the true reserves value. If the experimental designs do not encompass all the true case parameters, but the true reserves value is covered by the experiments, the integrated mismatch method may still bracket

the true case. This applies if there is a strong correlation between mismatch and closeness to the true reserves value. The integrated mismatch method does not need a large number of simulation runs for the uncertainty analysis, while some other methods need hundreds of runs.

DEDICATION

This thesis is dedicated to:

My wife, Ying Gu, and my parents for their love, encouragement, and support.

The professors in the petroleum engineering and geology and geophysics departments who have given me academic or financial support for my graduate studies at Texas A&M University.

ACKNOWLEDGEMENTS

I would like to express my sincere gratitude to the following people who significantly contributed to the completion of this dissertation:

- Dr. Duane A. McVay, chair of my advisory committee, for his valuable guidance, encouragement, and great efforts in helping me finish this dissertation.
- Dr. Joel Watkins for serving as a member of my advisory committee and for his strong contributions and financial support for my graduate study.
- Dr. Walter Ayers and Dr. John Lee for serving as members of my advisory committee and for their guidance, suggestions, and help for my dissertation.
- Dr. Thomas A. Blasingame for his great help for my graduate study.
- Darla-Jean Weatherford for her suggestions to improve the technical writing style.
- Paul White and the student workers for their computer support.

TABLE OF CONTENTS

	Page
TABLE OF CONTENTS`	vii
LIST OF TABLES	ix
LIST OF FIGURES.....	xi
 CHAPTER	
I INTRODUCTION	1
1.1 Integrated Reservoir Study	1
1.2 Uncertainty Analysis	3
II METHODOLOGIES OF UNCERTAINTY ANALYSIS.....	8
2.1 Monte-Carlo Method.....	8
2.2 Experimental Design and Response Surface Method	13
2.3 Multiple Realization Tree Method	19
2.4 Relative Variation Factor Method.....	21
2.5 Bayesian Method.....	30
III INTEGRATED MISMATCH METHOD	31
3.1 Quantifying Mismatch.....	32
3.2 Model Probabilities	33
3.3 Weighting Function.....	35
3.4 Sample the Parameter Space	36
3.5 Reserves Distribution	38
IV EXAMPLE APPLICATION 1: PABST FIELD	39
4.1 Introduction	39
4.2 Research Objectives	40

CHAPTER	Page
4.3 Reservoir Simulation Model	41
4.4 Uncertainty Analysis	48
4.4.1 Experimental Design and Response Surface Method	49
4.4.2 Multiple Realization Tree Method	54
4.4.3 Relative Variation Factor Method	57
4.4.4 Integrated Mismatch Method	64
4.4.5 Multiple Method Comparisons	68
4.4.6 Limitations	69
 V EXAMPLE APPLICATION 2: PUNQ-S3 PROJECT	 71
5.1 Introduction	71
5.2 Research Objectives	72
5.3 Reservoir Simulation Model	74
5.4 Uncertainty Analysis	77
5.4.1 Integrated Mismatch Method	77
5.4.2 Multiple Method Comparisons	105
 VI LIMITATIONS AND FUTURE WORK	 108
 VII CONCLUSIONS	 110
 NOMENCLATURE	 112
 REFERENCES	 114
 APPENDIX A PUNQ-S3 ECLIPSE DATA FILE	 119
 VITA	 139

LIST OF TABLES

	Page
Table 4.1 Gas in Place After History Matching.....	47
Table 4.2 Reservoir Parameters After History Matching	48
Table 4.3 Reservoir Parameters and Their Distributions	49
Table 4.4 Three Parameter Factorial Design	50
Table 4.5 Reservoir Parameters and Their Distributions	54
Table 4.6 Decision Tree Leaf Probabilities	56
Table 4.7 Parameters That Affect the Hydrocarbon Volume.....	57
Table 4.8 Triangular Distributions for Porosity and Thickness Factor	57
Table 4.9 Influential Parameters for the Recovery Factor.....	60
Table 4.10 Triangular Distributions for Permeability, Skin and Fault Transmissibility Factor.....	60
Table 4.11 Reservoir Parameters and Their Distributions.....	64
Table 4.12 Factorial Design for the Three Reservoir Parameters	65
Table 4.13 Mismatch Coefficients.....	67
Table 4.14 Reserves Coefficients	67
Table 5.1 Four-Factor Experimental Design, Case 1	81
Table 5.2 Reserves Coefficients (Case 1).....	82
Table 5.3 Mismatch Coefficients (Case 1).....	84
Table 5.4 Key Variable Range and Step Size	86
Table 5.5 Regressed Model Runs and Probability Calculation	87
Table 5.6 Four-Factor Experimental Design, Case 2	90
Table 5.7 Reserves Coefficients (Case 2).....	91
Table 5.8 Mismatch Coefficients (Case 2).....	91

	Page
Table 5.9 Four-Factor Experimental Design, Case 3	96
Table 5.10 Random Permeability and Porosity Multipliers for Case 4.....	98
Table 5.11 Four-Factor Experimental Design, Case 4.....	99
Table 5.12 Reserves Coefficients (Case 4).....	100
Table 5.13 Mismatch Coefficients (Case 4).	100
Table 5.14 Four-Factor Experimental Design, Case 5	104

LIST OF FIGURES

	Page
Fig 2.1 Monte Carlo simulation schematic	9
Fig 2.2 Monte Carlo method vs. discrete approaches	12
Fig 2.3 Tornado diagram	16
Fig 2.4 The 2^n factorial design	16
Fig. 2.5 Composite design.....	17
Fig. 2.6 Multiple realization tree procedure.....	22
Fig. 2.7 Multiple realization tree structure based on reserves estimation	23
Fig. 2.8 Reserves CDF	24
Fig. 2.9 Triangular distribution	27
Fig. 3.1 Pressure mismatch quantification	33
Fig. 3.2 Sample the sample space–stochastic method.....	37
Fig. 3.3 Sample the sample space–the integrated mismatch method.....	38
Fig. 4.1 Location of Pabst field	40
Fig. 4.2 Structure map of 10,300-ft sand.....	42
Fig. 4.3 10,300-ft sand net-gas isopach map.....	43
Fig. 4.4 Sidewall core analysis.....	44
Fig. 4.5 Pressure-transient test results	44
Fig. 4.6 Simulation grid.....	45
Fig. 4.7 Well A2 pressure history match	46
Fig. 4.8 Well A4 pressure history match	46
Fig. 4.9 Well A9 pressure history match	47
Fig. 4.10 Regressed reserves vs. reserves from simulator	51
Fig. 4.11 Probability distribution of porosity	51

	Page
Fig. 4.12 Probability distribution of skin factor	52
Fig. 4.13 Probability distribution of fault transmissibility	52
Fig. 4.14 Reserves distribution of experimental design method	53
Fig. 4.15 Reserves cumulative distribution function of experimental design method..	53
Fig. 4.16 Multiple realization tree	55
Fig. 4.17 Reserves distribution.....	56
Fig. 4.18 Probability density function of porosity factor	58
Fig. 4.19 Probability density function of thickness variation factor	58
Fig. 4.20 Hydrocarbon volume distribution of relative variation method.	59
Fig. 4.21 Probability density function of permeability factor	60
Fig. 4.22 Probability density function of the factor of skin factor	61
Fig. 4.23 Probability density function of fault transmissibility factor	61
Fig. 4.24 Probability distribution of recovery factor.....	62
Fig. 4.25 Probability distribution of reserves.....	63
Fig. 4.26 Cumulative distribution function of reserves.....	63
Fig. 4.27 Mismatch response surface	66
Fig. 4.28 Reserves response surface.....	66
Fig. 4.29 Reserves cumulative distribution function of integrated mismatch method..	68
Fig. 4.30 Multiple method reserves comparisons	69
Fig. 5.1 Typical production data for a well	73
Fig. 5.2 PUNQ-S3 3D reservoir model	74
Fig. 5.3 Well PRO-1 oil-production rate	75
Fig. 5.4 Well PRO-1 bottomhole pressure.....	75
Fig. 5.5 Well PRO-1 gas/oil ratio	76
Fig. 5.6 Well PRO-1 water cut	76

	Page
Fig. 5.7 Well PRO-11 bottomhole pressure true case.....	78
Fig. 5.8 Well PRO-11 bottomhole pressure half-porosity nonoptimal case.....	79
Fig. 5.9 Predicted vs. observed reserves (Case 1).....	82
Fig. 5.10 Reserves response surface residual analysis (Case 1).....	83
Fig. 5.11 Predicted vs. observed mismatch (Case 1).....	84
Fig. 5.12 Mismatch response surface residual analysis (Case 1).....	85
Fig. 5.13 Mismatch-reserves crossplot (Case 1).....	89
Fig. 5.14 Predicted vs. observed reserves (Case 2).....	92
Fig. 5.15 Reserves response surface residual analysis (Case 2).....	92
Fig. 5.16 Predicted vs. observed mismatch (Case 2).....	94
Fig. 5.17 Mismatch response surface residual analysis (Case 2).....	94
Fig. 5.18 Mismatch-reserves crossplot (Case 3).....	97
Fig. 5.19 Predicted vs. observed reserves (Case 4).....	101
Fig. 5.20 Reserves response surface residual analysis (Case 4).....	101
Fig. 5.21 Predicted vs. observed mismatch (Case 4).....	102
Fig. 5.22 Mismatch response surface residual analysis (Case 4).....	102
Fig. 5.23 Multiple case comparisons.....	106
Fig. 5.24 Multiple method comparisons from different participants.....	107

CHAPTER I

INTRODUCTION

In an integrated reservoir study, a multidisciplinary team of geophysicists, geologists, petrophysicists, and engineers works closely towards a common goal – better understanding of the reservoir and formation of an optimal reservoir development plan. In spite of modern technology advancements and the multidisciplinary team’s efforts to integrate people, data, technology, and tools, many uncertainties still exist for various reasons. The objectives of this work are to quantify uncertainties associated with integrated reservoir studies, enabling sound reservoir management decisions at different stages of reservoir development.

1.1 Integrated Reservoir Study

Traditionally, reservoir studies were not integrated. Each discipline worked on its own specialty separately; projects often followed a linear approach: geophysics, geology, and then reservoir engineering. People did not realize the interdependency of other groups’ results, even though they were working for a mutual objective. Sometimes geoscientists and engineers got different conclusions because they did not communicate effectively. Within the last two decades, the value of integrated reservoir studies has been recognized gradually. Different disciplines have realized that they depend on each other, and their goals can be accomplished with mutual support. Working as a team, they feel a sense of ownership for their jobs because they are committed to the goals they helped to

This dissertation follows the style and format of SPE Reservoir Evaluation & Engineering

establish. They work more effectively and efficiently as teams than as individuals, and thus their synergy realizes a whole greater than the sum of its parts.

With the recognition of the importance and advantages of integrated reservoir studies, people are employing them more and more. The members of a multidisciplinary team formed for integrated reservoir study meet periodically to discuss the problem and the progress, fix possible disagreements as early as possible, and solve the problem in a timely, efficient manner, avoiding the inconsistent results reached by different disciplines. In the process of integrated reservoir study, the team members usually learn as they become familiar with each other's expertise, which is definitely beneficial to the whole team and the project, and which is one purpose of integrated reservoir study. Usually, trust is established among the team members, and they can do a better job on the next project.

Integrated reservoir study has been conducted for various purposes. Juan Diego *et al.*¹ conducted an integrated reservoir study of a carbonate reservoir developed with waterflooding. They developed a geological/petrophysical model, evaluated the past reservoir performance, predicted future performance for various operating plans, and made appropriate recommendations based upon technical and economic considerations. A large-scale integrated study² was performed in the Bachaquero Intercampos field, Lake Maracaibo, Venezuela, with the aim of identifying new reserves and defining a new development plan. In early 2000, LUKOil and PetroAlliance³ completed one of the

largest integrated reservoir studies in the western Siberian basin, which contains some of the largest oil fields in Russia and the former Soviet Union. They used state-of-the-art technology to create a new 3D geological model of Vatyogan's six major producing zones, which range in age from Upper Jurassic to Upper Cretaceous and cover a wide range of depositional environments. With the new model, they estimated reserves and prepared a drilling program in the undeveloped areas, identified areas of by-passed oil, and developed an optimal infill drilling and enhanced recovery program to improve production in the developed areas. Bouman *et al.*⁴ conducted an integrated reservoir study to solve the puzzle of the rapidly declining reservoir pressure in the Obaiyed Field. Cosentino *et al.*⁵ simulated the irregular water advance observed in part of the field as a consequence of peripheral water injection.

1.2 Uncertainty Analysis

What do we mean by uncertainty? It means being less than 100% sure about something. In the petroleum industry, people are extremely concerned about quantities such as original hydrocarbon in place, reserves, and the time for the recovery process, which are all critical to the economic returns. Those quantities play a key role in making important decisions for both the oil producers and the investors at different phases of reservoir development. But being certain of these quantities is usually impossible.

In the past 10 to 15 years, probabilistic expressions of reserves estimates have been gradually accepted and adopted in the industry. The traditional method involves

specifying a deterministic value for the reserves estimate, which usually is calculated with a mathematical model. Unlike the probabilistic method, the traditional method does not consider the uncertainty associated with the reserves estimate; it simply takes for granted that the deterministic reserves value is the most likely value. As a matter of fact, when we talk about reserves prediction, we are never completely sure about its correctness: there is always some degree of uncertainty, big or small, associated with it. Therefore, a statistical approach or probabilistic approach is more appropriate for reserves prediction. When we talk about reserves prediction in this study, we mean a reserves distribution—a probability density function for reserves.

All of the uncertainties among oilfield variables, such as geological characteristics, rock and fluid properties, oil price, capital expenditures, and operating costs, result in uncertainty in the expected profitability of the project. Capital investment for hydrocarbon extraction increases as exploration and development extend to distant areas such as offshore and Alaska, compounding the economic uncertainty.

Uncertainty comes from several sources⁶: measurement error, mathematical model error, and incomplete data sets. All field and laboratory measurements, such as production and PVT data, involve some degree of error or inaccuracy, which may result from poor tool calibration or even human error. This kind of error can be reduced to some extent by using more accurate tools or increased human effort, but it will never be eliminated. When geoscientists and engineers try to evaluate the values of reservoir parameters from

various mathematical models, uncertainty is incurred. None of the mathematical models are perfect; they were built either by empirical methods or on the basis of assumptions that are not always applicable to the real situations. The development of a finite-difference reservoir simulator involves some assumptions and numerical computational error. In real situations, we never have a complete data set for the study. Often, we lack some kind of data and we try to make a reasonable guess based on our knowledge and experience. The process, of course, introduces errors to the prediction.

The paucity of available data in the appraisal stage of a field, or incomplete reservoir description even during the development stage, increases the risks associated with investment decisions. Quantification of these uncertainties and evaluation of the risks would improve decision making.⁷ However, estimating these uncertainties is complicated because it requires an understanding of both the reservoir's static structure and dynamic behavior during production. Even a producing field can result in a financial loss,^{8,9} and even mature fields have uncertainties in the reservoir description. Uncertainty analysis methods provide new and comprehensive ways to evaluate and compare the degree of risk and uncertainty associated with each investment choice. The result is that the decision-maker is given a clear and sharp insight into potential profitability and the likelihood of achieving various levels of profitability. When we talk about uncertainty analysis for the reserves prediction in this study, we generally refer only to technological uncertainty. We do not convert the reserves distribution into monetary value distribution, which is usually done in a risk analysis. However, the reserves distribution can be

converted into a net present value distribution once an oil and gas price prediction is made.

Uncertainty analysis methods attempt to reduce the complexity and difficulty of quantifying uncertainty. Uncertainty analysis methods have some advantages⁹:

- Uncertainty analysis forces a more explicit look at the possible outcomes that could occur if the decision-maker accepts a given development scheme.
- Certain techniques of uncertainty analysis provide excellent ways to evaluate the sensitivity of various factors relating to overall worth.
- Uncertainty analysis provides a means to compare the relative desirability of various candidate projects.
- Uncertainty analysis is a convenient and unambiguous way to communicate judgments about risk and uncertainty.

Exceedingly complex investment options can be analyzed using uncertainty analysis techniques. To economically develop reservoirs and maximize the return, oil producers have to characterize and, if possible, manage to reduce the uncertainties.

Usually people are interested in obtaining a reserves distribution at a specific time. The methods developed for uncertainty analysis in the petroleum industry use various techniques such as experimental design, response surface, multiple realization tree, and Monte Carlo simulation. However, they do not consider the mismatch between the

modeled and actual production history. This study introduces a method—the integrated mismatch method—that incorporates the quality of the history match into the reserves prediction in order to quantify its uncertainty. Although starting from non-optimal reservoir models that underpredict or overpredict the reserves, the method yields prediction ranges that cover the true reserves values.

CHAPTER II

METHODOLOGIES OF UNCERTAINTY ANALYSIS

Statistical methods of uncertainty analysis developed or introduced for the petroleum industry for many years have various assumptions and limitations associated with them. This chapter reviews those methods of quantifying uncertainties with production forecast: Monte Carlo, experimental design and response surface, multiple realization tree, relative variation method, and Bayesian rule methods.

2.1 Monte Carlo Method

Monte Carlo is a powerful statistical method that has been used for more than half a century. It has been applied extensively in the petroleum industry for decades. As early as 1969, it was used for pressure transient analysis.¹⁰ The Monte Carlo method has been used for various other purposes in the industry such as reserves estimation,¹¹ material balance analysis,¹² workover risk assessment,¹³ and producing property estimation.¹⁴ It is an alternative to both deterministic estimation and the scenario approach that presents pessimistic, most likely, and optimistic case scenarios.¹⁵

The Monte Carlo method begins with a mathematical model in which a dependent variable is a function of the independent variables. The dependent variable usually is the quantity of interest such as original hydrocarbons in place or cumulative oil production at a future time. The independent variables are the reservoir parameters, such as porosity, permeability, and saturation. Different independent variables might have

different statistical distributions, or they might have different parameters even though they are the same kind of distribution. For example, two normal distributions can have different parameters: mean and standard deviation. After the mathematical model is built, many random numbers are generated for each independent variable based on their specific statistical distributions. To generate random numbers for the independent variables, we need probability density functions for them. Thus, those probability density functions have to be determined before Monte Carlo method can be applied.

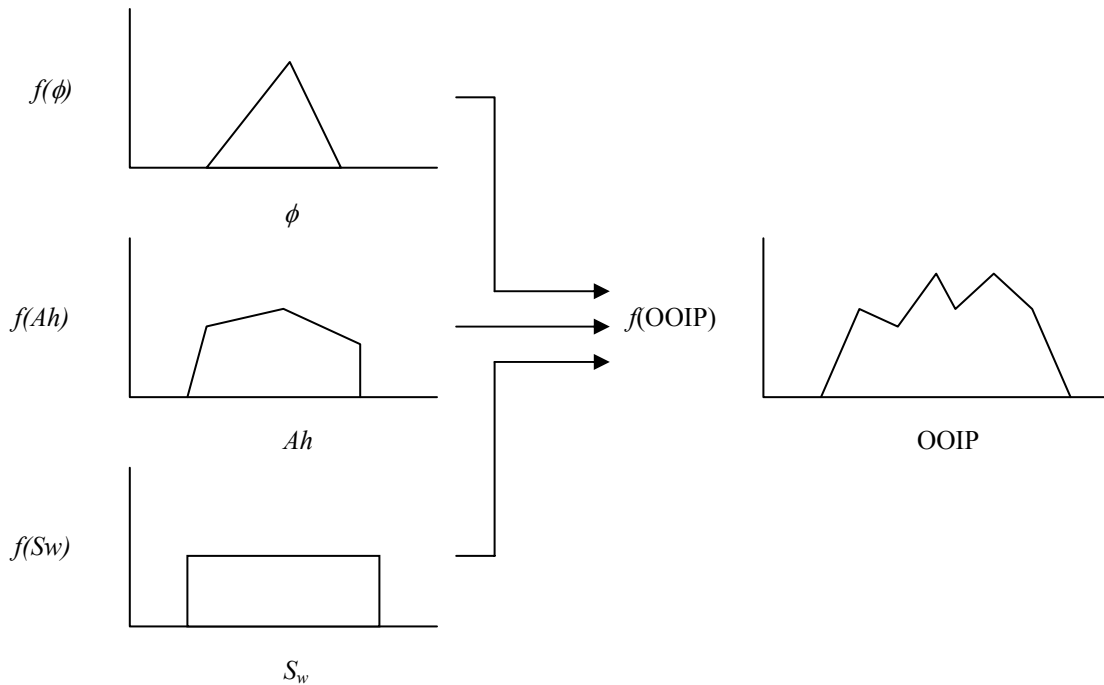


Fig. 2.1—Monte Carlo simulation schematic.

Statistical distributions are characterized by different numbers of parameters. A normal distribution has two character parameters: mean and variance. A triangular distribution has three parameters: low limit, most likely value, and high limit. A random number of

each independent variable is plugged into the mathematical model, and a dependent variable is calculated. Thus, many values of the dependent variable are obtained by using those values of the independent variables. A distribution can be formed with the values of the dependent variable (Fig. 2.1).

For the purposes of illustration, we use reserves estimation—by far the most frequent use of Monte Carlo as an example.^{16, 17} The original oil in place (OOIP) is given by Eq. 2-1.

$$OOIP = \frac{\phi(1 - S_w)Ah}{B_{oi}} \dots\dots\dots (2-1)$$

Ah is the reservoir volume, B_{oi} is the oil formation volume factor, S_w is the water saturation, and ϕ is formation porosity. In this example, Eq. 2-1 is the mathematical model for the original oil in place calculation. OOIP is the dependent variable; porosity, water saturation, and reservoir volume (we use a fixed value for oil formation factor here) are the independent variables. A random number generator in a computer program (like Microsoft Excel) generates random numbers for all the independent variables, porosity, water saturation, and reservoir volume, from their user-specified probability density functions. Then the original oil in place is calculated by the mathematical model (Eq. 2-1). This process is repeated an arbitrarily large number of times (hundreds or thousands). We get a lot of values of original oil in place from the process above using the mathematical model. From those values, we can come up with the probability density function (PDF) and cumulative distribution function (CDF) for the original oil in place, from which summary statistics such as the mean and median can be calculated as well.

The probability density function and cumulative distribution function of the dependent variable depend directly on the input parameter distributions. Poor input parameter distributions will result in a low-quality estimation of the quantity of interest (like original oil in place). Given that the results are sensitive to the input parameter distributions, we need good-quality input parameter distributions. The commonly used distributions include normal, triangular, lognormal, and uniform.

Selecting distributions and their character parameters is critical to the successful application of Monte Carlo method. Guidance for selecting input parameter distributions can be obtained from three sources¹⁶: fundamental principles, expert opinion, and historical data. According to statistical principles, products of variables tend to have lognormal distributions; sums of variables tend to have normal distributions. Monte Carlo simulation is much like a black box. Without any previous knowledge about the distributions or character parameters of independent variables, expert opinions might be quite useful at the early stage of Monte Carlo application for some projects. With time elapsing, more and more data become available. The available data can be used to investigate the distributions of the independent variables of interest.

The Monte Carlo method can be quite computationally intensive. If many independent variables are random and they all have large variabilities, a larger number of runs of the mathematical model may be needed to recognize the range of the dependent variable

response. An important point about the Monte Carlo method is that the outputted dependent-variable distribution is sensitive to the input parameter distributions.

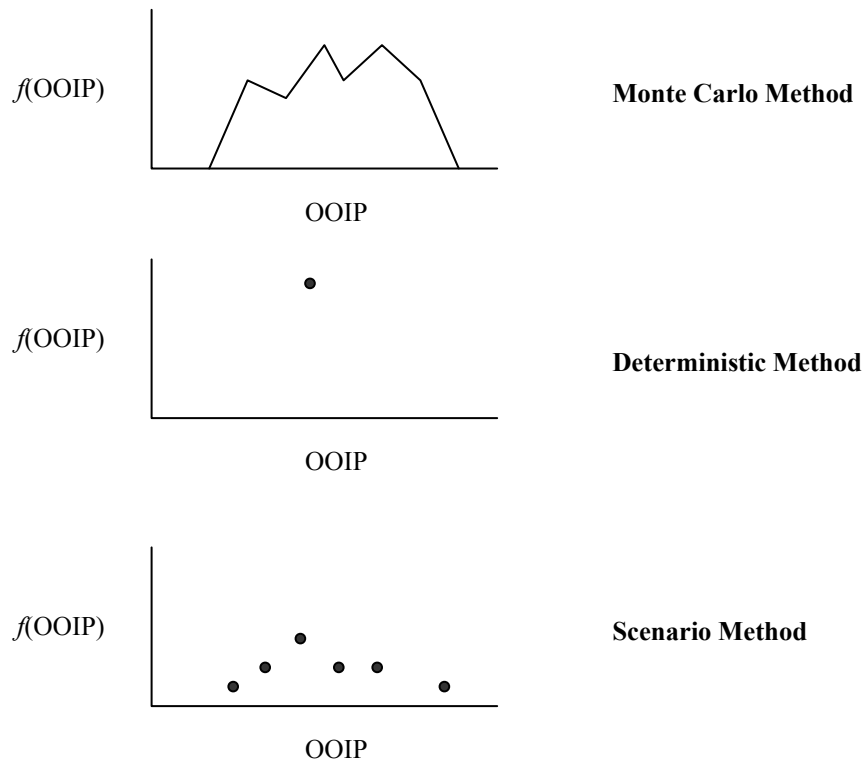


Fig. 2.2—Monte Carlo method vs. discrete approaches.

The Monte Carlo method has some advantages and disadvantages. The results contain more information about possible outcomes than the deterministic and scenario approach (Fig. 2.2). Monte Carlo results are continuous distributions such as probability density and cumulative-distribution functions instead of discrete points as from the deterministic or scenario approach. The Monte Carlo results give the users ideas about the probability of the most likely outcome, the pessimistic outcome, and the optimistic outcome. Thus, users can evaluate the kind of risks they are dealing with. The users can even obtain a

confidence interval for the predicted variable—how likely the predicted value will be located within an interval. However, the Monte Carlo method is a statistical method; therefore, some knowledge of statistics is prerequisite both for its correct application and for the interpretation of the results. This might be a barrier for its application in the industry. In addition, determining the input variable distributions and their character parameters involves some subjectivity. Despite its limitations, Monte Carlo simulation has been widely used in the petroleum industry for risk analysis,^{18, 19} project evaluation,^{20, 21} and even fracture-characteristic investigation.²²

2.2 Experimental Design and Response Surface Method

The experimental design and response surface method has been used in the medical and agricultural industry for many years. It was first introduced in reservoir engineering in the early nineties. The purpose is to obtain maximum information at the minimum experimental cost by varying all the uncertain parameters simultaneously. Since then, the experimental design and response surface method have been used in petroleum industry for many purposes.²³⁻³⁶

Reservoir simulation differs from the experiments in medicine or agriculture in that it does not have random errors. The same input file will result in the same output file. Thus we can use this method in uncertainty analysis in reservoir engineering to gather optimal information from the results of the simulation runs. We need to come up with the response surface for the variables of interest by regression after the experimental

design is finished. With the response surfaces regressed, we can obtain the final reserves distributions by Monte Carlo simulation.

The experimental design and response surface method consists of the following steps:

- Identify the most influential reservoir parameters by sensitivity analysis after history matching.
- Use experimental design to come up with the simulation runs with different combinations of reservoir parameters.
- Conduct the experiment, using reservoir simulation to calculate the reserves for the simulation runs.
- Analyze the results of the experiments and establish a reserves response surface as a function of the reservoir parameters.
- Predict the reserves distribution with the aid of Monte Carlo simulation.

Sensitivity Analysis. Usually a number of reservoir parameters affect the final reserves distribution. Some of the reservoir parameters are more important than others, so they should not be missed in the reserves uncertainty analysis. However, we cannot afford to include too many reservoir parameters in the experimental design method. The number of reservoir simulation runs increases rapidly with the increase of the number of reservoir parameters included in the experimental design. A large number of simulation runs may be very expensive because of the time-consuming nature of reservoir simulation. Including many reservoir parameters in an experimental design might not

give a good result. Including nonsensitive reservoir parameters can deteriorate the response surfaces to the point that there is no response surface. Therefore, the first step of experimental design is to identify the influential reservoir parameters. To construct the reserves tornado diagram for n reservoir parameters, we need $2n+1$ reservoir simulation runs: one run for all the reservoir parameters at their most likely value—the history-matched model—plus two runs for each parameter—one at the pessimist value and the other at the optimistic value for each parameter. For every reservoir parameter that affects the final reserves, geoscientists and engineers work together to determine the most-likely, pessimistic, and optimistic values. The most-likely, pessimistic, and optimistic reserves values are then calculated with the corresponding reservoir parameter value. For example, for reservoir porosity, the optimistic reserves is calculated with the optimistic porosity value; the most likely reserves is calculated with the most likely porosity value; the pessimistic reserves value is calculated with the pessimistic value. Finally, a reserves range is obtained from the pessimistic and optimistic reserves values. A reserves tornado diagram (Fig. 2.3) is formed and the influential reservoir parameters can be determined from the diagram.

Designs. Factorial and composite designs are the most commonly used designs in the petroleum industry. Factorial designs have been popular in experimental design for some time. Fig. 2.4 illustrates the application of a 2^n factorial design with two parameters. If we have n parameters with two levels of change (the pessimistic and the optimistic value), 2^n experiments need to be conducted. Usually, each parameter has three levels of

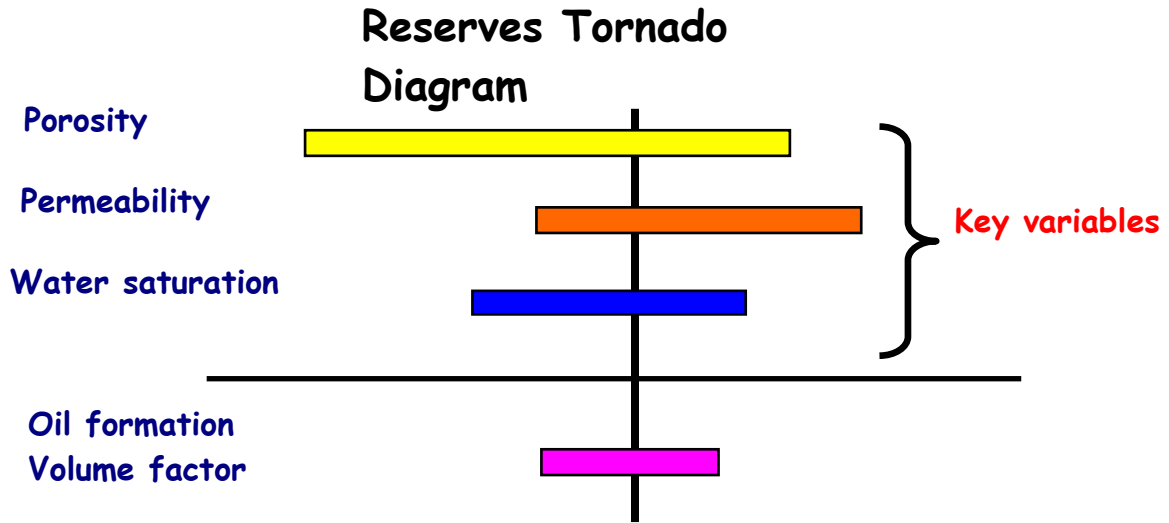
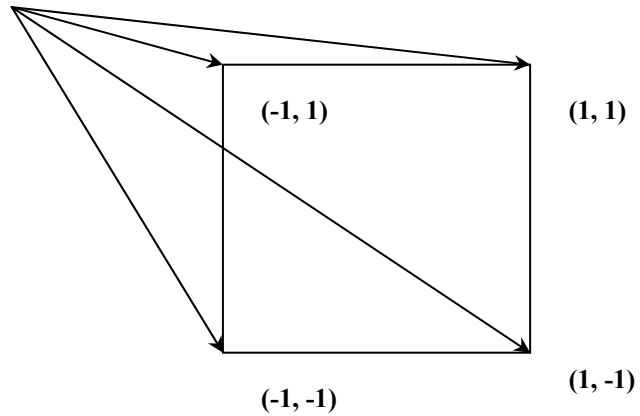


Fig. 2.3—Tornado diagram.

change (the pessimistic, the most likely, and the optimistic value); in this situation, we conduct 3^n experiments. Even for a modest set of five variables, the total number of

Conduct experiments at the corners

Experiment	X1	X2
1	1	1
2	1	-1
3	-1	1
4	-1	-1



Predict the outcome at the entire area

Fig. 2.4—The 2^n factorial design.

experiments is 243. In many situations, conducting this many experiments is too time-consuming or expensive. A compromise is to use the so-called Composite Designs (Fig. 2.5). These consist of 2^n factorial designs augmented by $2n$ star points: one variable

Experiment#	P1	P2	P3	P4
1	1	1	1	1
2	1	1	1	-1
3	1	1	-1	1
4	1	1	-1	-1
5	1	-1	1	1
6	1	-1	1	-1
7	1	-1	-1	1
8	1	-1	-1	-1
9	-1	1	1	1
10	-1	1	1	-1
11	-1	1	-1	1
12	-1	1	-1	-1
13	-1	-1	1	1
14	-1	-1	1	-1
15	-1	-1	-1	1
16	-1	-1	-1	-1
17	1	0	0	0
18	-1	0	0	0
19	0	1	0	0
20	0	-1	0	0
21	0	0	1	0
22	0	0	-1	0
23	0	0	0	1
24	0	0	0	-1
25	0	0	0	0

Fig. 2.5—Composite design.

at its pessimistic or optimistic value and all other variables at their most likely values. The central point has all the variables at their most likely values. There are four parameters in the composite design in Fig. 2.5 (i.e, $n=4$). Thus it has $2^4 = 16$ factorial designs, $2 \times 4 = 8$ star points, and 1 central point. The total number of designs is 25. In

the table, -1 represents the pessimistic value; 0 represents the most-likely value; 1 represents the optimistic value.

Conduct Experiments. After the design is finished, the next step is to conduct the experiments. This is done by reservoir simulation runs. One experiment needs one reservoir simulation run. The composite design in Fig. 2.5 needs 25 reservoir simulation runs.

Response Surface. Once the designs are done and the simulations finished, the results must be interpreted with tools provided by the response surface^{33, 36} technique, the aim of which is to approximate a process by a simple regression model that fits the true response surface well. A response surface model is an empirical fit of experimental or computed responses. The responses are measured from the experimental designs. The response surface is a function of the most influential parameters in the experimental design (Eq. 2-2). The response surface model is usually a polynomial fit with linear regression. Some examples will be given in Chapters IV and V.

$$S = f(\bar{x}) + \varepsilon . \dots\dots\dots (2-2)$$

The residual—the difference between the so-called observed and the predicted value—is one important criterion for the quality of the response surface. If the residual does not change much with the predicted values, and appears to be randomly distributed, the quality of the regression usually will be adequate. Otherwise, there might be problems with the regressed model; thus the response surface model is in question. The problems might result from inappropriate selection of the regressors, not correctly considering the

interactions between the regressors, powers of the regressors set too low, or nonexistent response surfaces for the given regressors. It is entirely possible that no good response surface exists for a given set of regressors.

Reserves Distribution. After the response surface is formed, we can obtain the reserves distribution by Monte Carlo simulation. For every parameter in the response surface function, we generate a set of random numbers from a statistical distribution, and then plug the random numbers into the response surface function to get a set of numbers for the reserves. The final results we get are the reserves distribution. We can conduct statistical analysis of the reserves distributions. The statistics parameters, such as mean and standard deviation, can be estimated from those distributions. On the basis of the results analysis, we will have some ideas of the probability that the reserves will be over a certain value. The results will be very helpful in the decision making process.

2.3 Multiple Realization Tree Method

The multiple realization tree method^{30,35,36} has been used in the petroleum industry to estimate ultimate recovery and field reserves. This method is a powerful method that helps decision making.

The general procedure of this method includes:

- Construct tornado diagrams to identify the key uncertainties from the reservoir parameters to simplify the multiple realization trees after history matching.
- Create multiple realization trees to define the reserves.

- Assign probabilities to the branches of the multiple realization trees based on discretisation of the continuous probability functions.
- Analyze simulation runs to form the probability distribution function of the reserves.

Fig. 2.6 is a schematic of the procedure described above.

The first step is the same as the experimental design and response surface method. The recovery or reserves is the root of the multiple realization tree; the most influential parameter is located at the first level, and all the other key parameters are located at different levels based on their importance from the tornado diagram. Fig. 2.7 shows the multiple realization trees. The parameter porosity here is the most important one for reserves; therefore, it is the first level. Permeability and skin factor are located at the second and third level. In this example, we have three important parameters.

The probabilities for each branch – the pessimistic, the most likely, and the optimistic value – are assigned on the basis of the best knowledge of the integrated reservoir study. If we have n reservoir parameters in the multiple realization tree, the tree will have n levels (not including the root “reserves”), and $3n$ leaves (three probabilities for each reservoir parameter). Fig. 2.7 shows three levels: porosity, permeability, and skin factor, and $3^3 = 27$ leaves, which are located at the very bottom of the tree. The probability for each leaf is the product of the probabilities of all its ancestors. For example, the probability of the left-most leaf is the product of the probabilities of pessimistic porosity, pessimistic permeability, and pessimistic skin factor. For each leaf, we have to conduct

one simulation run to get the reserves or recovery. After the reservoir simulation runs are finished and the probability for each leaf is calculated, we can get the reserves distribution (Fig. 2.8).

2.4 Relative Variation Factor Method

The relative variation factor method⁷ consists of three steps:

- Quantify the sources of uncertainties concerning the reservoir volume (original oil/gas in place);
- Quantify the factors affecting the oil recovery factor;
- Quantify the uncertainty range of the recoverable volume.

Hydrocarbon Volume

In the first step, the most influential reservoir parameters for hydrocarbon volume are selected from all the reservoir parameters. These most influential parameters are kept at their most likely values from the existing data/tests and the most likely hydrocarbon volume is calculated from these values. The resultant hydrocarbon volume is called a base case or reference value. After the most influential reservoir parameters are determined by integrated reservoir study and the reference hydrocarbon volume is calculated with these reservoir parameters at their most likely values, the probability density functions of hydrocarbon volume are obtained. To determine the probability density function of hydrocarbon volume, we select one parameter from the most influential parameters for the hydrocarbon volume at a time and keep all the other

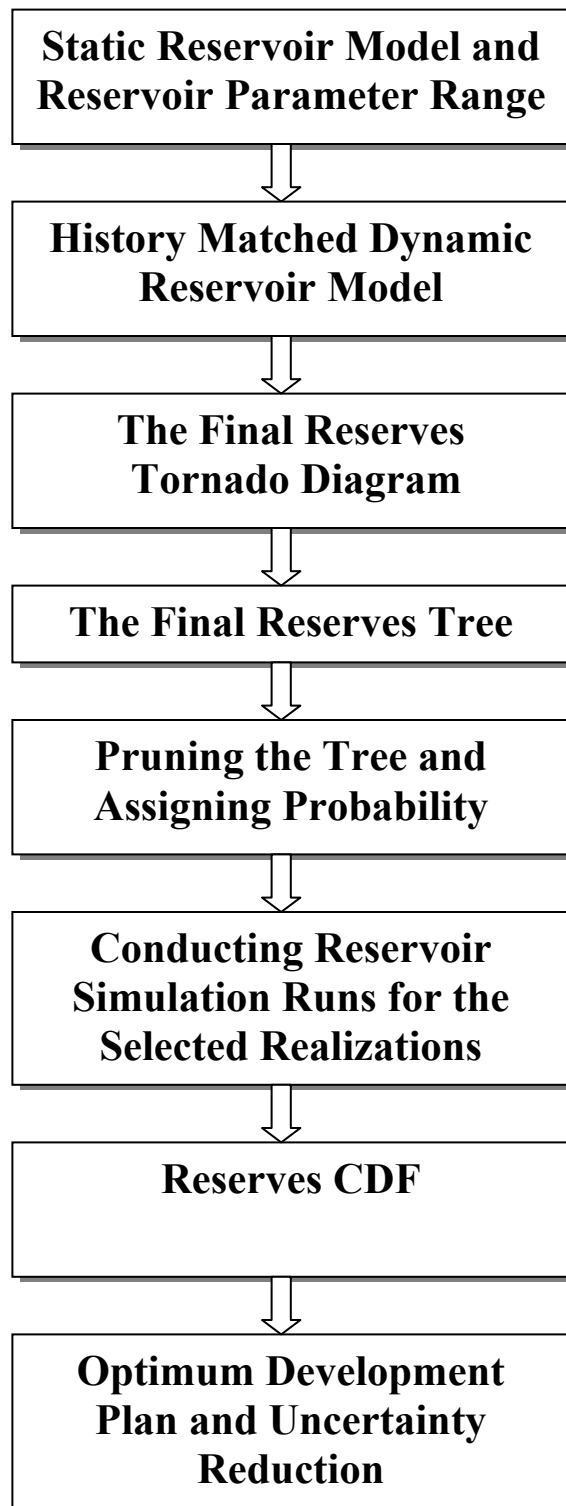


Fig. 2.6—Multiple realization tree procedure.

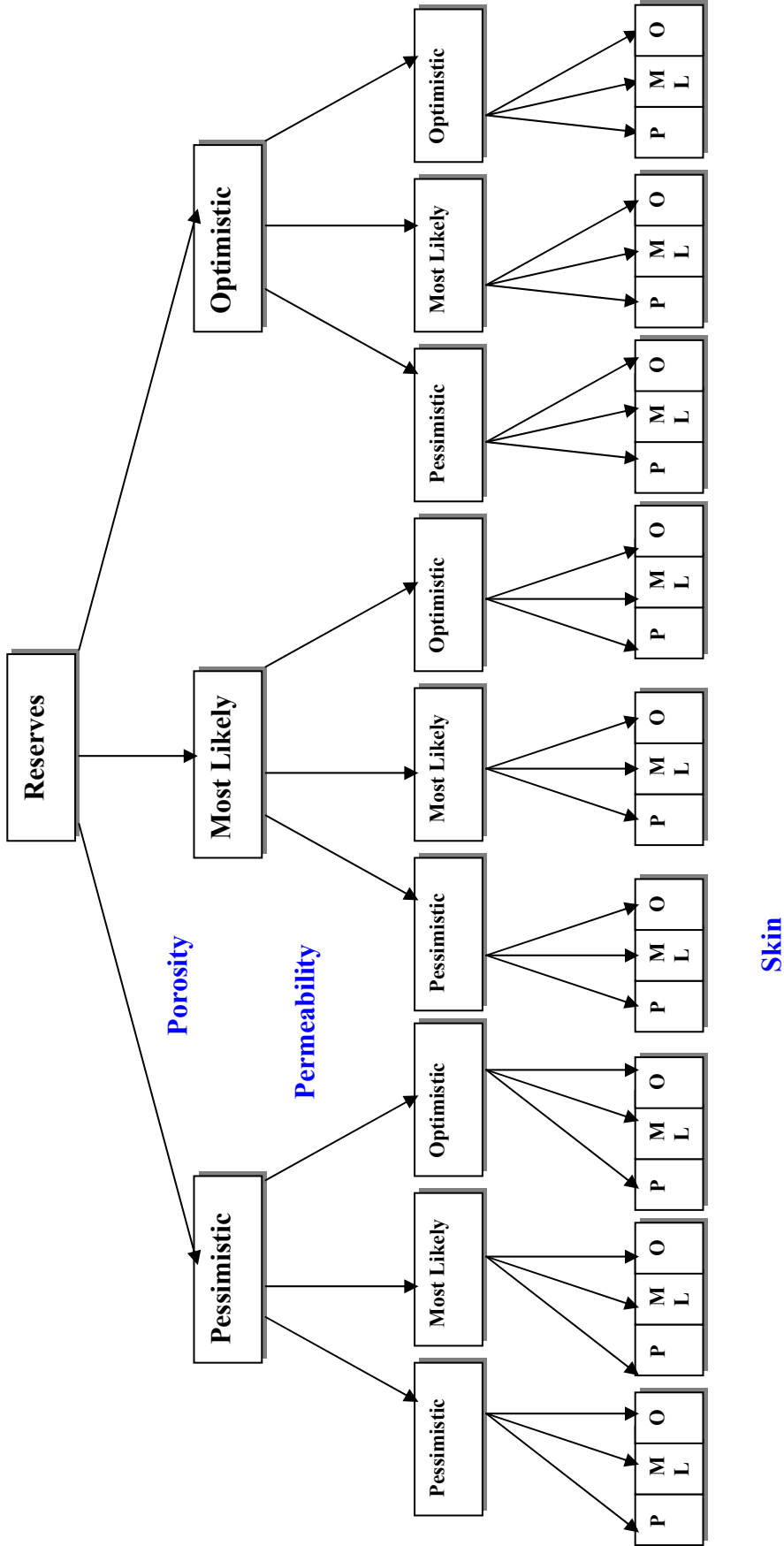


Fig. 2.7—Multiple realization tree structure based on reserves estimation.

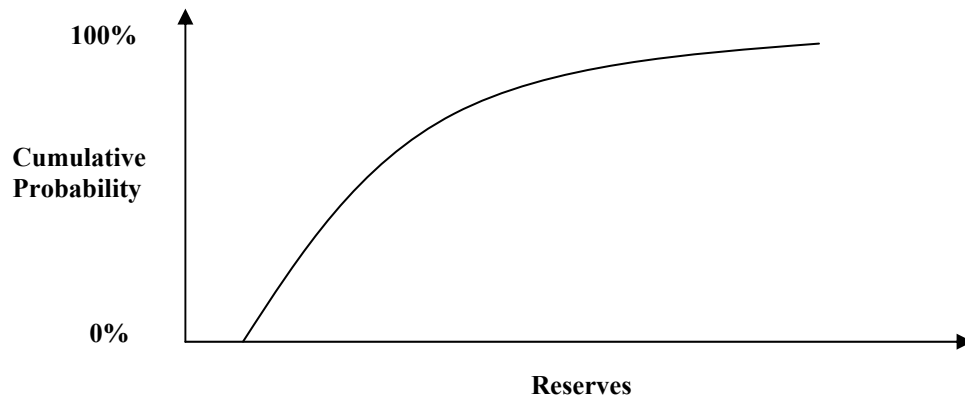


Fig. 2.8—Reserves CDF.

parameters at their base or reference values. To calculate the hydrocarbon volume of the reservoir, we do not need to conduct reservoir simulation runs. After the reservoir simulation model is constructed from the available data set and inputted into the computer, the hydrocarbon volume can be outputted whenever a reservoir parameter is changed. If we have n most influential reservoir parameters, we will have to calculate the hydrocarbon volume $2n+1$ times, including the base case in which every reservoir parameter is set to its most likely value. Each of the most influential reservoir parameters for hydrocarbon volume is set to the pessimistic and optimistic value (all the other parameters are kept at their most likely values), and the hydrocarbon volume is calculated; we have n parameters, so we get $2n$ calculations. If we include the base case, there are $2n+1$ calculations in total.

Then, we calculate the hydrocarbon volumes at three levels of the selected parameter: the pessimistic value, the most likely, and the optimistic value. After that, dividing the resultant three hydrocarbon volumes by the base case hydrocarbon volume results in three values: a real number less than 1, 1, and a real number greater than 1. At this point, we can construct a triangular distribution—relative variation factor—with these three numbers, which is the probability density function for the selected parameter. The probability density functions for other most influential parameters for hydrocarbon volume can be obtained likewise. The probability density function of hydrocarbon volume is the product of the reference hydrocarbon volume and the probability density functions of the most influential reservoir parameters for hydrocarbon volume. This is done with Monte Carlo simulation. Random numbers are generated for the relative variation factors, and a set of resultant hydrocarbon volumes is calculated. Finally, a hydrocarbon volume distribution is formed. The hydrocarbon volume of the reservoir can be calculated by the following equation:

$$N = N_{REF} \times \Delta_1 \times \Delta_2 \times \cdots \times \Delta_n \dots\dots\dots (2-3)$$

N is the distribution of the hydrocarbon volume; N_{REF} is the value of the hydrocarbon volume for the base/reference case; Δ is the distribution of the variation factors for the influential reservoir parameters that affect the hydrocarbon value. An example is available in Chapter IV.

The reservoir parameters that affect the hydrocarbon volume include porosity, oil saturation, porous thickness, depositional boundaries, faults, and contacts between

reservoir fluids (oil, gas, and water). Those parameters usually are obtained by indirect means. Porosity is obtained by log interpretation, core analysis, or correlations. Core analysis and log interpretation are the main means to get saturations. Seismic interpretation is used to determine the depositional boundaries and the fault locations. Log interpretation is the main method to obtain the contact locations between reservoir fluids. Most of the methods above are interpretation processes, which are not precise, and very easy to input errors to the final results. Even for the direct measurements like core analysis, errors can be involved because of systematic or measurement errors, not to mention that usually the reservoirs are not homogeneous and the cores are not necessarily good representations of the whole reservoirs. The quality and availability of seismic data, core samples, and tests also have a significant effect on the uncertainties for the reservoir parameters. Clearly, there are a lot of uncertainties with those reservoir parameters.

Integrated reservoir study is an excellent method to determine the possible ranges for those reservoir parameters. The engineers and the geoscientists work closely as a team to investigate the possible errors and the range for those reservoir parameters, and to come up with the most likely value, the pessimistic value, and the optimistic value for every reservoir parameter.

When we calculate the hydrocarbon volume distribution with Eq. 2-3 by Monte Carlo simulation, we need a random number generator for the variation factors of the

influential reservoir parameters that affect the hydrocarbon volume. Microsoft Excel can be used to generate the random numbers for regular statistics distribution such as normal distribution. However, we assume that the distributions for the parameters in Eq. 2-3 are triangular distributions, which are not regular distributions, and cannot be generated by Excel. In this situation, we need to generate random numbers with triangular distributions.

The triangular distribution is defined by a range (a,b) and a point p where the distribution has its mode (Fig. 2.9). Give a standard uniform random variate U , a random variate T from such a triangular distribution is obtained by the following formula. If

$$U < (p - a)/(b - a),$$

$$\text{then } T = a + \sqrt{(b - a)(p - a)U} ;$$

$$\text{else } T = b - \sqrt{(b - a)(b - p)(1 - U)} . \dots\dots\dots (2-4)$$

Random numbers for Monte Carlo simulation can be generated by Eq. 2-4.

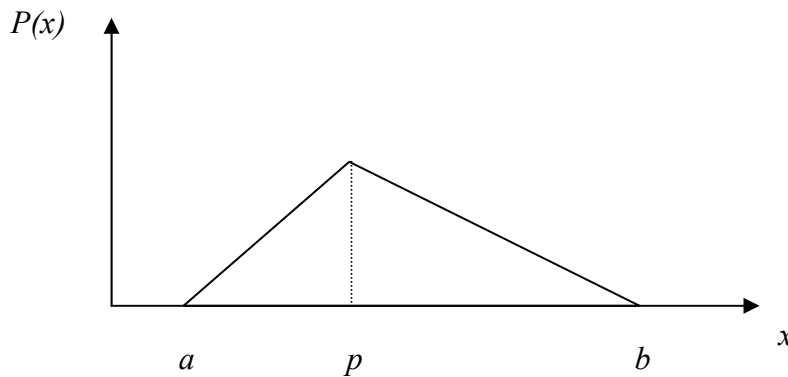


Fig. 2.9—Triangular distribution.

Recovery Factor

The reservoir parameters that affect recovery factor include horizontal permeability, vertical permeability, relative permeability between the phases, fault transmissibility, fluid viscosities, reservoir heterogeneity, and the productivity of the wells. Just like the reservoir parameters that affect hydrocarbon volume, those parameters have multiple uncertainties. The main challenge is how to study all of these parameters at the same time, and how to determine the probability density functions for them without many simulation runs.

As discussed before, the approach comprises the following procedure: starting from a base case, in which all the parameters are assigned with the most likely values, perform two additional simulation runs (the pessimistic and the optimistic cases), to estimate the influence of each considered variable, and suppose a fixed distribution of its effect on the oil recovery. With an equation similar to the calculation of the hydrocarbon volume, calculate the recovery factor with Eq. 2-5:

$$RF = RF_{REF} \times \Delta_1 \times \Delta_2 \times \cdots \times \Delta_n \dots\dots\dots (2-5)$$

RF is the distribution of the recovery factor. An example is available in Chapter IV.

Alternatively, the distribution of the recovery factor may be calculated with Monte-Carlo simulation.

When we try to get the probability density function of the recovery factor, we need to resort to reservoir simulation. As discussed before, if we have n most influential

reservoir parameters for recovery factor, we will have to conduct $2n+1$ reservoir simulation runs. We should not have any problem with this because of the number of the simulation runs. Usually the number of the most influential parameters is less than 8; thus, the maximum number of simulation runs is 17. This number is much lower than for the experimental design and response surface method.

Recoverable Hydrocarbon

The third step of this method is to calculate the reserves distribution. Now that we have the hydrocarbon volume and the recovery factor distributions, the recoverable hydrocarbons (reserves) can be obtained with the following straightforward equation:

$$R = N \times RF \dots\dots\dots (2-6)$$

Given the distributions of oil/gas volume and recovery factor, final reserves are obtained by Monte Carlo simulation. The hydrocarbon volume and recovery factor probability density functions can be displayed with histograms of the numbers calculated by Eq. 2-4 and 2-5. A set of random numbers is generated for the hydrocarbon volume and the recovery factor; with Eq. 2-6, many values of the reserves are obtained; the final reserves distribution is formed with these values. An example is available in Chapter IV.

2.5 Bayesian Method

The Bayesian approach^{37,38} has been applied in uncertainty analysis in the petroleum industry for some years. Bayes' theorem relates the *a posteriori* probability distribution function to an *a priori* probability distribution function and likelihood function. The prior

model characterizes the uncertainty before the production data are considered. The prior model is used to build the initial reservoir model. The posterior model characterizes the uncertainty after the production data are honored. The likelihood function measures the probability that the actual production data would have observed for any given model of the reservoir.

In the importance sampling method, many reservoir models are generated from the prior model and reservoir simulation is conducted for each model; then the objective function value is calculated. The contribution of each model to the posterior distribution for reserves is weighted by its likelihood function. If the prior model is good enough that many initial reservoir models match the production data very well, no history match process is needed. On the other hand, a large number of reservoir models might be needed before a good model that matches the production data is obtained. This is a limitation of this method.

In the pilot-point method, many reservoir models are generated from the prior model. Each model is then history matched. During the history match process, values at certain points in the reservoir are changed, and the changes are propagated to the rest of the reservoir model by Kriging. The process continues until each is matched. One problem with this method is that the values at the pilot-points of the reservoir might become extreme during the history match process. There are some variations to this method.

CHAPTER III

INTEGRATED MISMATCH METHOD

In Chapter II, I reviewed some existing methods for quantifying uncertainties with reserves: relative variation method, multiple realization tree method, and experimental design and response surface method. In some of those methods, estimates of reservoir uncertainty are attempted, after the history match is completed, by making extra runs of the simulator. These runs are made by systematically varying the reservoir description from the base case (history-matched model) and are called "sensitivity analysis" runs. Then, a response surface function is obtained by multivariate regression based on the reservoir description parameters. Probability distributions are assigned to the reservoir description parameters, and are input into the response surface function, and finally Monte Carlo simulation is conducted for many input parameter realizations.

When "sensitivity analysis" runs are made by perturbing from a calibrated model, these extra runs will not match the historical data as well because of the change in parameters; thus, the runs upon which the response surface function is based are not equiprobable. This is an inherent weakness of existing techniques. Another problem with existing methods is that probability distributions for reservoir parameters are not usually obtained by scientific methods; they are assumed and, thus, subjective. A method that incorporates the mismatch of the sensitivity analysis runs in the estimation of uncertainties in performance predictions to eliminate both of these deficiencies is proposed in this chapter.

3.1 Quantifying Mismatch

To measure the extent to which a reservoir model is conditioned to the available historical data, we must define a measure to quantify the mismatch between the simulated response of the reservoir model and the historical data. We call this an objective function, or mismatch function. The purpose of the history match is to minimize the mismatch function. The mismatch between the simulated production data and the observed production data can be quantified by using a sum of squares. For each parameter, like bottomhole pressure (BHP), gas/oil ratio (GOR), and water cut (WCT), at each time when the observed data are available, the sum of the square of the product of the weight factors and the differences between the observed and the simulated values divided by the standard deviation is calculated.

$$M = \left\{ \frac{1}{N} \sum_{j=1}^N \frac{1}{N_{ij}} \sum_{i=1}^{N_{ij}} \left[w_{ij} \frac{y_{ij}^{cal} - y_{ij}^{obs}}{\sigma_{ij}} \right]^2 \right\}^{\frac{1}{2}} \dots\dots\dots (3-1)$$

In Eq. 3-1, M is the mismatch value. It is a dimensionless quantity because it is a normalized value; the difference and the standard deviation of one parameter have the same units. The mismatch quantifies the distance between the reservoir simulation model and the true reservoir model. The smaller the mismatch value, the closer the reservoir simulation model is to the true reservoir model. A mismatch value of 0 gives a perfect reservoir model conditioned to all the production data; a mismatch value of 1 means that the match is within the measurement error, on average. The purpose of history matching is to obtain a mismatch value as small as possible for the given production data. The weight factor in the mismatch function gives more flexibility for

weight control of observed data type in the mismatch function. Different weight factors can be given to different observed data types or different data points for the same data type. Given the accuracy or relative importance of different data types or different data points, bottom hole pressure may appear to be more important to match than oil production rate; in that case, greater weight can be assigned to bottomhole pressure.

3.2 Model Probabilities

Usually, after the reservoir simulation model is built based on the integrated reservoir study, we try to reproduce the production history; this process is called history matching, or conditioning to the historical data. As shown in Fig. 3.1, we have different

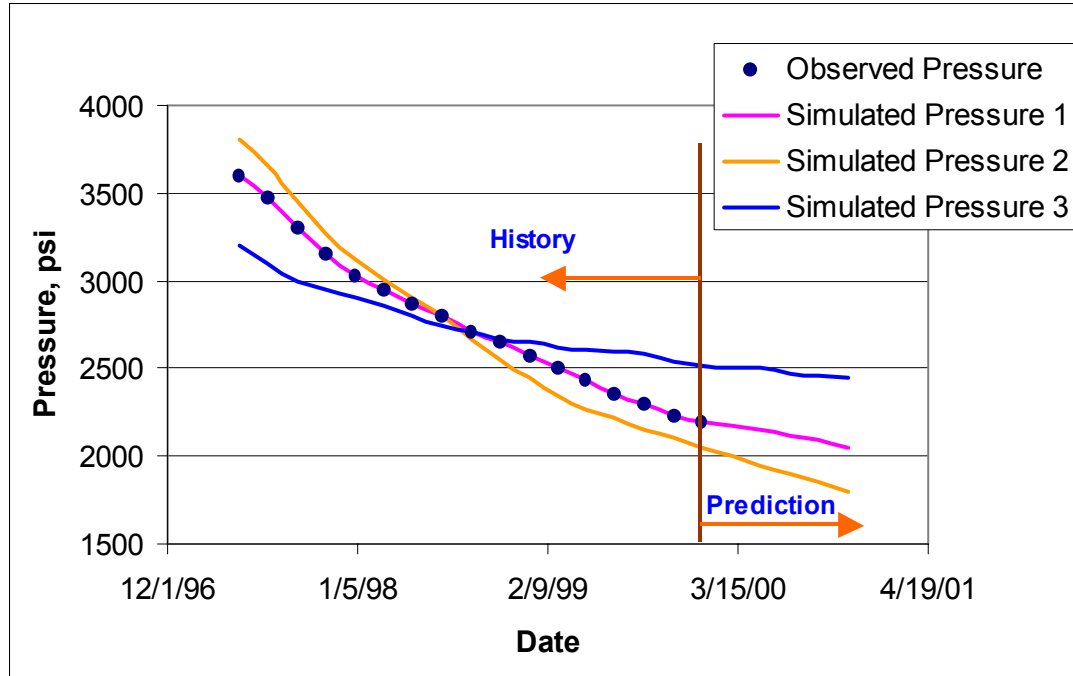


Fig. 3.1—Pressure mismatch quantification.

simulation runs during the history matching process. It is desirable that we find a model that can perfectly match the production history (Simulated Pressure 1 in Fig. 3.1). The mismatch we defined should be zero for this perfect model; however, we seldom find a perfect reservoir model. In practice, the history matching process will be complete when a model is found that can closely match the production history, because it is neither economic nor feasible to find the perfect model. For the deterministic method, when the history matching process is finished, the resultant reservoir model is used to make predictions for different scenarios as desired.

In Fig. 3.1, we can see that the reservoir models have different “distances” from the production history. Reservoir model 1 (“Simulated Pressure 1”) overlies all the observed data; thus its “distance” is 0 from the production history. The next closer reservoir model to production history is Reservoir Model 2; Reservoir Model 3 has the largest “distance” from the production history. It is intuitive that the smaller “distance” from the production history a reservoir model has, the more likely it is to represent the true reservoir description. In Fig. 3.1, the probability of Reservoir Model 1 is the largest; the probability of reservoir model 3 is the smallest. When a reservoir model’s distance from the production is bigger, the mismatch is bigger; its probability is smaller. The proposed method incorporates this in the probability assignment for different simulation runs.

3.3 Weighting Function

As different reservoir models give different mismatch values to a given production history, their probabilities are not the same in the final distribution. The probability of a reservoir model is inversely related to its mismatch value. A useful weighting function³⁸ for the probability of a reservoir model is given in Eq. 3-2:

$$L = c \exp\left[-\frac{N}{2} M^2\right] \dots\dots\dots (3-2)$$

where L is the likelihood and c is normalization constant such that the probabilities of all the possible reservoir models sum up to unity. M is the mismatch value and N is the total number of observed data points. Eq. 3-2 is an exponential function, which gives sharp differences for reservoir models with different mismatch values; reservoir models with small differences in mismatch values can have large differences in their probabilities in the final reserves distribution. By using a weighting function, reservoir models with smaller mismatch values are given more weight in their contributions to the final reserves distribution.

The procedure of this proposed method includes the following steps.

1. Conduct history matching.
2. Perform sensitivity analysis of hydrocarbon reserves for the reservoir description parameters to obtain the most influential parameters.
3. Apply experimental design to come up with an optimal design to cover as much information as possible with the least number of experiments.

4. Conduct the experiments with a reservoir simulator to get reserves and the mismatch in the history match for different combinations of the most influential reservoir description parameters.
5. Use multivariate regression to obtain the regression coefficients for the response surface functions for the reserves and history mismatch.
6. Sample the parameter space with different step sizes to calculate reserves and history mismatch with the response surface functions.
7. Calculate the likelihood (Eq. 3-2) to assign the probabilities for different parameter combinations (reservoir models) according to the mismatch.
8. Obtain the reserves distribution from the results of step 7.

3.4 Sampling the parameter space

After experimental design of the reservoir simulation is finished and response surfaces of reserves and mismatch are obtained from the simulation runs, we need to sample the possible reservoir parameter ranges to get the final reserves distribution. Traditionally, stochastic methods sample the sample space by a random number generator. Fig. 3.2 shows this kind of sampling for a domain that has only two reservoir parameters: porosity and permeability. We can clearly see that this kind of sampling does not completely cover the whole sample space with a limited number of samples. Usually, it is not affordable to use a large number of samples because each sample needs a reservoir simulation run that is time consuming and sometimes expensive.

For the integrated mismatch method, we sample the response surfaces, which are much less expensive. Thus, the sampling completely sweeps the whole sample space by setting a range and a step size for each reservoir parameter, using multiple loops to sweep through all the possible combinations of all the reservoir parameters. Fig. 3.3 is a schematic for a domain that has only two reservoir parameters: porosity and permeability. Every dot represents a reservoir model including a porosity value and a permeability value. Compared with Fig. 3.2, we can easily see that this sampling is more complete.

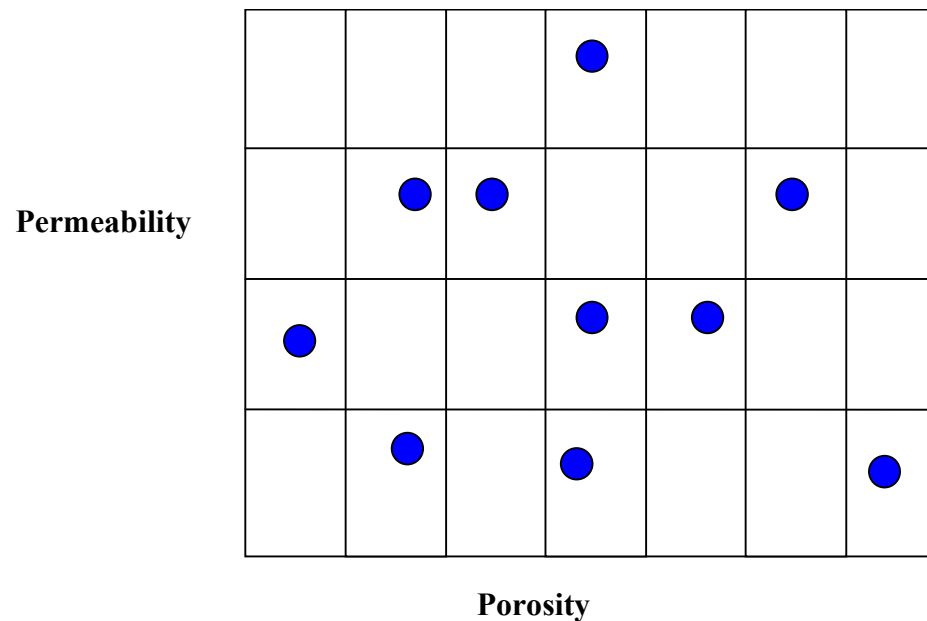


Fig. 3.2—Sample the sample space—stochastic method.

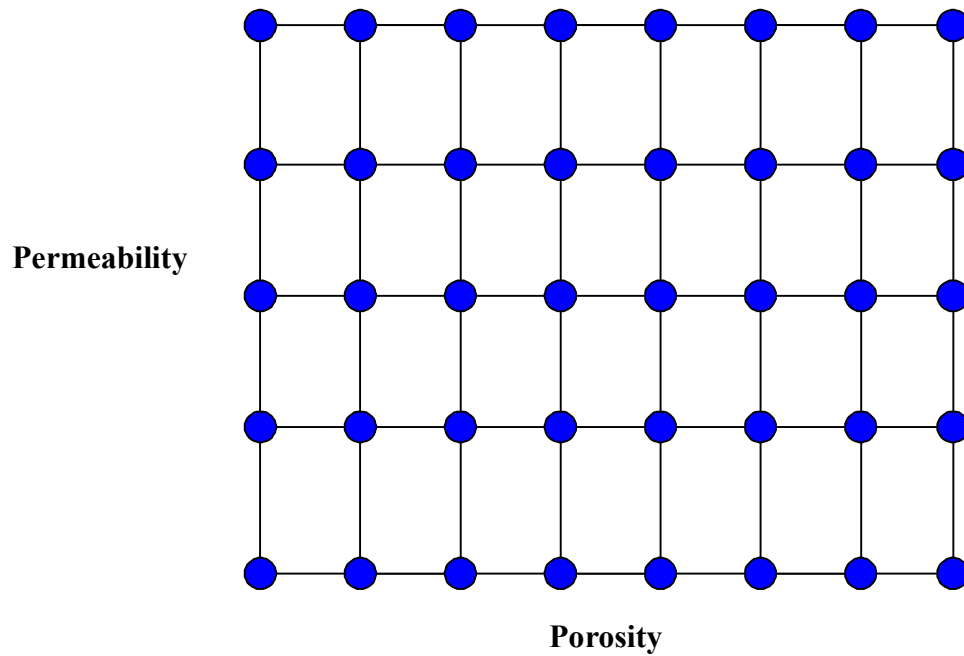


Fig. 3.3—Sample the sample space—the integrated mismatch method.

3.5 Reserves Distribution

On completion of sampling the sample space, we get a reserves value and an associated probability for every reservoir model. We can develop a reserves distribution with all the reservoir models and their reserves and probability values. Because we use a normalization constant in the weighting function, the probabilities of all the reservoir models from the sample space sums to unity. Now we order all the reservoir models by reserves values from high to low, then get a specific percentage for the reserves. If we wish to get a 90% range for reserves, we can read the high 5% and the low 5% of the reserves distribution.

CHAPTER IV

EXAMPLE APPLICATION 1: PABST FIELD

In the previous chapters, we have reviewed the importance of integrated reservoir study, and some methods of uncertainty analysis. Also we proposed a new method, the integrated mismatch method. In this chapter, we will illustrate the applications of all the methods of uncertainty analysis with a real field—Pabst Field, Gulf of Mexico.

Comparisons will be made with the methods for the field.

4.1 Introduction

Development of deepwater Gulf of Mexico fields is an expensive undertaking that involves considerable analysis and evaluation of both engineering and geologic data. In this context, failure to recognize reservoir compartmentalization can add significantly to field development capital and result in less-than-optimal reservoir management and profitability. For all of these reasons, early recognition of reservoir compartmentalization is advantageous. Over the past 10 years, a number of case studies employed geochemistry to recognize reservoir compartmentalization. In other cases, production performance was used to investigate the compartments of reservoirs. However, geochemistry and production are not enough for identifying reservoir compartmentalization in many situations. Many cases have illustrated the application of integrated reservoir studies for reservoir management in the past. By using integrated reservoir study, we modeled the sealing capacity of two major faults at Pabst field, Gulf of Mexico. Pabst field is located in Main Pass 259 Block Gulf of Mexico, offshore

Louisiana (Fig. 4.1). It was discovered in 1990. There are 24 wells in total; 13 are in production. Production is from 7,700 ft to 11,500 ft. The field produces mostly gas and some condensate. Nearby fields include Petronius, Tahoe, and Ram-Powell.

4.2 Research Objectives

The objectives of this project include determining the sealing capacity of two major faults, delineating the reservoir compartments, evaluating the potential of a new well, and finally characterizing the uncertainties of the reserves.

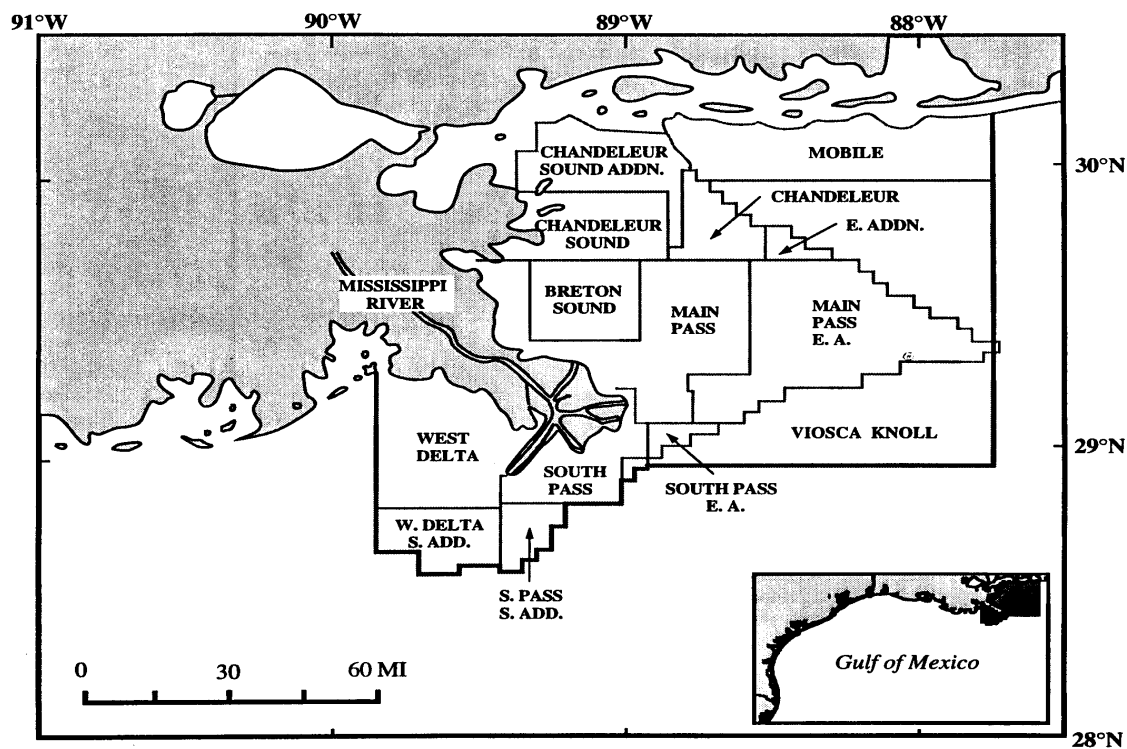


Fig. 4.1—Location of Pabst field.

4.3 Reservoir Simulation Model

There are several reservoirs in this field: Texas W1, Texas W2, Texas W6, 7,700-ft Sand, 10,000-ft Sand, 10,150-ft Sand, and 10,300-ft Sand. Our investigation focused on the 10,300-ft Sand. The operator wanted to investigate the sealing capacity of two major faults in the field; and on the basis of the results, they would consider drilling more wells to optimally develop the reservoir. Based on the reports from the former operator, the depositional environment of this reservoir is a slope fan. Some channels might exist, but they are not believed to be in communication with each other.

For this reservoir, we had 3D seismic data, well logs for some wells, sidewall core analysis for some wells, pressure transient tests for some wells, and pressure data and production data for all the wells under development through July 2000. Fig. 4.2 is the structure map of the 10,300-ft Sand from the seismic interpretation.

We clearly see the two large NW-SE trending faults. Fig. 4.3 is the net gas isopach map of the 10,300-ft Sand. Well A4 is separated from wells A7, A2, and A9 by the two major faults. The reservoir produces mostly gas and some condensate. Very little water is produced, so for simplicity, we treated the reservoir as a dry-gas reservoir. Well logs, sidewall core analysis, and pressure-transient test interpretation were used to determine porosity. Fig. 4.4 is the sidewall core analysis. Fig. 4.5 is the results of a pressure transient test. The initial reservoir pressure was around 5,000 psi. Four wells are currently producing from this reservoir.

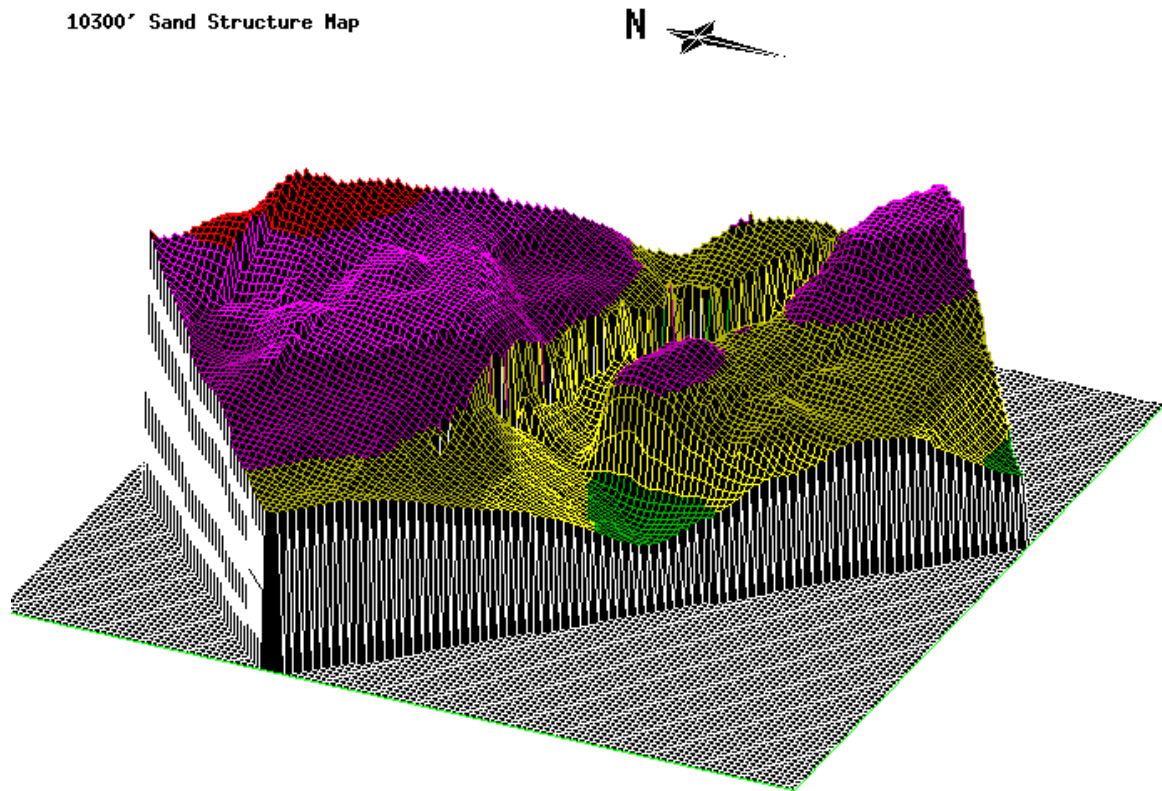


Fig. 4.2—Structure map of 10,300-ft sand.

For this project, we employed a multidisciplinary approach. Geologists, geophysicists, geochemists, and petroleum engineers worked closely together to achieve the single goal. Geoscientists interpreted the seismic data, well logs, and core data. Petroleum engineers interpreted the pressure transient test data and carried out reservoir simulation. We built a reservoir simulation model by integrating geophysical, petrophysical, production and well test data, and modeled the sealing capacities of faults by modifying the transmissibility between grid blocks along the fault traces.

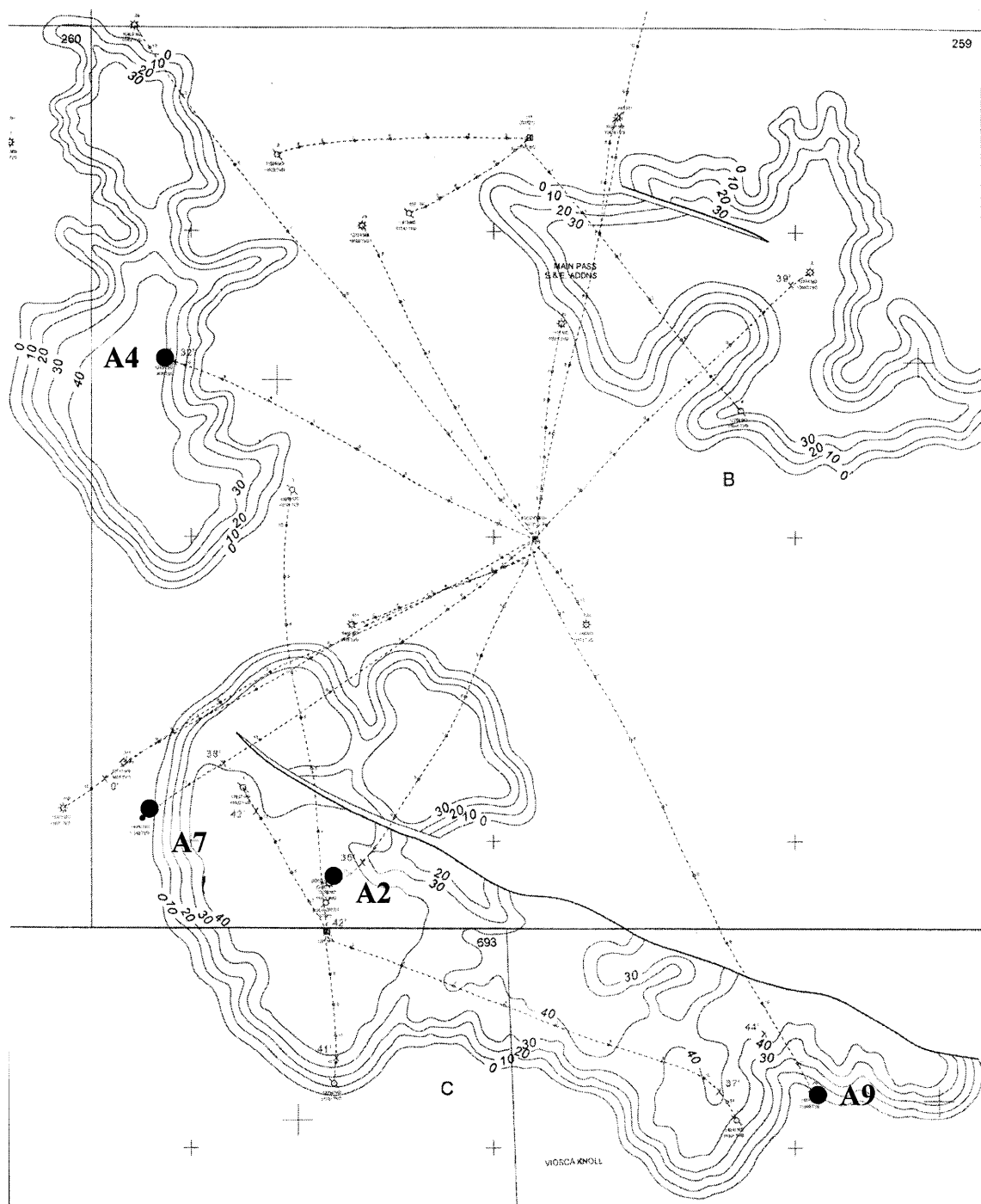


Fig. 4.3—10,300-ft sand net-gas isopach map.

SIDEWALL CORE ANALYSIS

In. Rec.	Sample Depth Feet	Permeability mD	Porosity %	Pore Volume		Prod Prod	Bulk Volume		Comb. Gas	Con. Water %	Q4 Factor	Core
				Saturation Oil %	Waste %		Saturation Oil %	Gas %				
0.8	12635.0	4.4	16.9	3.6	74.5	(6)	0.6	3.7	0	67	3	Sd vfg vsilty vshy lam slks yl-
0.5	12637.0	15.0	23.0	2.4	62.7	Cond	0.6	8.0	0	67	2	Sd vfg vsilty shy vft flu
0.5	12646.0	85.0	26.3	3.6	41.3	Cond	0.9	14.5	0	55	2	Sd vfg vsilty sshy yl-wh flu
0.5	12650.0	66.0	25.5	4.1	58.3	Cond	1.0	9.6	0	56	3	Sd vfg vsilty shy yl-wh flu
0.5	12654.0	56.0	25.4	1.1	70.3	Cond	0.3	7.3	0	56	3	Sd vfg vsilty shy yl-wh flu
0.5	12660.0	26.0	24.1	1.1	52.0	Cond	0.3	11.3	0	64	2	Sd vfg vsilty shy yl-wh flu
0.5	12671.0	19.0	22.7	1.4	55.1	Cond	0.3	9.9	0	65	2	Sd vfg vsilty shy ft yl-wh flu
0.6	12673.0	9.5	20.7	4.5	61.4	(6)	0.9	7.0	0	69	2	Sd vfg vsilty vshy lam slks yl-
0.5	12675.0	110.0	25.9	2.9	61.8	Cond	0.7	9.1	0	52	3	Sd vfg vsilty sshy ft flu
0.5	12680.0	130.0	26.1	0.9	47.4	Cond	0.2	13.5	0	50	3	Sd vfg vsilty sshy ft yl-wh flu
0.5	12682.0	57.0	23.4	1.0	62.6	Cond	0.2	8.5	0	54	2	Sd vfg vsilty shy yl-wh flu
0.5	12684.0	40.0	24.2	1.0	49.5	Cond	0.2	12.0	0	60	2	Sd vfg vsilty shy ft yl-wh flu
0.4	12684.0	50.0	23.4	1.7	64.1	Cond	0.4	8.0	0	56	3	Sd vfg vsilty shy ft yl-wh flu
0.0	12684.0											Misfire
0.0	12687.0											Misfire
0.5	12691.0	33.0	21.8	0.9	71.6	Cond	0.2	6.0	0	58	3	Sd vfg vsilty shy ft yl-wh flu
0.6	12693.0	34.0	24.5	0.8	66.1	Cond	0.2	8.1	0	63	2	Sd vfg vsilty shy ft yl-wh flu
0.6	12696.0	44.0	23.8	3.3	61.1	Cond	0.8	8.5	0	60	3	Sd vfg vsilty shy ft yl-wh flu
0.7	12698.0	600.0	30.7	1.1	75.4	Cond	0.3	7.2	0	38	3	Sd vfg vsilty ft yl-wh flu
0.0	12698.0											Misfire
0.0	12698.0											Misfire
0.0	12698.0											Misfire
0.7	12701.0	265.0	27.7	3.3	53.4	Cond	0.9	12.0	0	44	3	Sd vfg sily sshy yl-wh flu
0.8	12702.0	90.0	25.5	8.9	60.8	Oil	2.3	7.7	0	52	3	Sd vfg vsilty shy yl-wh flu 32
1.2	12704.0											Mudcake
1.0	12707.0	125.0	25.8	13.6	42.3	Oil	3.5	11.4	0	50	3	Sd vfg vsilty shy yl-wh flu
1.0	12710.0	41.0	24.1	5.7	53.2	Oil	1.4	9.9	0	60	2	Sd vfg vsilty shy ft flu
0.8	12712.0	39.0	24.2	4.4	54.9	Oil	1.1	9.8	0	60	3	Sd vfg vsilty shy ft yl-wh flu
0.8	12713.0	42.0	24.1	4.2	43.0	Oil	1.0	12.7	0	60	2	Sd vfg vsilty shy lam slks ft y

Fig. 4.4—Sidewall core analysis.

WBS Model :	Constant Storage
Storage Coeff. (C1) :	0.02
Dimensionless Storage (CD) :	129.251
CD1 :	129.251
Near Well Model :	Skin Model
Skin :	115.5
Reservoir Model :	Homogeneous
Permeability :	75
User Input PI (psia) :	4800
Back Calculated Pi (psia) :	4794.372
Time Match (TD/dt) :	2.45E+05
Pressure Match (PD/dp) :	2.49E-07
Boundary Model :	Closed Circle
Drainage Radius :	2500

Fig. 4.5—Pressure-transient test results.

The reservoir was modeled (Fig. 4.6) with one layer, and the grid was $30 \times 15 \times 1$. The size of the grid was set with $\Delta x = 779$ ft and $\Delta y = 779$ ft; Δz was sampled from the net-gas isopach map. Individual well pressures were matched by adjusting reservoir porosity and permeability.

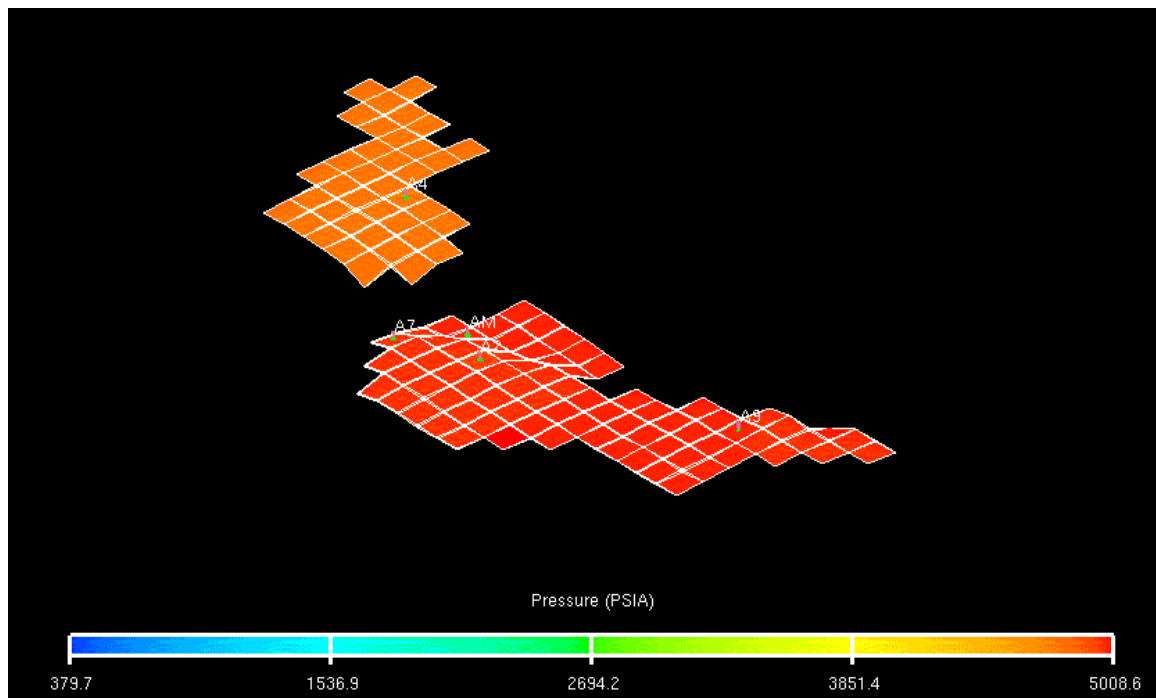


Fig. 4.6—Simulation grid.

In addition, to determine the sealing capacities of the two major faults, the sealing capacities of faults were varied by modifying the transmissibilities between grid blocks along the fault traces. A very good pressure history match was reached (Fig. 4.7, Fig. 4.8 and Fig. 4.9).

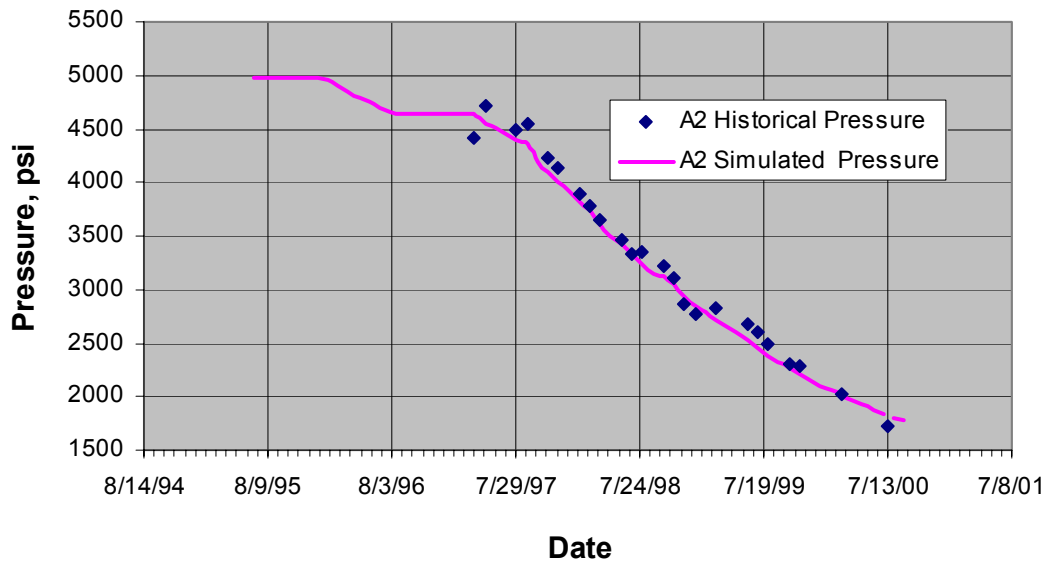


Fig. 4.7—Well A2 pressure history match.

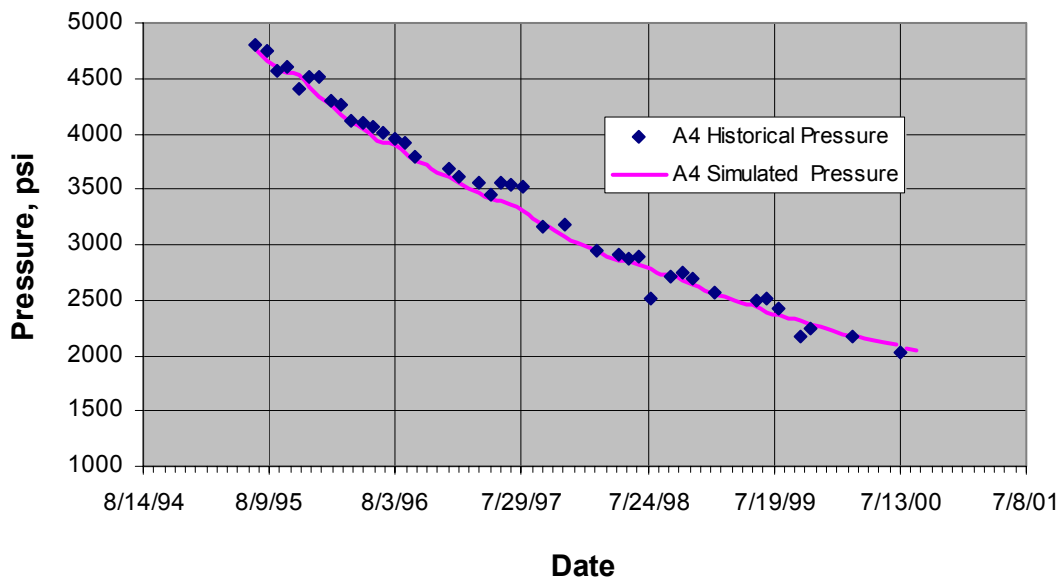


Fig. 4.8—Well A4 pressure history match.

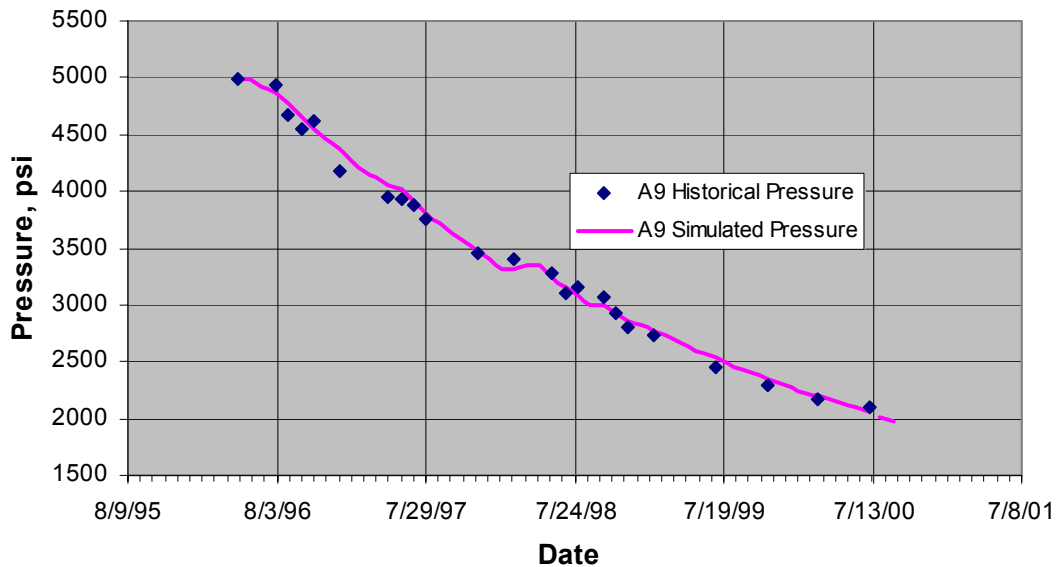


Fig. 4.9—Well A9 pressure history match.

From the simulation studies, the reservoir properties and continuity are as follows: porosity about 0.25, permeability 75 md; Well A2, A4, and A9 are separate; Well A2 and A7 are in communication; the two major faults are sealing. The gas in place for different compartments is listed in Table 4.1.

Table 4.1—Gas in Place After History Matching.

Compartment	Gas in place (Bcf)
Well A4	28.36
Well A2 and A7	25.87
Well A9	30.67

From the simulation studies, an untapped area with an estimated 9.7 Bcf gas in place was determined to be separated from other wells by the two major sealing faults. Well

A2 penetrates three sands: TEX W1, TEX W2, and the 10,300-ft Sand. At present, it has stopped producing from the TEX W1 (March 1995) and TEX W2 (March 1997). At the current rate, its BHP in the 10,300-ft Sand will decrease to an abandonment pressure of 700 psi in 500 days. Therefore, we recommend sidetracking from Well A2 to the untapped area after its pressure in the 10,300-ft Sand decreases to the abandonment pressure. Simulation results indicate Well A2 will produce 7.2 Bcf gas from the new untapped area within 600 days, assuming a target rate of 8MMscf/day and a minimum BHP of 700 psi. Final recovery for the untapped area is predicted to be around 74% of the original gas in place.

4.4 Uncertainty Analysis

In this section, I show the reserves uncertainty for the untapped area as determined by the methods we presented or proposed in Chapters II and III; the best estimates of the reservoir parameters for the untapped area after history matching are listed in Table 4.2.

Table 4.2—Reservoir Parameters After History Matching.

Reservoir Parameter	Value
Porosity	0.204
Permeability	50 md
Fault Transmissibility	0
Skin Factor	5
Thickness	35 ft

4.4.1 Experimental Design and Response Surface Method

There are only four parameters in our study: porosity, permeability, fault transmissibility, and skin factor. Compared to other parameters, the permeability is not sensitive; thus, the other three parameters are used in the experimental design. The pessimistic, most likely, and optimistic values are determined from integrated reservoir study and are listed in Table 4.3. The fault transmissibility cannot be negative, and our most likely value is 0; therefore, we do not have a pessimistic value for it. We have three parameters, one of which has two levels. The factorial design needs $3 \times 3 \times 2 = 18$ simulation runs, which is affordable. The experimental design is shown in Table 4.4.

Table 4.3—Reservoir Parameters and Their Distributions.

	Pessimistic value (-1)	Most likely value (0)	Optimistic value (+1)
Porosity	0.18	0.204	0.27
Fault Transmissibility Multiplier	1	0	N/A
Skin Factor	20	5	0

After the 18 simulation runs were finished and the reserves for each one was obtained, a reserves response surface was formed by regression. Fig. 4.10 shows the regressed reserves vs. experimental reserves. Almost all the points fall into a 45° straight line that passes through the origin. That means that almost all the regressed reserves values equal the experimental reserves values, which is what the response surface model tries to

achieve. We want to find a response surface that is a close representative of the experimental values, which we achieved in this case.

Table 4.4—Three Parameter Factorial Design.

Experiment #	Fault Trans	Porosity	Skin	Reserves (Bcf)
1	0	1	1	10.633
2	0	1	0	10.537
3	0	1	-1	10.253
4	0	0	1	8.026
5	0	0	0	7.945
6	0	0	-1	7.744
7	0	-1	1	7.078
8	0	-1	0	7.013
9	0	-1	-1	6.824
10	-1	1	1	8.921
11	-1	1	0	8.463
12	-1	1	-1	7.322
13	-1	0	1	7.437
14	-1	0	0	6.992
15	-1	0	-1	5.95
16	-1	-1	1	6.891
17	-1	-1	0	6.46
18	-1	-1	-1	5.455

With a good response surface model for the reserves, we used Monte-Carlo simulation to obtain the final reserves distribution. We assumed a triangular distribution for porosity, fault transmissibility, and skin factor. Figs. 4.11, 4.12, and 4.13 show the probability density functions for those three parameters. The modes of the triangles are the most likely values of the three parameters. The two ends are the pessimistic and optimistic values for the three parameters.

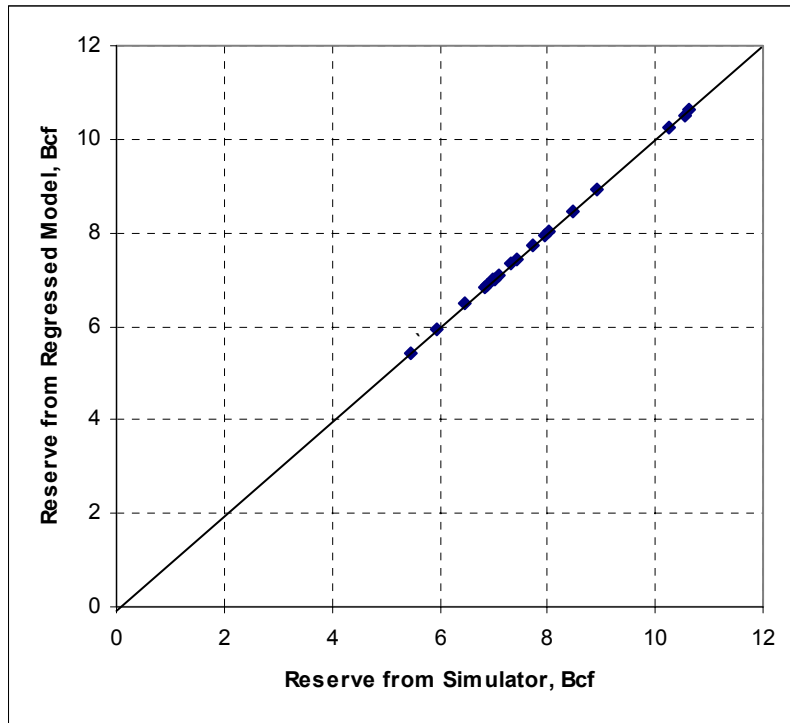


Fig. 4.10—Regressed reserves vs. reserves from simulator.

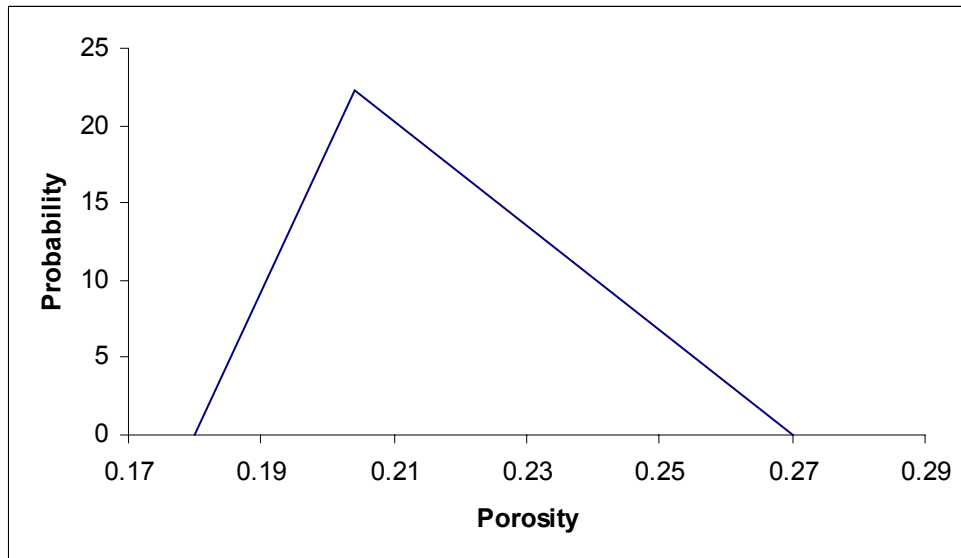


Fig. 4.11—Probability distribution of porosity.

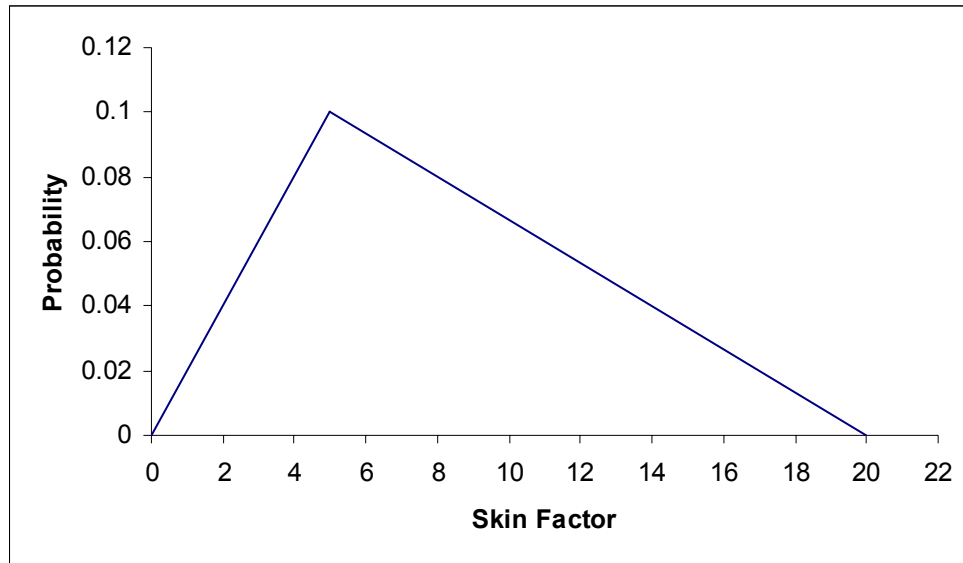


Fig. 4.12—Probability distribution of skin factor.

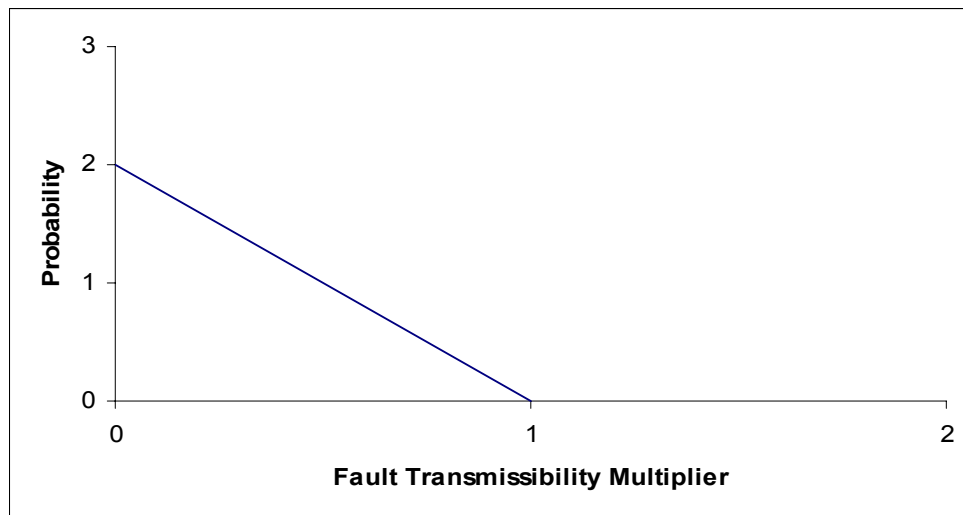


Fig. 4.13—Probability distribution of fault transmissibility.

One thousand random numbers were generated from the probability density function for each of three parameters, and then they were plugged into the response surface function

to get the final reserves distribution. A histogram of the reserves distribution is shown in Fig. 4.14. The reserves cumulative distribution function is shown in Fig. 4.15.

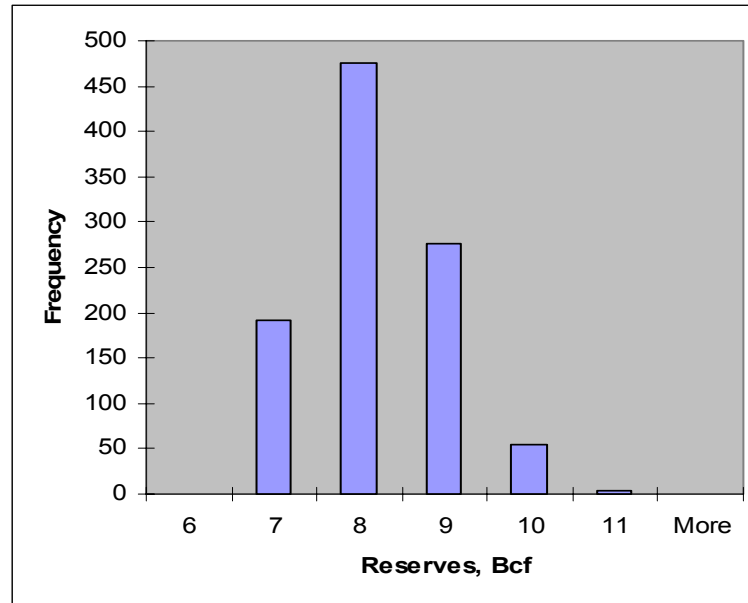


Fig. 4.14—Reserves distribution of experimental design method.

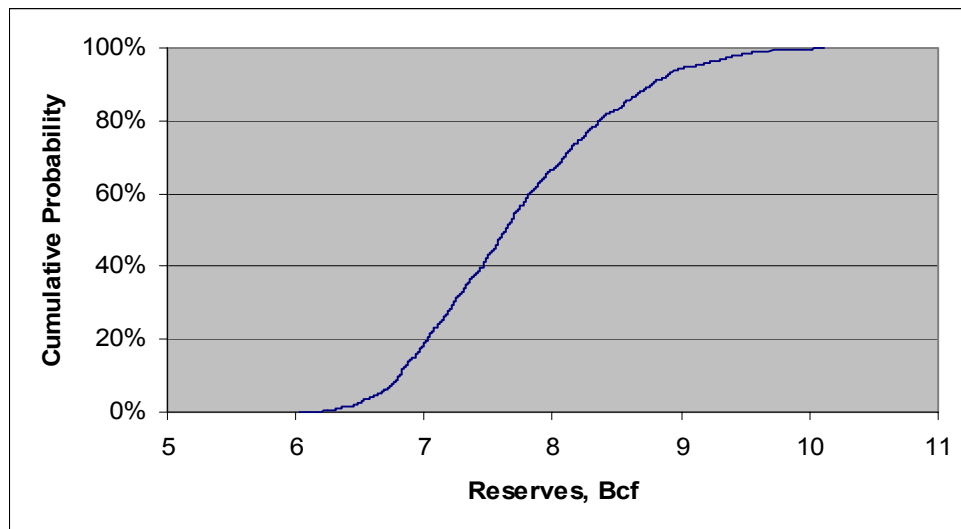


Fig. 4.15—Reserves cumulative distribution function of experimental design method.

4.4.2 Multiple Realization Tree Method

The influential parameters were determined by the same method as the experimental design and response surface method. The influential parameters and their pessimistic, most likely, and optimistic values are listed in Table 4.2. The root of the tree is the reserves; since porosity is the most important parameter, it is located at the second level. Fault transmissibility is the second most important parameter; it is located at the third level. Skin factor is the third most important parameter; thus, it is located at the fourth level. The probabilities for the pessimistic, most likely, and optimistic values of the parameters are determined by integrated reservoir study and listed in Table 4.5.

Table 4.5—Reservoir Parameters and Their Distributions.

	Pessimistic probability	Most likely probability	Optimistic probability
Porosity	25%	50%	25%
Fault Transmissibility	20%	80%	
Skin Factor	25%	50%	25%

The total number of leaves is $3 \times 2 \times 3 = 18$; their probabilities are listed in Table 4.6, which sums to unity. The realization tree is shown in Fig. 4.16.

After the reserves value for every leaf is calculated by a reservoir simulator (Table 4.3), the final reserves CDF is formed (Fig. 4.17).

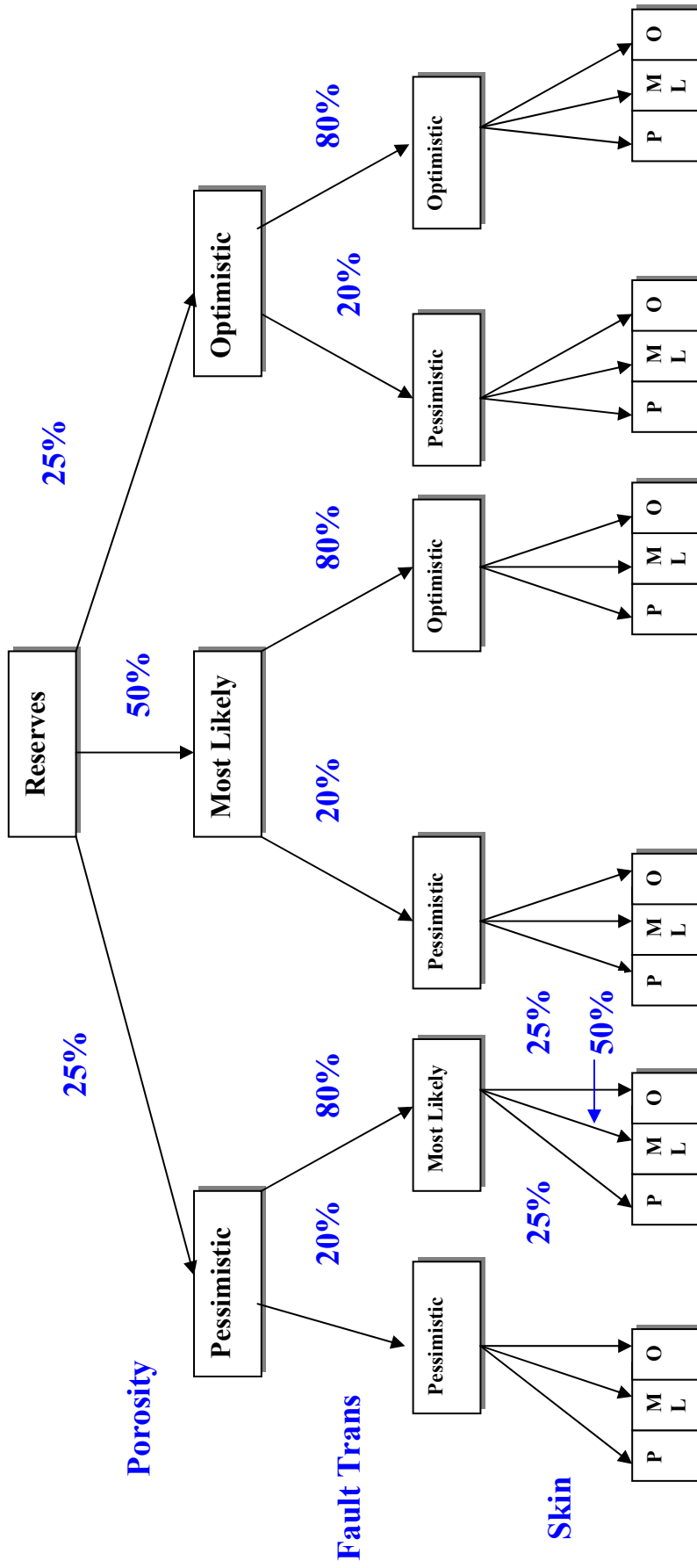


Fig. 4.16—Multiple realization tree.

Table 4.6—Decision Tree Leaf Probabilities.

Porosity	Fault Trans	Skin	Probability
1	0	1	0.05
1	0	0	0.1
1	0	-1	0.05
0	0	1	0.1
0	0	0	0.2
0	0	-1	0.1
-1	0	1	0.05
-1	0	0	0.1
-1	0	-1	0.05
1	-1	1	0.0125
1	-1	0	0.025
1	-1	-1	0.0125
0	-1	1	0.025
0	-1	0	0.05
0	-1	-1	0.025
-1	-1	1	0.0125
-1	-1	0	0.025
-1	-1	-1	0.0125

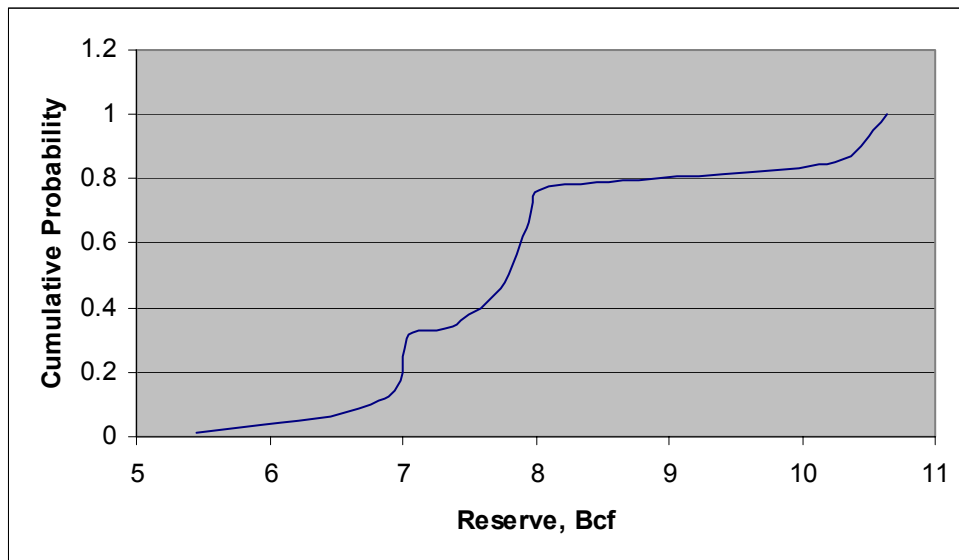


Fig. 4.17—Reserves distribution.

4.4.3 Relative Variation Factor Method

After integrated reservoir study, the pessimistic, most likely, and optimistic values of the most influential parameters were determined.

A net-gas isopach map was used in the study; thus, the gas saturation is 1. The base case hydrocarbon volume was 9.69 Bcf. Porosity and thickness were chosen as the parameters that most affect the hydrocarbon volume of the Pabst field. The possible value ranges for those parameters are listed in Table 4.7. After dividing by the most likely values, we get the triangular distributions for porosity and thickness factors (Table 4.8).

Table 4.7—Parameters That Affect the Hydrocarbon Volume.

Parameter	Pessimist Value	Most Likely Value	Optimist Value
Porosity	0.18	0.204	0.27
Thickness (ft)	30	35	40

Table 4.8—Triangular Distributions for Porosity and Thickness Factor.

Parameter	Pessimist Value	Most Likely Value	Optimist Value
Porosity ($\Delta 1$)	0.88	1	1.32
Thickness ($\Delta 2$)	0.86	1	1.14

The probability density functions of porosity factor and thickness factor are shown in Figs. 4.18 and 4.19. Now the reference hydrocarbon volume and the probability density

functions for all the factors that affect hydrocarbon volume are available. One thousand random numbers are generated and plugged into Eq. 2-3. The distribution of hydrocarbon in place is shown in Fig. 4.20 as a histogram.

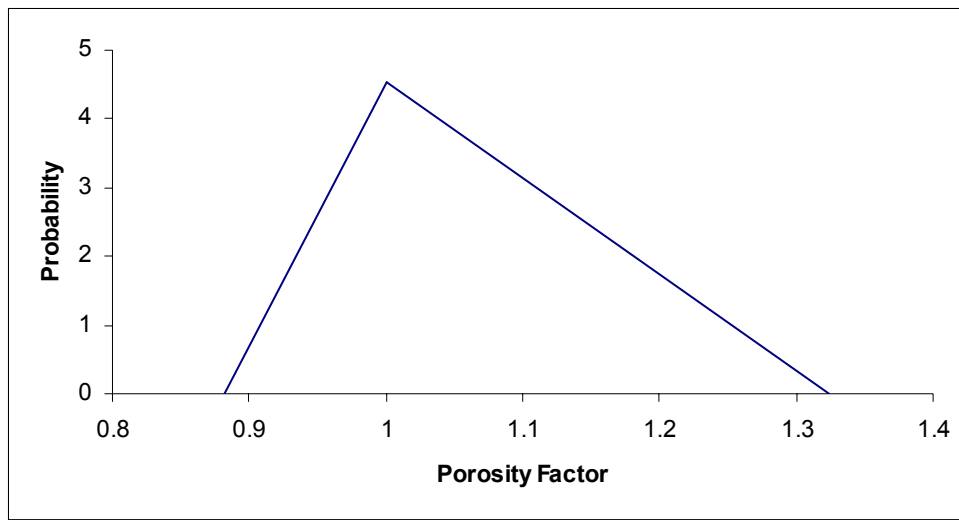


Fig. 4.18—Probability density function of porosity factor.

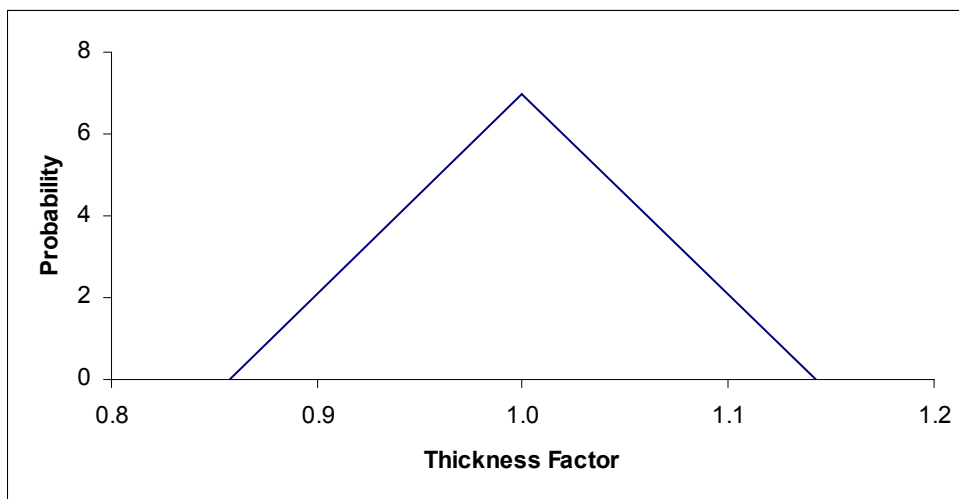


Fig. 4.19—Probability density function of thickness variation factor.

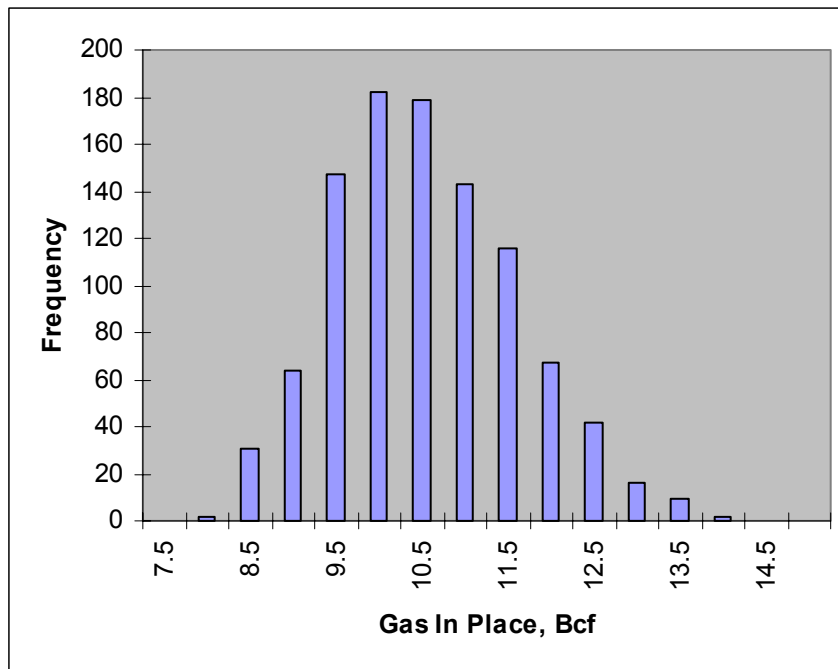


Fig. 4.20—Hydrocarbon volume distribution of relative variation method.

The parameters that affect the recovery factor of the Pabst field include permeability, skin factor, and fault transmissibility. The possible value ranges for those parameters are listed in Table 4.9. After dividing by the most likely values, we obtain triangular distributions for permeability, skin factor and fault transmissibility factors (Table 4.10). The probability density functions of permeability, skin factor, and fault transmissibility factors are shown in Figs. 4.21 4.22, and 4.23.

Table 4.9— Influential Parameters for the Recovery Factor.

Parameter	Pessimist Value	Most Likely Value	Optimist Value
Permeability (md)	30	50	80
Skin Factor	20	5	0
Fault Transmissibility	1	0	N/A

Table 4.10—Triangular Distributions for Permeability, Skin and Fault Transmissibility Factor.

Parameter	Pessimist Value	Most Likely Value	Optimist Value
Permeability ($\Delta 1$)	0.9953	1	1.0047
Skin Factor ($\Delta 2$)	0.9947	1	1.0102
Fault Transmissibility ($\Delta 3$)	0.88	1	

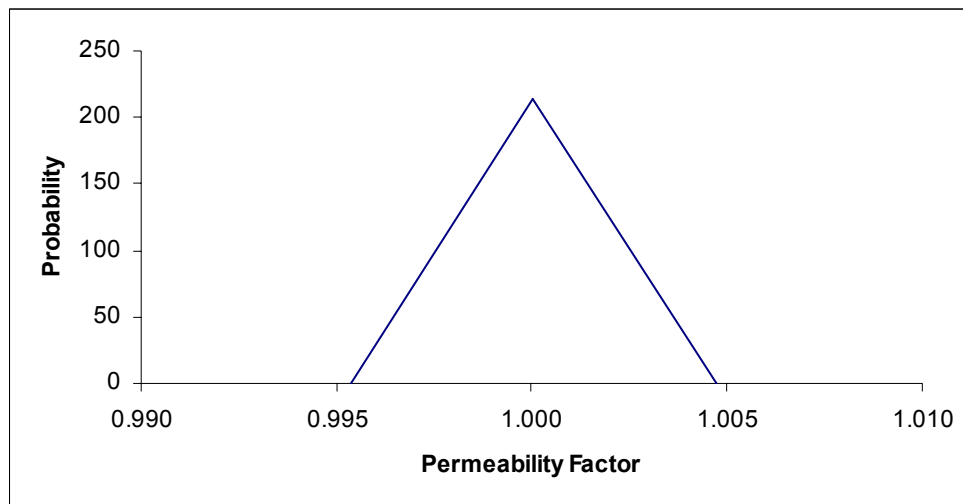


Fig. 4.21—Probability density function of permeability factor.

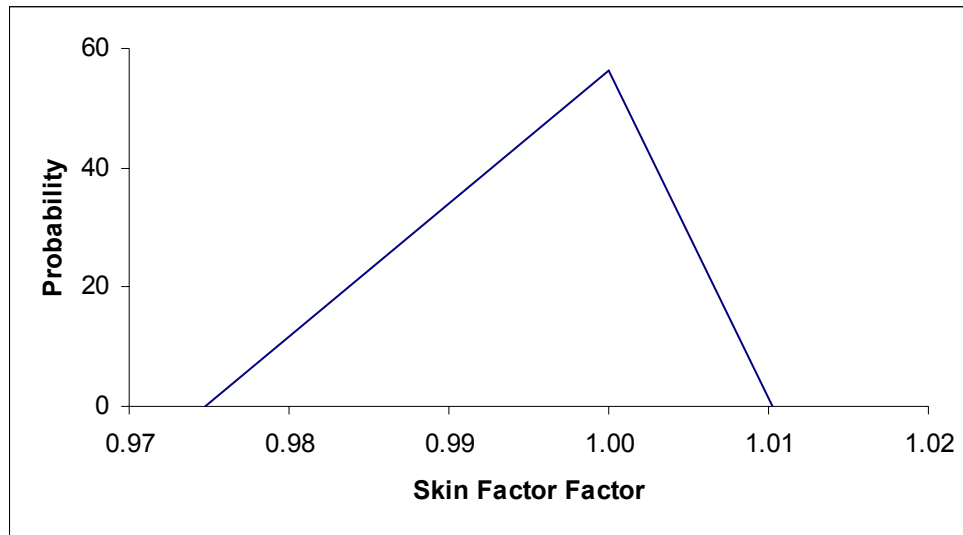


Fig. 4.22—Probability density function of the factor of skin factor.

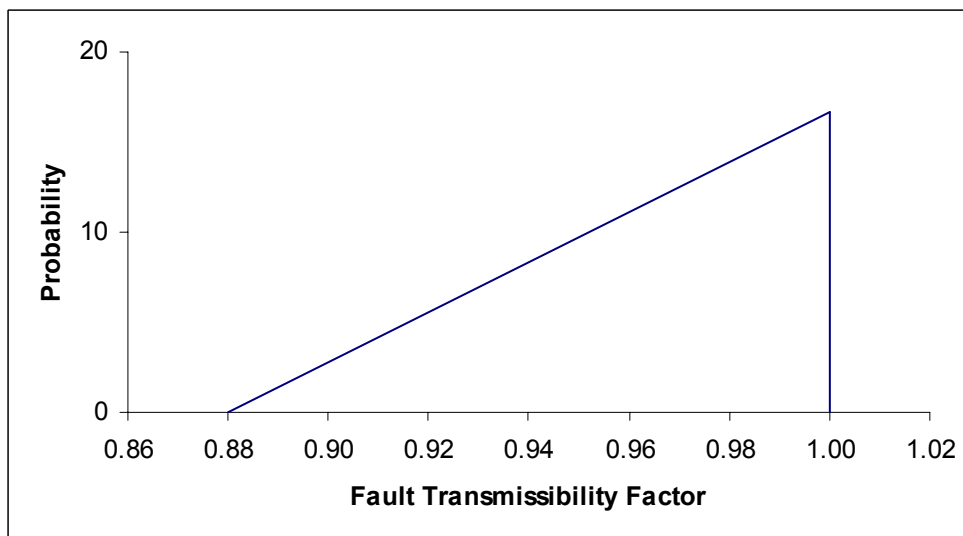


Fig. 4.23—Probability density function of fault transmissibility factor.

Monte Carlo simulation was used to get the recovery factor and final reserves distribution. One thousand random numbers for each factor were generated and plugged into Eq. 2-5 to obtain the recovery factor distribution (Fig. 4.24). Likewise, the final reserves distribution (Fig. 4.25) is obtained from Eq. 2-6, i.e., a set of random numbers for hydrocarbon volume multiplied by a set of random numbers for recovery factor. Fig. 4.26 shows the cumulative distribution function of the reserves.

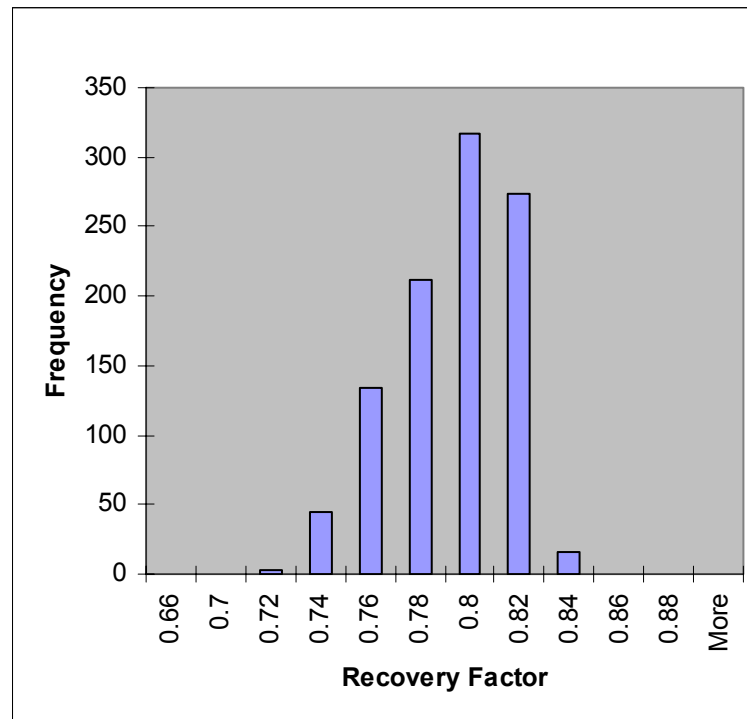


Fig. 4.24—Probability distribution of recovery factor.

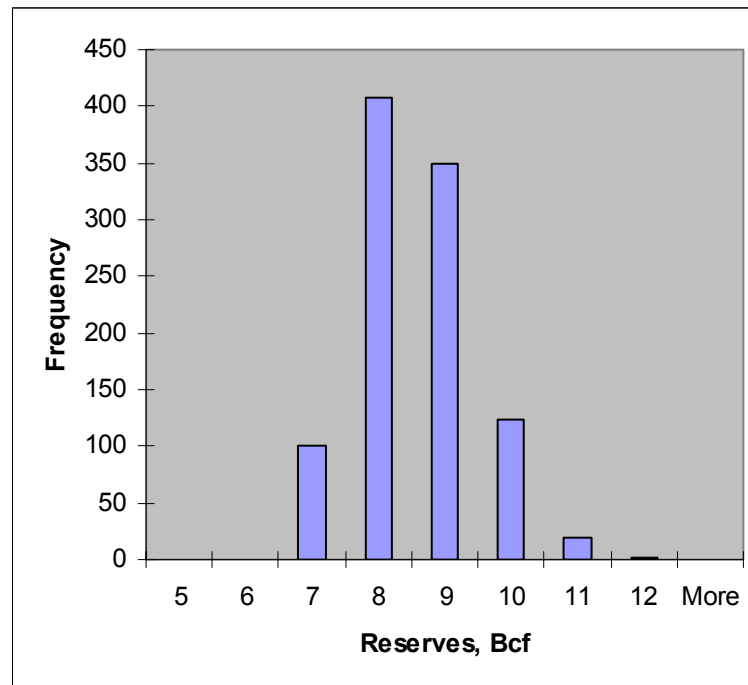


Fig. 4.25—Probability distribution of reserves.

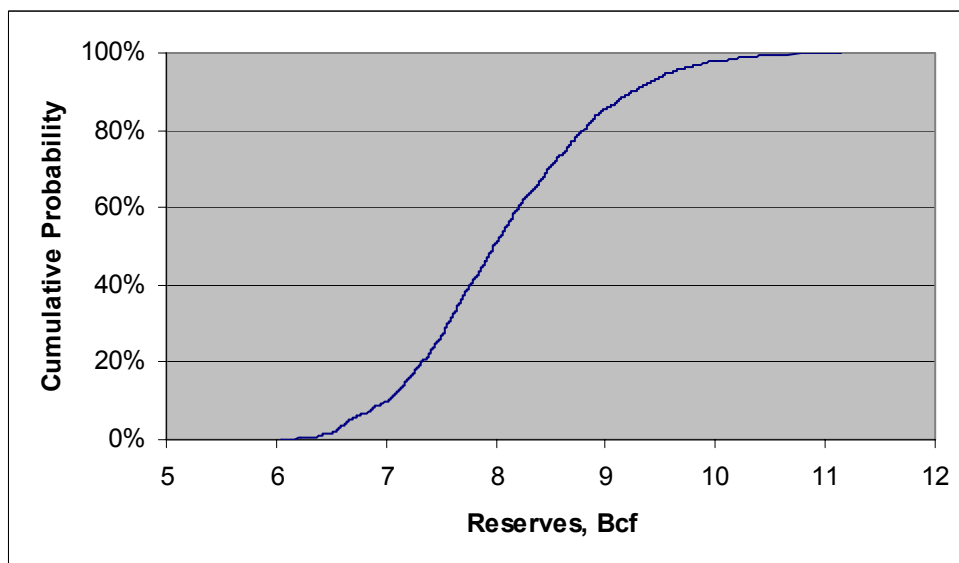


Fig. 4.26—Cumulative distribution function of reserves.

4.4.4 Integrated Mismatch Method

The parameters used in this analysis are fault transmissibility multiplier, porosity, and permeability. For porosity and permeability, we use three levels—the pessimistic, the most likely, and the optimistic values—for the uncertainty analysis; for the fault transmissibility multiplier, we use two levels—the most likely and the pessimistic values—for the uncertainty analysis. Table 4.11 shows the values for the most influential reservoir parameters for this method.

Table 4.11—Reservoir Parameters and Their Distributions.

	Pessimist value	Most likely value	Optimist value
Porosity	0.18	0.204	0.27
Permeability (md)	30	50	80
Fault Transmissibility	1	0	

After the most influential reservoir parameters and their ranges are determined, we use factorial design for these three parameters because the total number of simulation runs is 18. Table 4.12 is the factorial design for the three reservoir parameters.

The reservoir simulation runs are conducted after the experimental design is finished. Then, the mismatch is calculated for different simulation runs. We have only pressure data (no GOR or WCT available), so the mismatch is only from the pressure. The weight for every pressure difference at the time when the observed pressures are

available is set to 1. The mismatch and reserves values for all the reservoir simulation runs are listed in Table 4.12.

Table 4.12—Factorial Design for the Three Reservoir Parameters.

Experiment #	Fault Trans	Porosity	Permeability	Reserves (bcf)	Mismatch
1	0	1	1	10.660	10.41
2	0	1	0	10.634	9.85
3	0	1	-1	10.596	8.87
4	0	0	1	8.069	1.76
5	0	0	0	8.026	1.89
6	0	0	-1	7.983	2.56
7	0	-1	1	7.116	5.14
8	0	-1	0	7.078	5.78
9	0	-1	-1	7.045	6.94
10	-1	1	1	13.010	18.18
11	-1	1	0	12.828	17.78
12	-1	1	-1	12.470	17.08
13	-1	0	1	7.596	10.40
14	-1	0	0	7.437	9.99
15	-1	0	-1	7.167	9.26
16	-1	-1	1	5.597	6.82
17	-1	-1	0	5.456	6.40
18	-1	-1	-1	5.245	5.68

The response surface for the mismatch is built from the selected reservoir parameters with a second-order polynomial (Fig. 4.27). Please see Eq. 4-1 for the mismatch response surface and Table 4.13 for the coefficients. We can see that this response surface is only fair. Likewise, the reserves response surface is regressed with the same set of reservoir parameters (Fig. 4.28). Please see Eq. 4-1 for the reserves response surface and Table 4.14 for the coefficients. We see that the reserves response surface fits the simulation data very well.

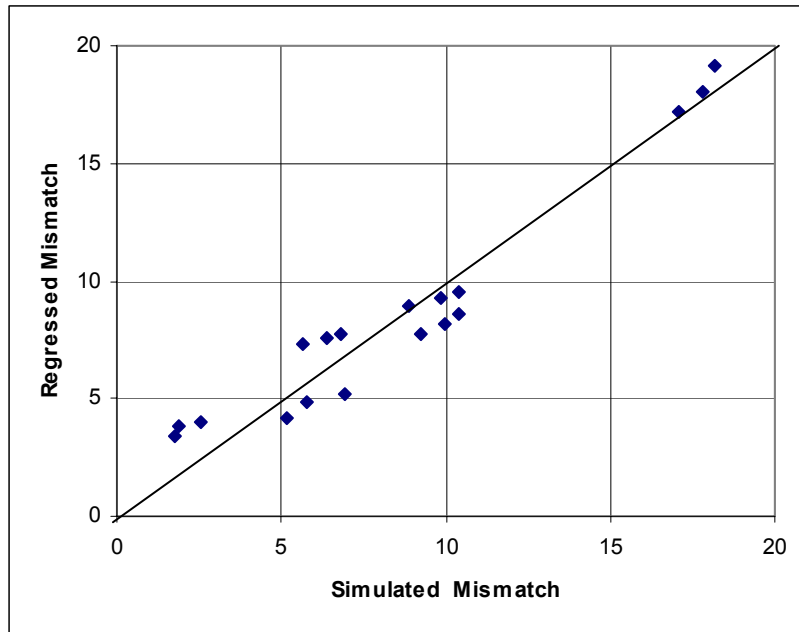


Fig. 4.27—Mismatch response surface.

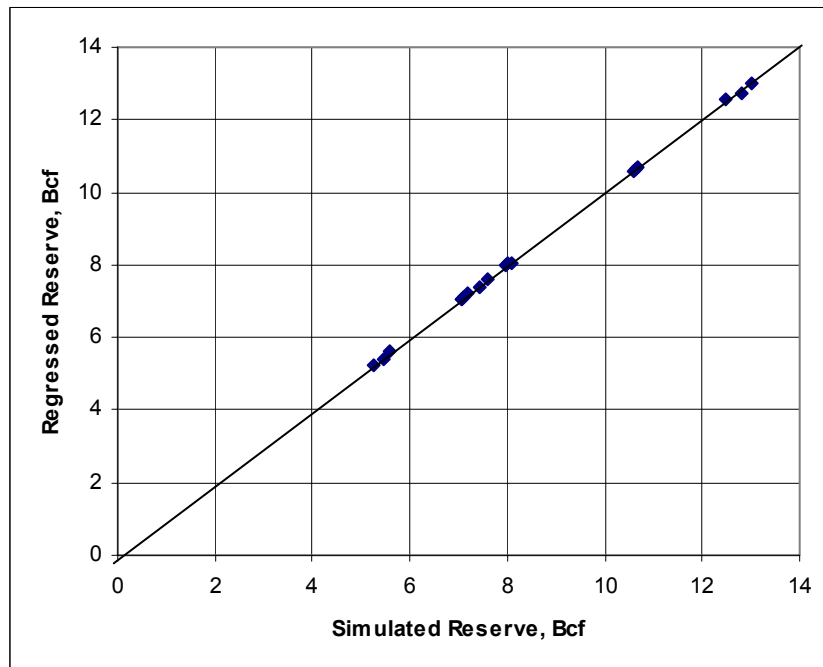


Fig. 4.28—Reserves response surface.

$$R = a_0 + a_1x_1 + a_2x_2 + a_3x_3 + a_4x_4 + a_5x_1^2 + a_6x_2^2 + a_7x_3^2 + a_8x_4^2 + a_9x_1x_2 + a_{10}x_1x_3 + a_{11}x_1x_4 + a_{12}x_2x_3 + a_{13}x_2x_4 + a_{14}x_3x_4 \quad \dots\dots\dots (4-1)$$

Table 4.13—Mismatch Coefficients.

a0	-0.05796	a8	-0.01128
a1	1.026052	a9	0.291103
a2	3.132839	a10	-0.04281
a3	0.139095	a11	0.051684
a4	0.10236	a12	-0.02808
a5	-0.37867	a13	-0.07144
a6	-0.96962	a14	0.006094
a7	-0.0107		

Table 4.14—Reserves Coefficients.

a0	-0.05796	a8	-0.01128
a1	1.026052	a9	0.291103
a2	3.132839	a10	-0.04281
a3	0.139095	a11	0.051684
a4	0.10236	a12	-0.02808
a5	-0.37867	a13	-0.07144
a6	-0.96962	a14	0.006094
a7	-0.0107		

Following the steps of the proposed method, we finally get the reserves cumulative distribution function for the untapped area (Fig. 4.29). This curve is not very smooth, and the biggest changes in reserves occur between 7 and 9 Bcf. The most likely reserves value is 8.026 Bcf. The reason the curve is not smooth is that the quality of the mismatch

response surface is not very good. The reserves contribution of a reservoir model is weighted by its mismatch.

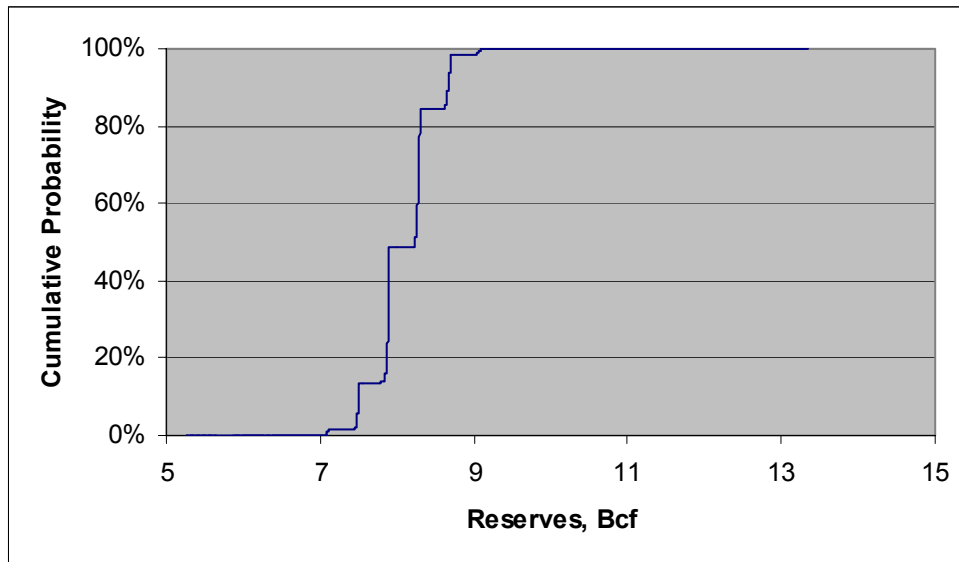


Fig. 4.29—Reserves cumulative distribution function of integrated mismatch method.

4.4.5 Multiple Method Comparisons

The cumulative distribution functions of reserves for the four methods—relative variation factor method, experimental design, multiple realization tree, and integrated mismatch method—are plotted together in Fig. 4.30. Although there are some differences between the four cumulative distribution functions, they are essentially close and centered at the most likely reserves value of 8.03 Bcf. The CDFs of the relative variation factor and experimental design method are smooth while the CDFs of the multiple realization tree and the integrated mismatch methods are not. The greatest change in the CDF for integrated mismatch occurs between 7 and 9 Bcf, which is

narrower than for other methods. Narrower ranges mean more certainty, which is usually what people want to have. The narrow ranges occur because the integrated mismatch method gives more weight to the reservoir models that have small mismatch.

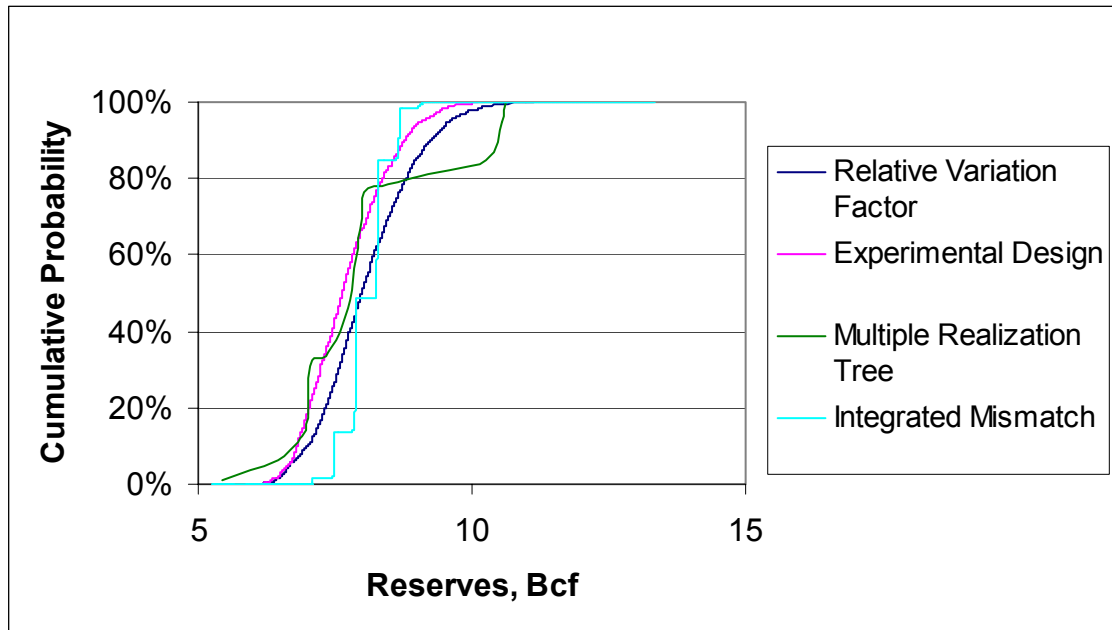


Fig. 4.30—Multiple method reserves comparisons.

4.4.6 Limitations

One important point needs to be made: all the studies were based on one geological model. Since there is also uncertainty in the geological model, failure to incorporate geological uncertainty will result in an overestimation in the certainty of reserves estimates.

Subsequent to these analyses, a new well was drilled in the untapped area. This well was a dry hole. The sand was wet, indicating the assumed geological model was incorrect.

None of the methods suggested the possibility of a dry hole, because geological uncertainty was not considered. This indicates that identification of the most influential parameters is a critical step in uncertainty analysis. Failure to consider all possible sources of uncertainty may lead to results that are quite incorrect and misleading.

CHAPTER V

EXAMPLE APPLICATION 2: PUNQ-S3 PROJECT

We introduced our proposed method—the integrated mismatch method—in Chapter III. In this chapter, we will apply the integrated mismatch method to the PUNQ-S3 problem.³⁷⁻

³⁹ PUNQ is an acronym for **P**roduction forecasting with **U**ncertainty **Q**uantification.

The project involved 10 universities, research institutes, and oil companies. The approaches employed by the project participants are mainly based on Bayesian methods. We will compare our result with others, and illustrate the advantages of ours.

5.1 Introduction

The PUNQ-S3 case is a synthetic reservoir model taken from a reservoir engineering study on a real field operated by Elf Exploration Production.³⁷⁻³⁹ It was characterized as a small-size industrial reservoir engineering model. The reservoir model contains 19×28×5 grid blocks, of which 1,761 blocks are active. This field is bounded to the east and south by a fault, and links to the north and west to a fairly strong aquifer. A small gas cap is located in the center of the dome-shaped structure. The field initially contains six production wells located around the gas oil contact. Due to the strong aquifer, no injection wells are present. The geometry of the field has been modeled using corner-point geometry.³⁹ The porosity/permeability fields were regenerated to have more control over the underlying geological/geostatistical model. A geostatistical model based on Gaussian random fields was used to generate the porosity and permeability fields. Geostatistical parameters, such as means and variograms, were chosen to be as

consistent as possible with the geological model. Through the use of collocated cosimulation, the porosity and permeability fields have been correlated statistically. This has resulted in correlated fields for porosity and horizontal and vertical permeability in each of the five layers.

The reservoir engineering model was completed with the PVT and aquifer data from the original model. There is no capillary pressure in the model. The production scheduling was inspired by the original model; i.e., a first year of extended well testing, followed by a three-year shut-in period, before field production commences. The well-testing year consists of four three-month production periods, each with a different production rate. During field production, two weeks of each year are used to do a shut-in test to collect shut-in pressure data for each well. The wells operate under constant-rate production constraints. After falling below a limiting bottomhole pressure, they will switch to a BHP-constraint. Fig. 5.1³⁹ shows typical production data for a well. Using this reservoir engineering model, a synthetic history was generated using the reservoir simulator ECLIPSE. The total simulation period is 16.5 years. Pressure, water-cut, and gas/oil ratio curves have been generated for each of the wells. Random errors are introduced into the data to reflect the inaccuracy of measurements.

5.2 Research Objectives

Each of the partners in the project was given the synthetic production history of the first 8 years. Note that this history includes 1 year of well testing, 3 years of field shut-in,

and 4 years of actual field production. The synthetic production data consisted of the BHP, WCT, and GOR for each of the six wells. All partners were asked to forecast the total oil production after 16.5 years, including uncertainty estimates. The purpose was to compare various techniques for quantification of uncertainty in future oil production when historical production data are available. Thus, the reservoir needs to be conditioned to both static and dynamic well data when used to quantify the uncertainty in future oil production.

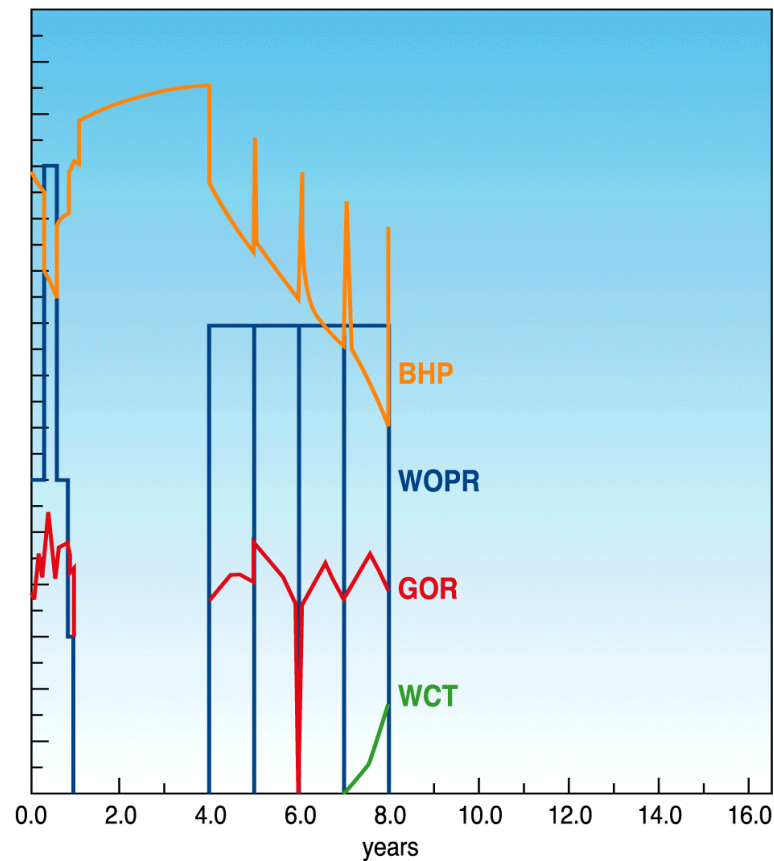


Fig. 5.1—Typical production data for a well.³⁹

5.3 Reservoir Simulation Model

Fig. 5.2 shows the 3D reservoir model for the PUNQ-S3 project (color represents porosity). The reservoir contains six production wells: PRO-1, PRO-4, PRO-5, PRO-11, PRO-12, and PRO-15. Figs. 5.3 through Fig. 5.6 show the production data for Well PRO-1.

PUNQ-S3 3D Reservoir Model

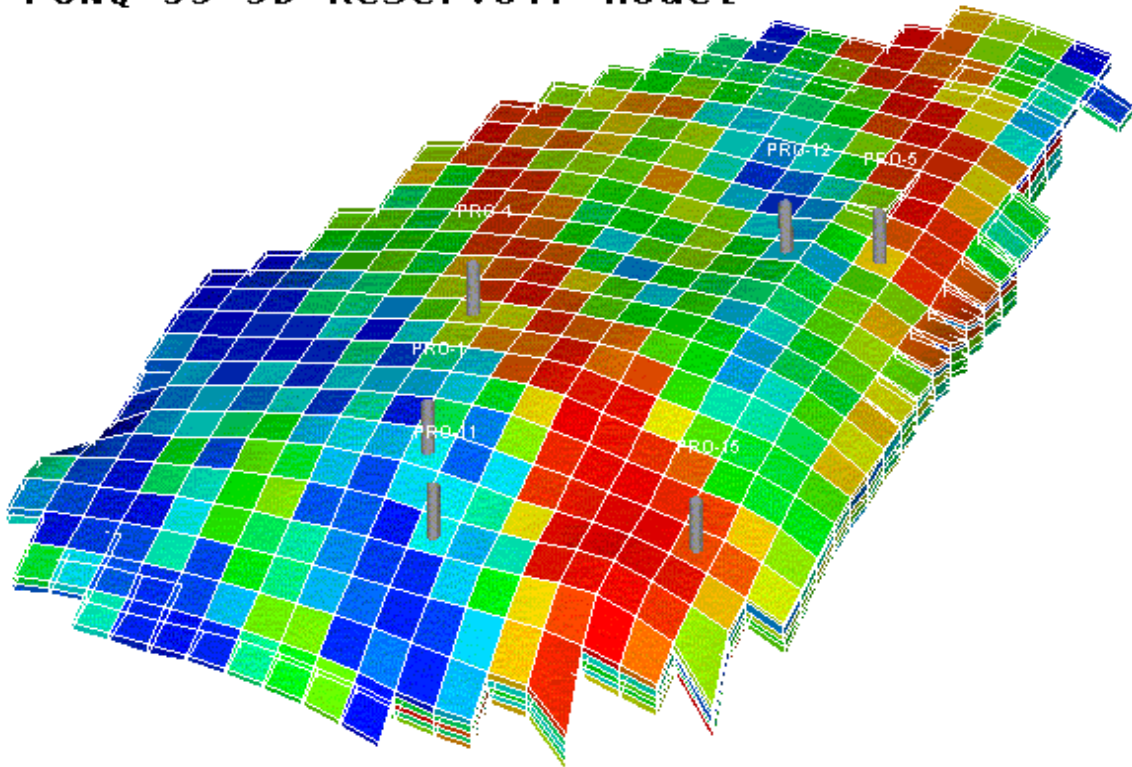


Fig. 5.2—PUNQ-S3 3D reservoir model.

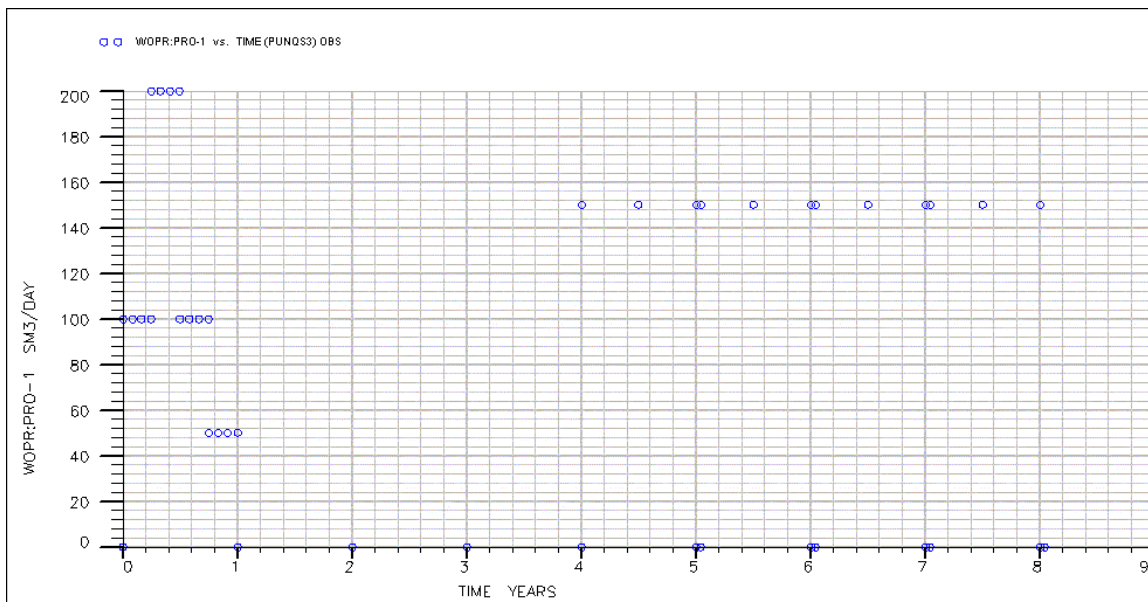


Fig. 5.3—Well PRO-1 oil-production rate.

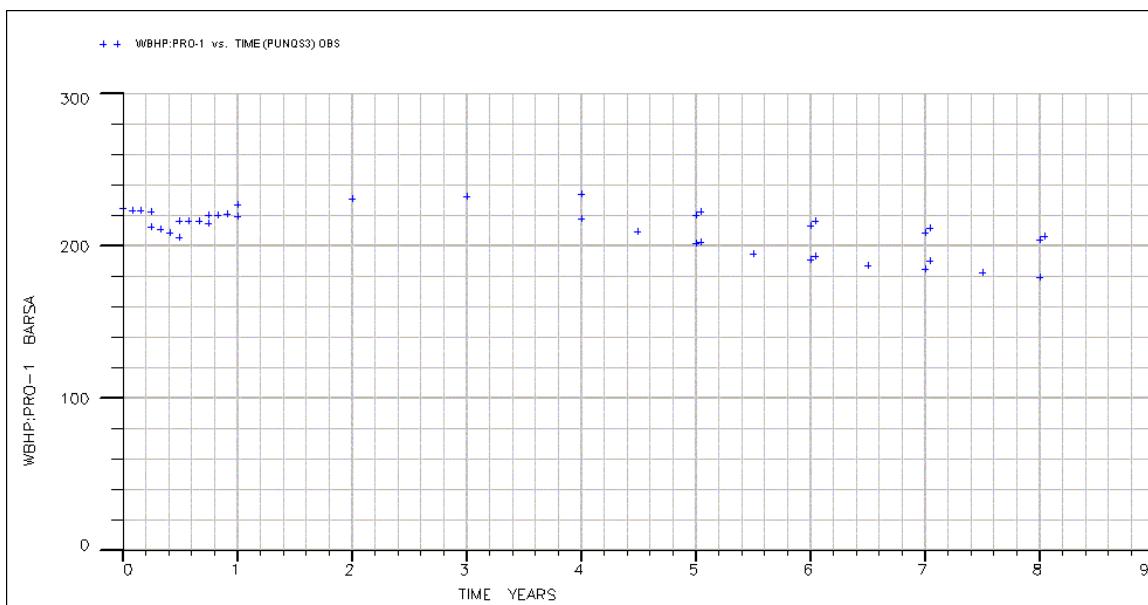


Fig. 5.4—Well PRO-1 bottomhole pressure.

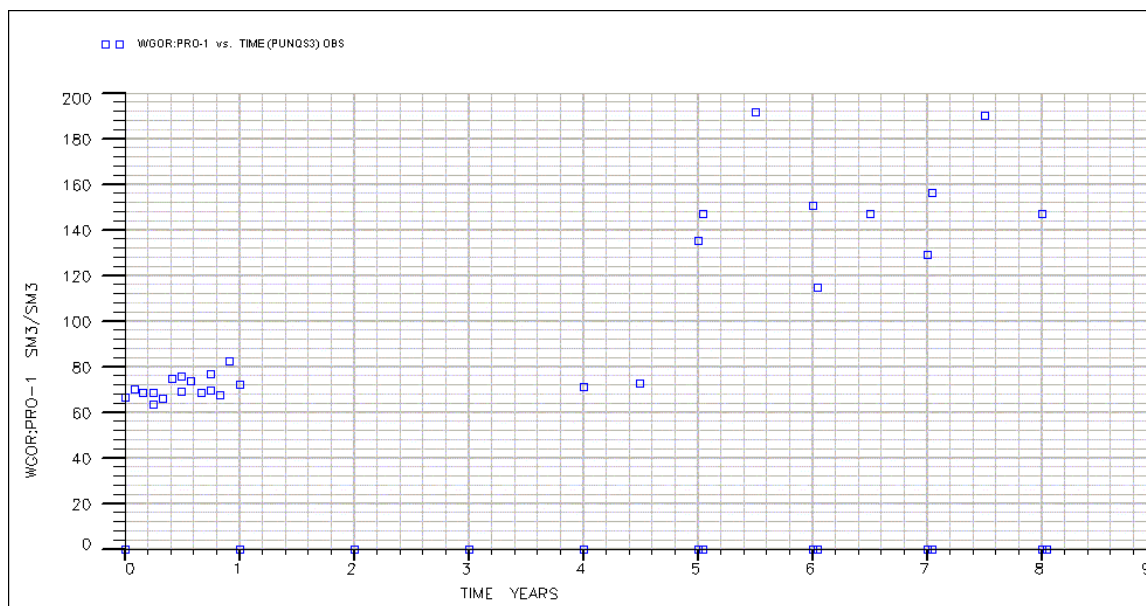


Fig. 5.5—Well PRO-1 gas/oil ratio.

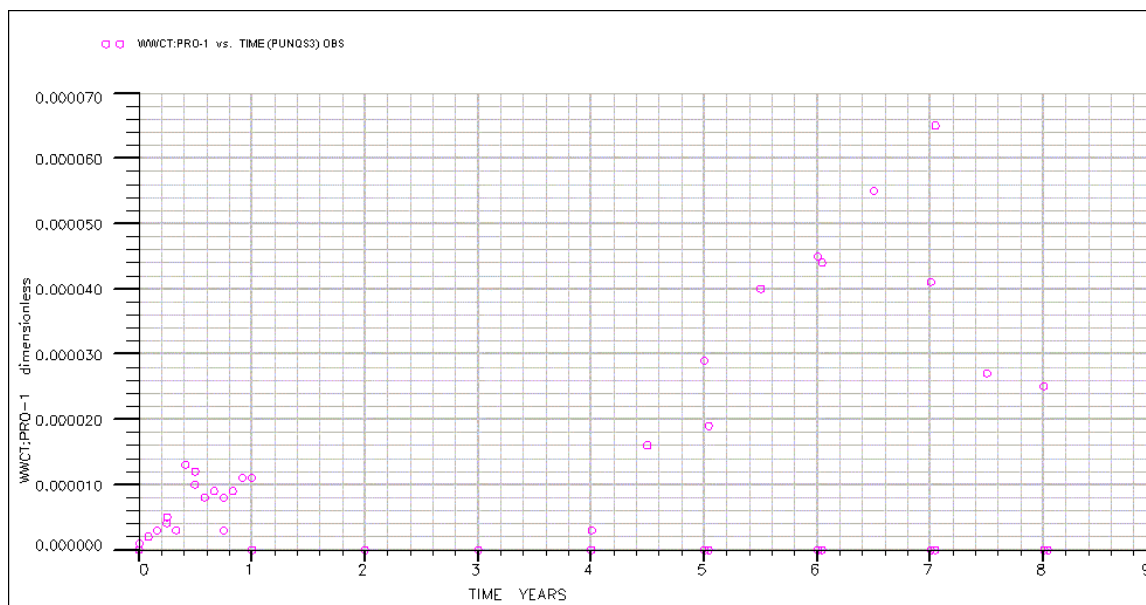


Fig. 5.6—Well PRO-1 water cut.

5.4 Uncertainty Analysis

In this part, we analyze the production forecasts after 16.5 years with our proposed method: the integrated mismatch method. As described in Chapter III, our method starts from a history-matched reservoir model. I used the true reservoir model as the history-matched model in my work. We will show in this section that the integrated mismatch method still gives good results when starting from nonoptimal reservoir models.

The participants of the PUNQ-S3 project were required to analyze the reserves uncertainty. Here, the purpose is to determine how well the proposed method works and how well the results compare with other methods. To start from nonoptimal reservoir models, I changed the porosity and permeability values of the true reservoir model by applying a random multiplier to different layers of the reservoir. In the following section, I apply the proposed method to six cases, each starting from different history-matched models of varying quality.

5.4.1 Integrated Mismatch Method

Case 1. In Case 1, I cut the porosity of the whole reservoir to half of the true value so that the reservoir model was far from the true model. The purpose was to determine if the new method would still cover the true case when starting from a nonoptimal history-matched reservoir model. In practice, the reservoir simulation engineer usually does not know if the history-matched model is close to true or not. The reason is that the result of a history match is not unique. Multiple reservoir models can give the same or

approximate quality of history match even though only one true model exists, and these history-matched models might not include the true one at all. Therefore, starting from a nonoptimal model is common. Fig. 5.7 shows the results of the true model for the bottomhole pressure of well PRO-11. The simulation does not match the observation data exactly because some random noise has been introduced into the data. Fig. 5.8 is the bottomhole pressure of well PRO-11 for the case where the porosity is cut to half of the true case. We can clearly see that the bottomhole pressure match is not good at all.

The cumulative oil production of the whole field is $3.87 \times 10^6 \text{ Sm}^3$ after 16.5 years for the true reservoir model. The cumulative oil production for this starting model is $3.18 \times 10^6 \text{ Sm}^3$, which is about 18% smaller than for the true case. Thus, this starting model significantly underpredicts the true reserves.

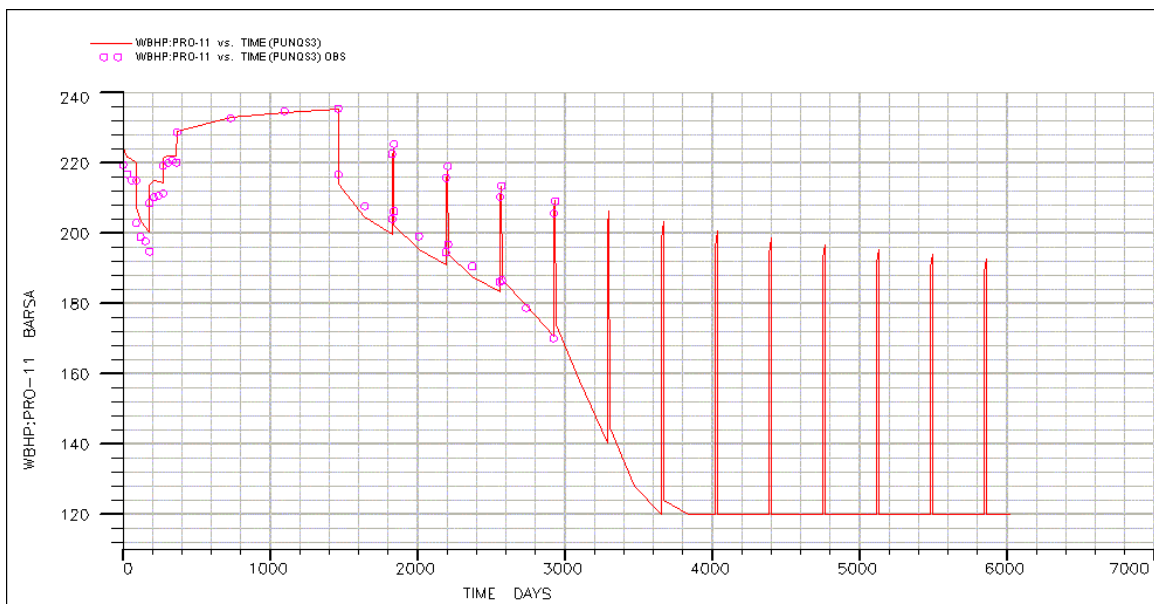


Fig. 5.7—Well PRO-11 bottomhole pressure true case.

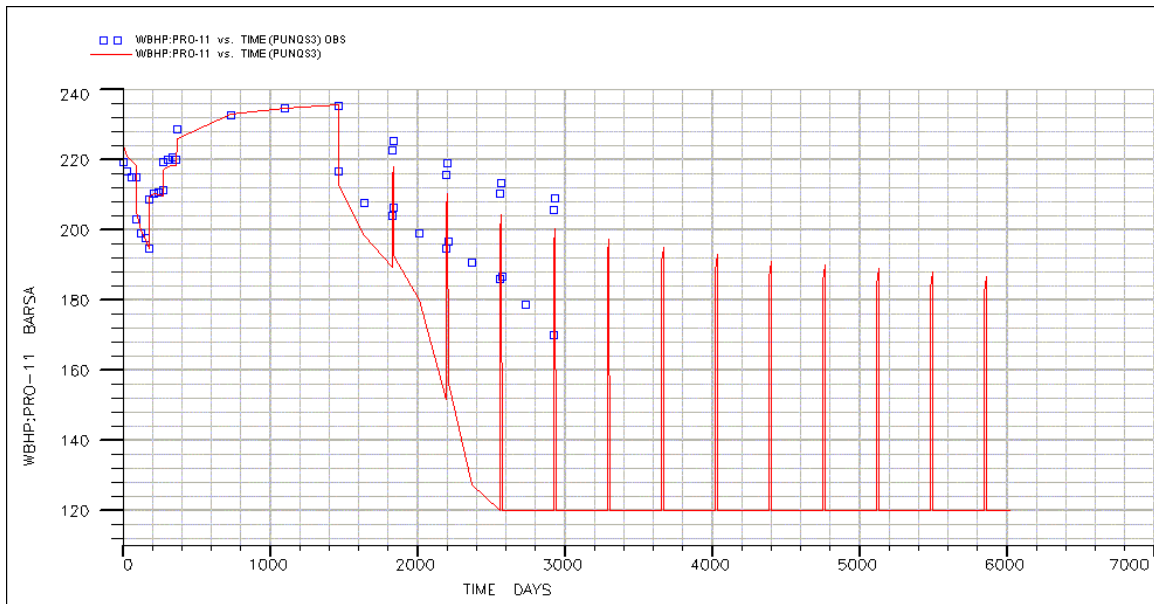


Fig. 5.8—Well PRO-11 bottomhole pressure half-porosity nonoptimal case.

As stated in Chapter III, the second step of the integrated mismatch method is experimental design. From the starting non-optimal model we obtained by changing the true case porosity, we identify the key variables for this reservoir study. Usually the variables include porosity, horizontal permeability, vertical permeability, relative permeability, the location of the faults, fault transmissibility, the locations of the oil/water contact and gas/oil contact, the reservoir boundaries, reservoir compartmentalization, and oil formation volume factor. For the PUNQ-S3 project, all the data including PVT, reservoir structure, boundary, faults, and aquifer, except the porosity and permeability, are given. Thus, the porosity and permeability are the only uncertain variables in this problem. From the geological description, we know that Layers 1, 3-5 have similar reservoir quality, while Layer 2 has poor reservoir quality.

We are interested in the cumulative oil production after 16.5 years for the whole reservoir, given the 8 years' production history. After some sensitivity runs, I decided to use four key variables: (1) porosity of Layers 1, 3-5, (2) porosity of Layer 2, (3) permeability of Layers 1, 3-5, and (4) permeability of Layer 2. I could have used more key variables by dividing the whole reservoir into different regions according to the geological description, and using porosity and permeability for each region. The problem is that using too many key variables requires a large number of simulation runs, and it will be harder to find a good response surface for all the variables and the production forecast. Selecting the right key variables is a very important step in the integrated mismatch method.

With these four key variables, three-level factorial design requires $3^4=81$ simulation runs. Although that is still affordable, we used a composite design, which saves some simulation runs. The composite design is shown in Table 5.1. Note that the table lists the permeability and porosity multipliers for Layers 1, 3-5 and Layer 2. All the simulation runs were conducted with GeoQuest's simulator—Eclipse. The cumulative oil production after 16.5 years and the mismatch for each run were obtained from the simulation results (Table 5.1).

The reserves response surface was built using multiple variable regression (Eq. 5-1). The coefficients are listed in Table 5.2. A very good response surface was found with a quadratic polynomial.

Table 5.1—Four-Factor Experimental Design, Case 1.

Permeability Factor Layers 1, 3-5	Porosity Factor Layers 1, 3-5	Permeability Factor Layer 2	Porosity Factor Layer 2	Reserves (10 ⁶ Sm ³)	Mismatch (dimensionless)
1.5	1.5	1.5	1.5	3.906	2.390
1.5	1.5	1.5	0.5	3.869	2.621
1.5	1.5	0.5	1.5	3.889	2.584
1.5	1.5	0.5	0.5	3.854	2.832
1.5	0.5	1.5	1.5	2.454	26.597
1.5	0.5	1.5	0.5	2.299	28.150
1.5	0.5	0.5	1.5	2.403	27.105
1.5	0.5	0.5	0.5	2.256	28.633
0.5	1.5	1.5	1.5	3.220	5.562
0.5	1.5	1.5	0.5	3.189	5.829
0.5	1.5	0.5	1.5	3.156	5.840
0.5	1.5	0.5	0.5	3.130	6.113
0.5	0.5	1.5	1.5	2.012	25.329
0.5	0.5	1.5	0.5	1.952	26.050
0.5	0.5	0.5	1.5	1.921	26.242
0.5	0.5	0.5	0.5	1.869	27.034
1.5	1	1	1	3.403	11.311
0.5	1	1	1	2.765	11.968
1	1.5	1	1	3.647	2.648
1	0.5	1	1	2.226	27.340
1	1	1.5	1	3.203	11.334
1	1	0.5	1	3.150	11.709
1	1	1	1.5	3.203	11.268
1	1	1	0.5	3.149	11.775
1	1	1	1	3.177	11.505

$$R = a_0 + a_1x_1 + a_2x_2 + a_3x_3 + a_4x_4 + a_5x_1^2 + a_6x_2^2 + a_7x_3^2 + a_8x_4^2 + a_9x_1x_2 + a_{10}x_1x_3 + a_{11}x_1x_4 + a_{12}x_2x_3 + a_{13}x_2x_4 + a_{14}x_3x_4 \dots (5-1)$$

Table 5.2—Reserves Coefficients (Case 1).

a0	-0.05796	a8	-0.01128
a1	1.026052	a9	0.291103
a2	3.132839	a10	-0.04281
a3	0.139095	a11	0.051684
a4	0.10236	a12	-0.02808
a5	-0.37867	a13	-0.07144
a6	-0.96962	a14	0.006094
a7	-0.0107		

Fig. 5.9 is the plot of predicted reserves vs. the simulated reserves. The figure shows that the predicted value with the regressed model and the observed value (from

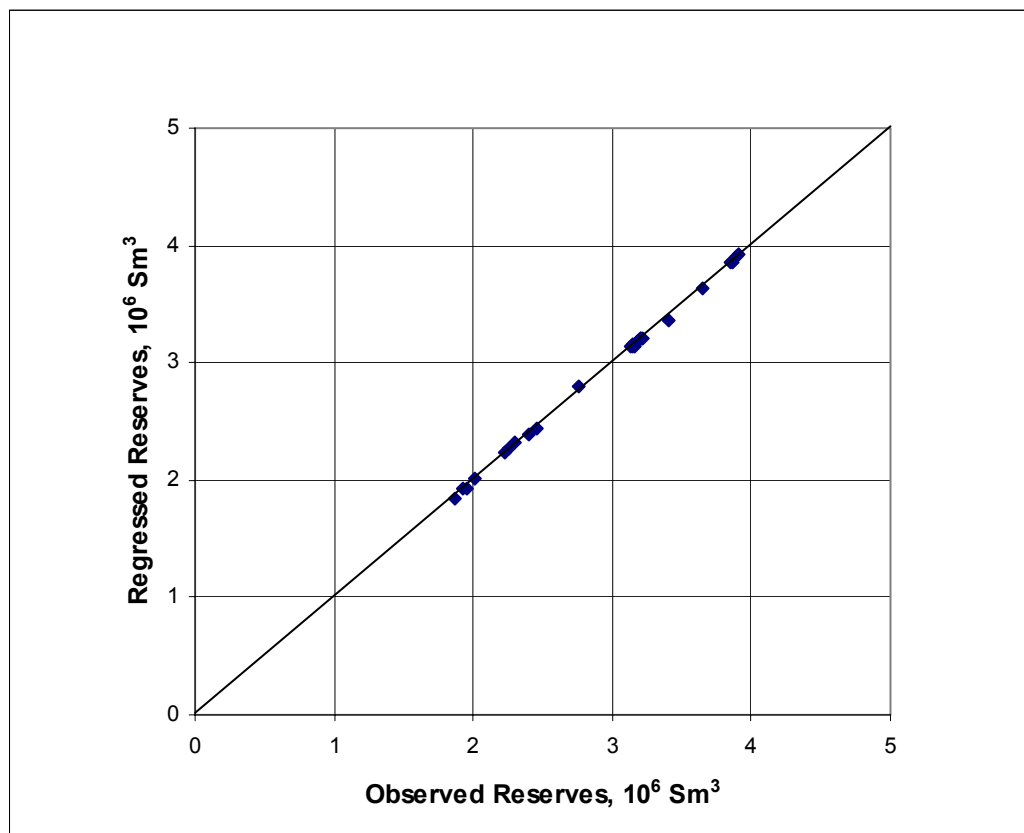


Fig. 5.9—Predicted vs. observed reserves (Case 1).

simulation) almost fall on the 45° line passing through the origin. That means that the model is an excellent one. We have high confidence that the response surface will correctly give the reserves value. The residual of reserves is plotted vs. the predicted reserves in Fig. 5.10. We can see that the residuals are randomly distributed and do not change with the predicted reserves, indicating a good quality response surface.

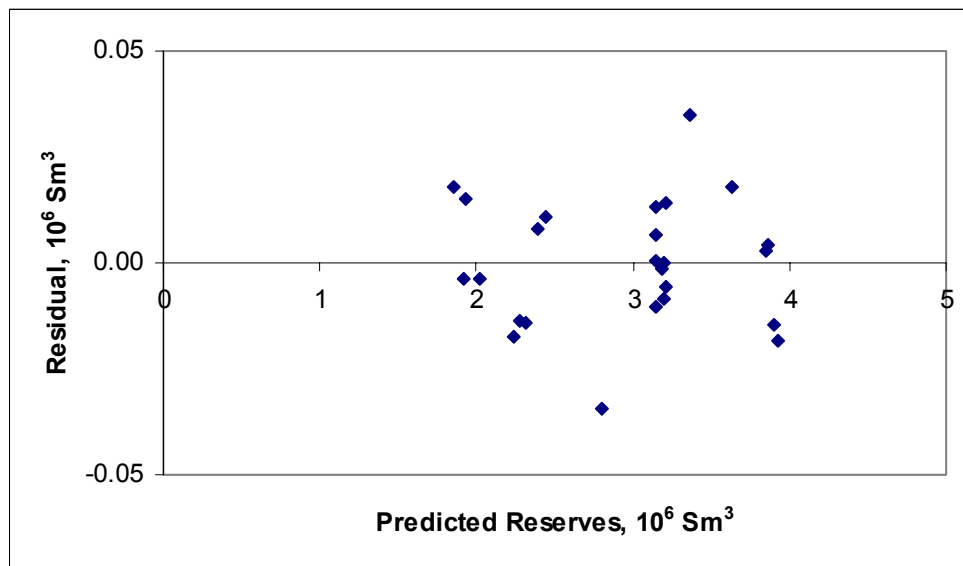


Fig. 5.10—Reserves response surface residual analysis (Case 1).

Likewise, I built the mismatch response surface based on the reservoir simulations from the experimental design. Eq.5-2 gives the mismatch response surface for this study, while Table 5.3 lists the coefficients.

$$M = b_0 + b_1x_1 + b_2x_2 + b_3x_3 + b_4x_4 + b_5x_1^2 + b_6x_2^2 + b_7x_3^2 + b_8x_4^2 + b_9x_1x_2 + b_{10}x_1x_3 + b_{11}x_1x_4 + b_{12}x_2x_3 + b_{13}x_2x_4 + b_{14}x_3x_4 \quad \text{..... (5-2)}$$

Table 5.3—Mismatch Coefficients (Case 1).

b0	49.5228	b8	0.565446
b1	1.867535	b9	-4.68643
b2	-48.5072	b10	0.265155
b3	-2.36072	b11	-0.37702
b4	-2.34382	b12	0.480572
b5	1.035171	b13	0.893924
b6	14.46184	b14	0.016289
b7	0.564411		

The predicted mismatch vs. the regressed mismatch is plotted in Fig. 5.11. Only one point is a bit off the 45° straightline; all the others seem to fall on the line. Thus, this is still a fairly good model.

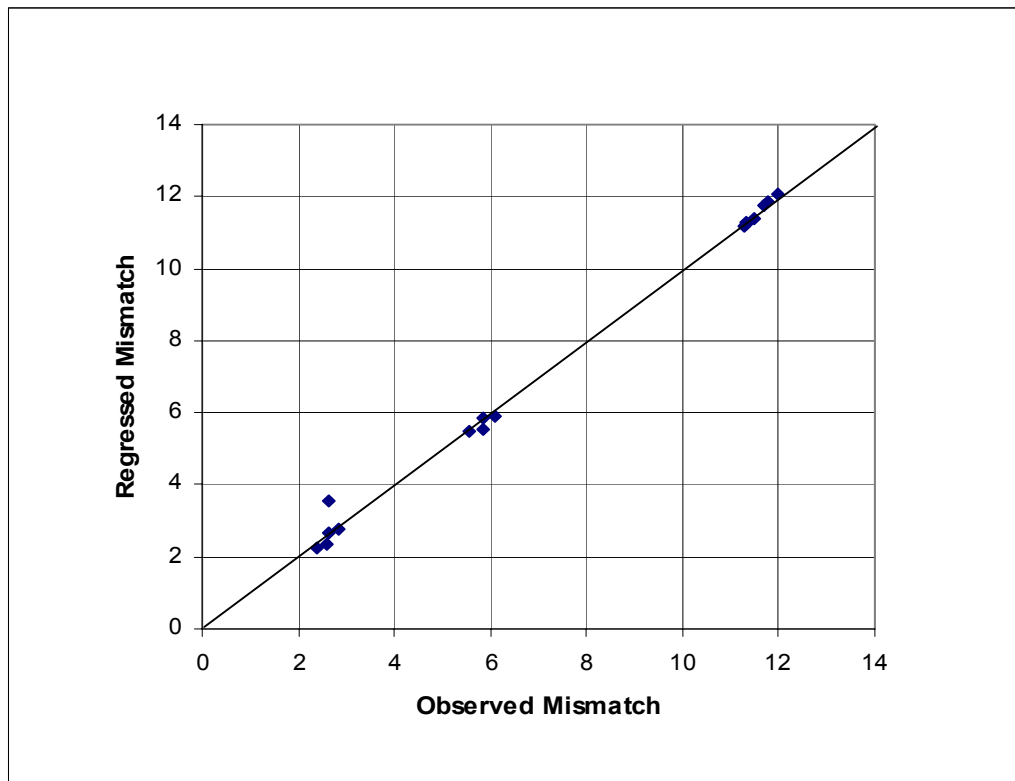


Fig. 5.11—Predicted vs. observed mismatch (Case 1).

The residual plot for mismatch (Fig. 5.12) shows that two residuals are bigger than others. Those two outliers, while of concern, do not severely affect the overall regression quality. If there are quite a few outliers for a regression model, the quality of the regression will be affected. Except for those two outliers, the residuals seem to be randomly distributed.

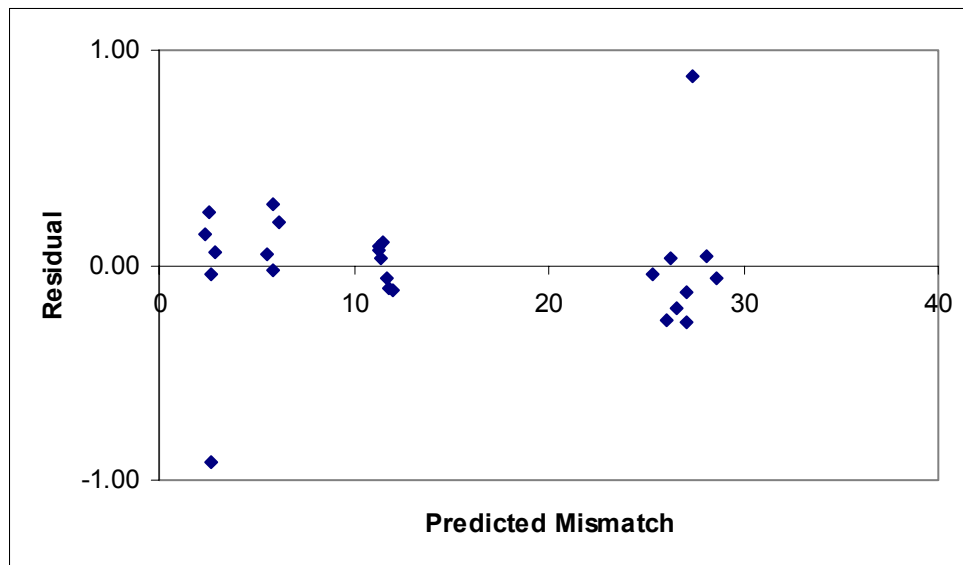


Fig. 5.12—Mismatch response surface residual analysis (Case 1).

With good reserves and mismatch response surface models, the next step is to sample the parameter space and quantify the uncertainty in reserves. As described in Chapter III, we set a step size for each key variable, use multiple loops to sweep all the possible combinations of all the key variables, and calculate the reserves and mismatch. The probability for each run—a combination of a set of key variables—will be assigned by the

weighting function (Eq. 3-2). According to the weighting function, the bigger the mismatch, the smaller the probability. A small difference in the mismatch might lead to a big difference in the probability between runs, because the weighting function (Eq. 3-2) is very sensitive to the mismatch. The step size and the ranges for the key variables are listed in Table 5.4.

Table 5.4—Key Variable Range and Step Size.

Variable Multiplier	Low Value	High Value	Step Size
Permeability Layers 1, 3-5	0.5	1.5	0.1
Porosity Layers 1, 3-5	0.5	1.5	0.1
Permeability Layer 2	0.5	1.5	0.25
Porosity Layer 2	0.5	1.5	0.25

Note that the ranges for the key variables are arbitrary and can be determined by integrated reservoir study. All the available data need to be considered when engineers and geoscientists work together to determine a range for each key variable. As for the step size for each key variable, smaller sizes need to be set for more sensitive key variables. The reason is that a small change in a sensitive variable can cause a big change in the response. Sampling the sample space more completely requires smaller sizes for the more sensitive key variables. In our case, permeability and porosity of Layers 1, 3-5, which have good reservoir quality, are the more sensitive (i.e., changing the variable has a greater effect on the reserves value) key variables in our study, while the permeability and porosity of Layer 2, which has poor reservoir quality, are not very

sensitive key variables. Therefore, the step size of the former key variables is set to 0.1, and the latter is set to 0.25. If the step size of one key variable is cut to half and all the other step sizes stay the same, the calculation will be doubled. Therefore, small step size will incur much more calculation. Fortunately, because we have a statistical model (response surface) to take the place of a reservoir simulator, we can afford an extremely large number of “simulation runs” with our regressed models. In practice, we can test the sensitivity of the step size for each key variable. If decreasing the step size of a key variable will not affect the final reserves distribution, the step size for that level is not very sensitive. Thus we do not need to decrease its step size at that level.

Table 5.5—Regressed Model Runs and Probability Calculation.

Permeability Factor Layer 1, 3-5	Porosity Factor Layer 1, 3-5	Permeability Factor Layer 2	Porosity Factor Layer 2	Mismatch	Reserve s	Normalized Probability
0.5	0.5	0.5	0.5	27.1555	1.85128	2.13E-161
0.5	0.5	0.5	0.75	26.8129	1.87164	2.20E-157
0.5	0.5	0.5	1	26.541	1.89059	3.12E-154
0.5	0.5	0.5	1.25	26.3398	1.90813	6.38E-152
0.5	0.5	0.5	1.5	26.2092	1.92426	1.97E-150
0.5	0.5	0.75	0.5	26.837	1.87461	1.16E-157
0.5	0.5	0.75	0.75	26.4954	1.89535	1.04E-153
0.5	0.5	0.75	1	26.2245	1.91468	1.32E-150
0.5	0.5	0.5	0.5	27.1555	1.85128	2.47E-148
...

Table 5.5 gives a partial list of the final regressed model runs and the probability calculations. In this case, there are 3,025 samples (different combinations) of the key

variables. The probability for each of the runs is normalized so that the sum of all the runs is unity. The reserves of all the samples are ordered from high to low. Each reserves value is associated with a probability value. Then the 90%, 50%, and 10% probabilities of the reserves are recorded, and they are considered as high, median, and low for the final reserves distribution (Fig. 5.23). The resultant reserves values are as follows: 90%= $3.91 \times 10^6 \text{ Sm}^3$, 50%= $3.87 \times 10^6 \text{ Sm}^3$, and 10%= $3.78 \times 10^6 \text{ Sm}^3$. The true case reserves value is $3.87 \times 10^6 \text{ Sm}^3$, which is exactly the same as our median value. In this example, our results range is very narrow, but still correctly covers the true value. The point here is that although the integrated mismatch method starts from a nonoptimal case, it still gives a narrow range for the reserves prediction and it does cover the correct result—the true case.

In this example, the maximum porosity in the experimental design is $1.5 \times 0.5 = 0.75$ of the true case porosity; the true case porosity was not bracketed by the designs. However, the true reserves value was bracketed in the predicted reserves range. The reason is that the greater permeability compensated for the smaller porosity. Fig. 5.13 is the crossplot of the reserves and mismatch for the designed simulation runs. We can clearly see that when the mismatches are smaller, the reserves are closer to the true case. Because the starting model underpredicted the reserves, the model with the greatest porosity and permeability (the first model in Table 5.1, i.e., all the porosities and permeabilities were multiplied by 1.5) gives the greatest reserves and the smallest mismatch. Although that

model's porosity is 0.75 of the true case, its permeability is 1.5 times that of the true case. Thus, the greater permeability compensates the smaller porosity.

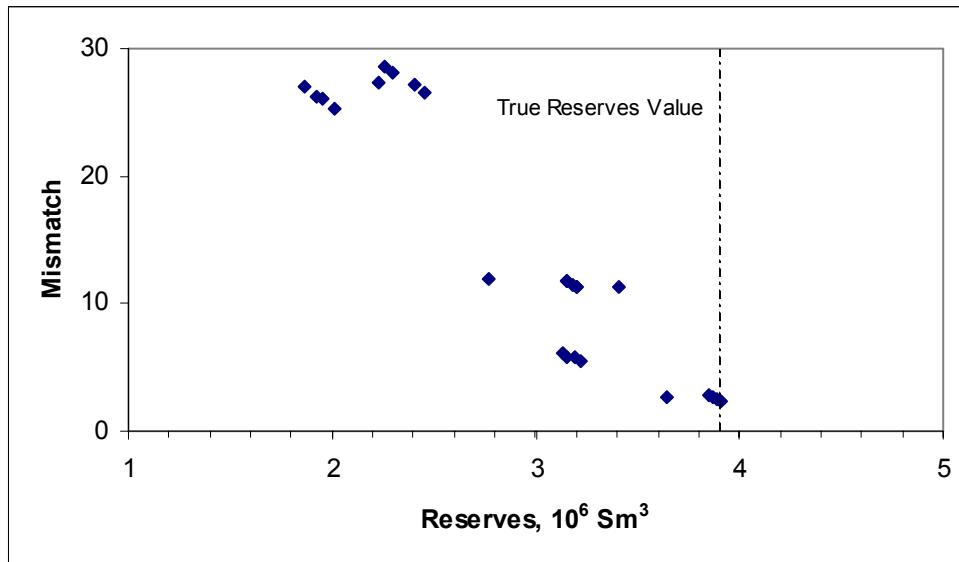


Fig. 5.13—Mismatch-reserves crossplot (Case 1).

Case 2. In Case 1, I multiplied the porosity of the entire true reservoir model by 0.5 to get a nonoptimal model. The result showed that the predicted range of reserves did cover the true case. In this Case 2, I not only changed the porosity but also the permeability of the true reservoir model. I multiplied the porosity and permeability for each of the five layers by 0.7, and then tested to see if the integrated mismatch method still bracketed the true case. By making this transformation from the true case, I got another nonoptimal case to test the proposed method. The cumulative oil production of the whole field is $3.87 \times 10^6 \text{ Sm}^3$ for the true reservoir model. The cumulative oil production for this

starting model is $3.32 \times 10^6 \text{ Sm}^3$, which is smaller than the true case. Thus, this starting model underpredicts the actual reserves as well. I used the same experimental design (Table 5.6) as Case 1.

Table 5.6—Four-Factor Experimental Design, Case 2.

Permeability Layer 1, 3-5	Porosity Layer 1, 3-5	Permeability Layer 2	Porosity Layer 2	Reserves (10^6 Sm^3)	Mismatch (dimensionless)
1.5	1.5	1.5	1.5	3.931	1.028
1.5	1.5	1.5	0.5	3.907	0.924
1.5	1.5	0.5	1.5	3.918	1.015
1.5	1.5	0.5	0.5	3.894	0.903
1.5	0.5	1.5	1.5	2.791	18.937
1.5	0.5	1.5	0.5	2.683	20.060
1.5	0.5	0.5	1.5	2.743	19.238
1.5	0.5	0.5	0.5	2.640	20.363
0.5	1.5	1.5	1.5	3.197	6.820
0.5	1.5	1.5	0.5	3.159	7.059
0.5	1.5	0.5	1.5	3.148	6.937
0.5	1.5	0.5	0.5	3.113	7.189
0.5	0.5	1.5	1.5	2.189	17.081
0.5	0.5	1.5	0.5	2.134	17.908
0.5	0.5	0.5	1.5	2.106	17.806
0.5	0.5	0.5	0.5	2.056	18.600
1.5	1	1	1	3.615	4.032
0.5	1	1	1	2.804	8.334
1	1.5	1	1	3.681	2.065
1	0.5	1	1	2.499	19.659
1	1	1.5	1	3.344	4.648
1	1	0.5	1	3.298	4.908
1	1	1	1.5	3.338	4.543
1	1	1	0.5	3.307	5.013
1	1	1	1	3.322	4.757

After conducting 25 reservoir simulation runs with Eclipse, I modeled the reserves and calculated the mismatches with Eq.3-1. After regressions, the response surfaces for

reserves and mismatch take the same form as Eq. 5-1 and Eq. 5-2, but the regression coefficients have changed, as given in Tables 5.7 and 5.8.

Table 5.7—Reserves Coefficients (Case 2).

a0	0.096272	a8	-0.001
a1	1.440739	a9	0.165556
a2	2.899187	a10	-0.03446
a3	0.120653	a11	0.020464
a4	0.078946	a12	-0.03278
a5	-0.45085	a13	-0.04875
a6	-0.93003	a14	0.003633
a7	-0.00522		

Table 5.8—Mismatch Coefficients (Case 2).

b0	42.46294	b8	-1.13748
b1	-3.78077	b9	-7.83428
b2	-55.0096	b10	0.273095
b3	1.278239	b11	0.01923
b4	0.851253	b12	0.452353
b5	4.481781	b13	0.899032
b6	23.20655	b14	-0.00734
b7	-1.13665		

The predicted reserves (also called the regressed reserves) is plotted vs. the observed values (the values calculated with the reservoir simulator) in Fig. 5.14. We can clearly see that the regression quality is excellent. All the points fall on the 45° line that passes through the origin. This means that the predicted and the observed values are almost the same. The residuals vs. predicted reserves values are plotted in Fig. 5.15. We can see from this plot that the residuals are randomly distributed, indicating a good quality regression.

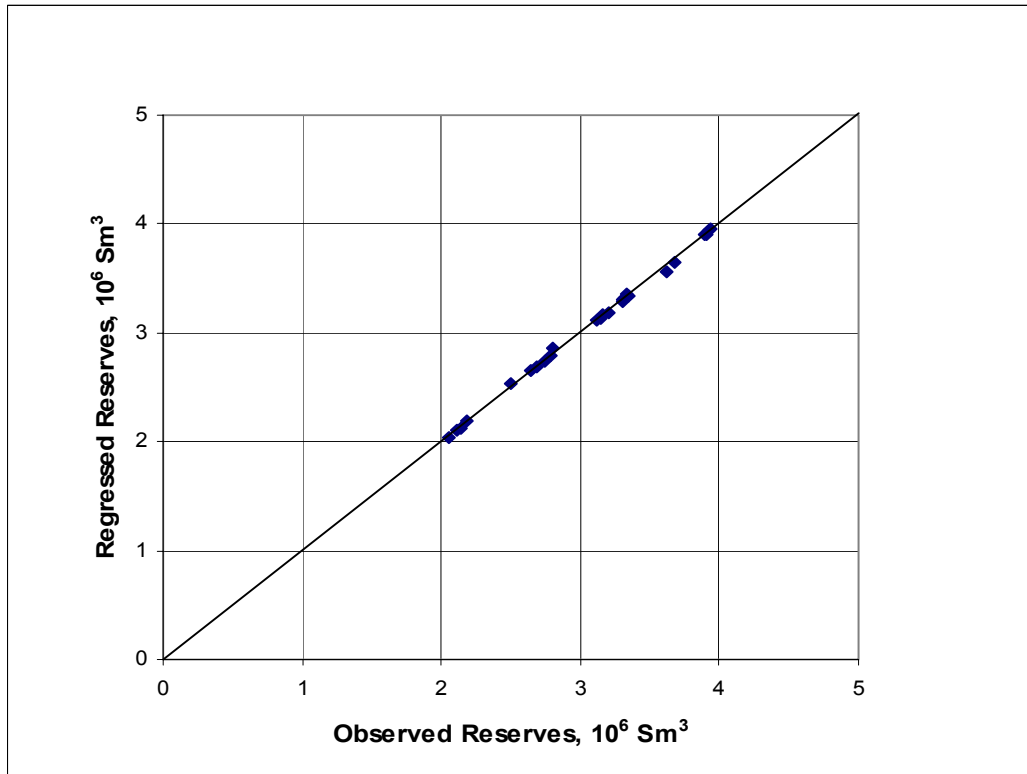


Fig. 5.14—Predicted vs. observed reserves (Case 2).

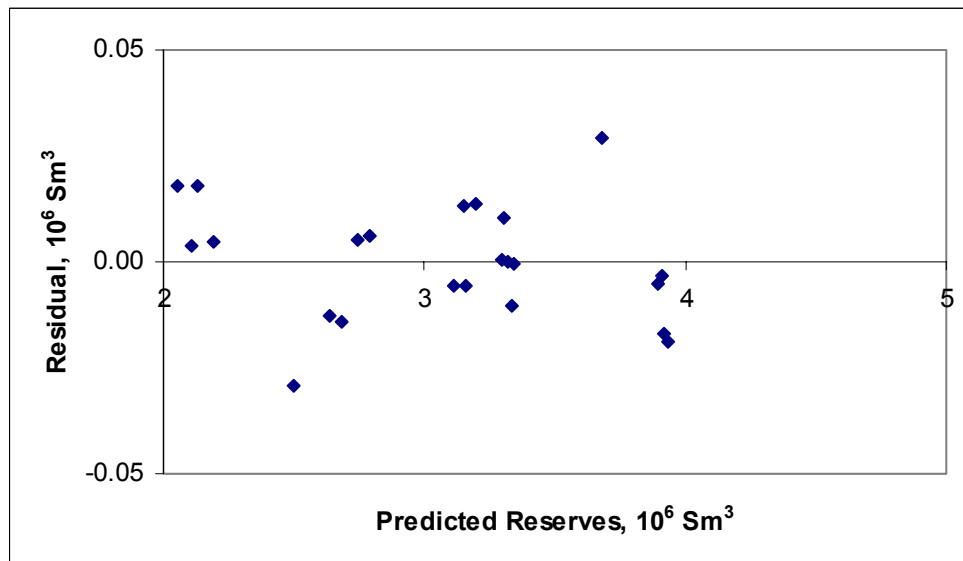


Fig. 5.15—Reserves response surface residual analysis (Case 2).

The predicted mismatch (also called the regressed mismatch) is plotted against observed mismatch (the values calculated from the reservoir simulation runs) in Fig. 5.16. The regression model is not as good; some of the points are off the 45° line that passes through the origin. However, we still regard this model as acceptable.

The residuals are plotted against the predicted mismatch values in Fig. 5.17. We can see from this plot that one point has a large residual; overall, the residuals seem randomly distributed. Thus, we can consider the regression model to be valid.

Following the same procedures as in Case 1, the reserves distribution after 16.5 years is 90%= $3.91 \times 10^6 \text{ Sm}^3$, 50%= $3.82 \times 10^6 \text{ Sm}^3$, and 10%= $3.67 \times 10^6 \text{ Sm}^3$. The true case reserves value is $3.87 \times 10^6 \text{ Sm}^3$, which is included within the 90% to 10% range. The porosity and permeability of the starting model is 0.7 of the true case; $1.5 \times 0.7 = 1.05 > 1$, thus the experimental design brackets the true case. In this example, our results mismatch (Case 2) range is greater than Case 1, but it still covers the true case (Fig. 5.23). This again illustrates that even when the integrated mismatch method starts from a nonoptimal case, it still gives a range for the reserves prediction that covers the correct result – the true case.

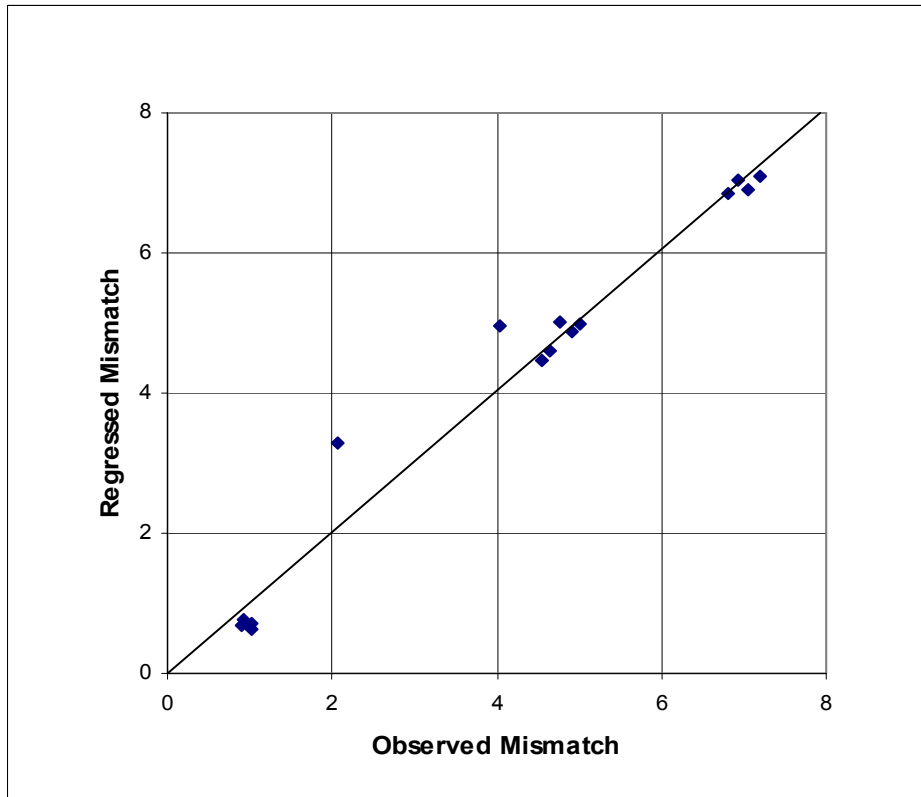


Fig. 5.16—Predicted vs. observed mismatch (Case 2).

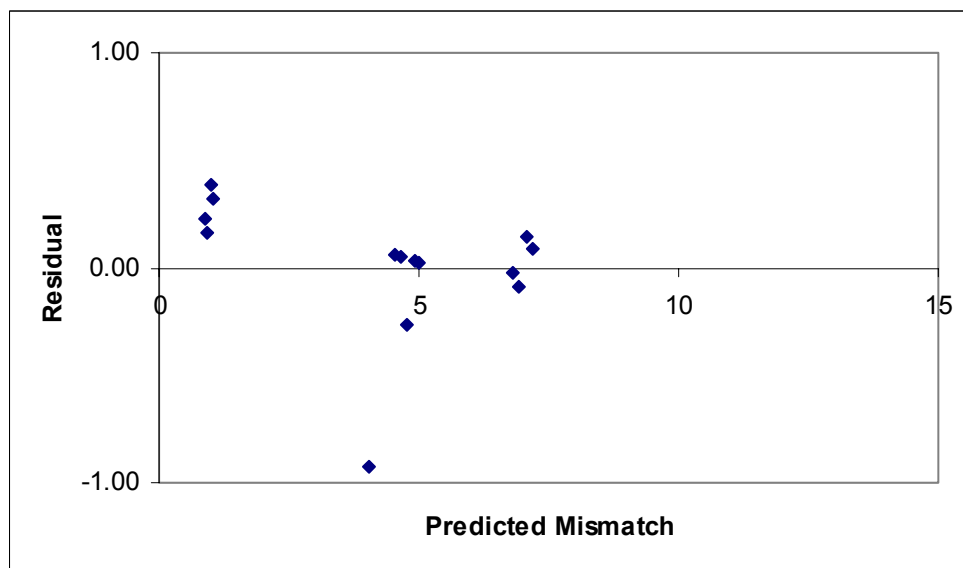


Fig. 5.17—Mismatch response surface residual analysis (Case 2).

Case 3. In Case 1, I multiplied the porosity of the whole reservoir by 0.5 and kept the permeability the same as the true case, and started to quantify reserves uncertainty from that model. The parameters ranged from 0.5 to 1.5 in the experimental design. Because $0.5 \times 1.5 = 0.75 < 1$, the biggest value of porosity in Case 1 was 0.75 of the true case. However, the predicted range of future oil production covers the true reserves value. In Case 2, I multiplied the porosity and permeability for each of the five layers by 0.7. Because $0.7 \times 1.5 = 1.05 > 1$, the parameter ranges also include the true case. Case 3 tests whether the integrated mismatch method will still bracket the true reserves value when both the permeability and porosity ranges in the experimental design do not cover the true case. In this case, I multiplied all the porosities and permeabilities of the five layers by 0.6, and used the same experimental design and the same ranges in the designs (0.5 – 1.5). Because $0.6 \times 1.5 = 0.9 < 1$, none of the possible combinations of porosity and permeability for the reservoir cover the true case. The cumulative oil production for this starting model is $3.05 \times 10^6 \text{ Sm}^3$, which is smaller than the true case ($3.87 \times 10^6 \text{ Sm}^3$). This case appears to be far enough from the true case that the ranges of parameter values in the experiments do not encompass the actual model. The experimental design, the reserves and the mismatch values are listed in Table 5.9.

From Fig. 5.18 and Table 5.9 we can see that when the reserves values are bigger, the mismatch values are smaller. That is because that the starting model underpredicts the reserves, and multiplying a number greater than 1 makes the model closer to the true case. The four experiments with porosity and permeability of Layers 1, 3-5 multiplied by

1.5 give the smallest mismatch values. The biggest reserves value in the table is $3.728 \times 10^6 \text{ Sm}^3$, which is smaller than the true reserves value ($3.87 \times 10^6 \text{ Sm}^3$). The smallest reserves value in the table is $1.794 \times 10^6 \text{ Sm}^3$.

Table 5.9—Four-Factor Experimental Design, Case 3.

Permeability Layer 1, 3-5	Porosity Layer 1, 3-5	Permeability Layer 2	Porosity Layer 2	Reserves (10^6 Sm^3)	Mismatch (dimensionless)
1.5	1.5	1.5	1.5	3.728	1.162
1.5	1.5	1.5	0.5	3.702	1.375
1.5	1.5	0.5	1.5	3.705	1.249
1.5	1.5	0.5	0.5	3.679	1.468
1.5	0.5	1.5	1.5	2.474	22.505
1.5	0.5	1.5	0.5	2.378	23.524
1.5	0.5	0.5	1.5	2.427	22.834
1.5	0.5	0.5	0.5	2.336	23.838
0.5	1.5	1.5	1.5	2.891	8.229
0.5	1.5	1.5	0.5	2.852	8.485
0.5	1.5	0.5	1.5	2.843	8.354
0.5	1.5	0.5	0.5	2.809	8.553
0.5	0.5	1.5	1.5	1.912	19.526
0.5	0.5	1.5	0.5	1.864	20.299
0.5	0.5	0.5	1.5	1.837	20.270
0.5	0.5	0.5	0.5	1.794	21.021
1.5	1	1	1	3.323	7.551
0.5	1	1	1	2.504	9.820
1	1.5	1	1	3.449	3.539
1	0.5	1	1	2.206	22.991
1	1	1.5	1	3.071	7.916
1	1	0.5	1	3.019	8.211
1	1	1	1.5	3.061	7.859
1	1	1	0.5	3.028	8.394
1	1	1	1	3.046	8.089

Following the same procedures as in Cases 1 and 2 resulted in the following for the reserves distribution after 16.5 years: 90%= $3.73 \times 10^6 \text{ Sm}^3$, 50%= $3.68 \times 10^6 \text{ Sm}^3$, and 10%= $3.60 \times 10^6 \text{ Sm}^3$. The true case reserves value is $3.87 \times 10^6 \text{ Sm}^3$, which is not included in the above 90% and 10% range. These results indicate that the predicted reserves distribution will not encompass the true value if the results from the experiments in the design do not bracket the true value. Therefore, when we design the experiments, we need to keep this in mind. The limitations of this method will be covered in a later chapter, and suggestions will be given as well.

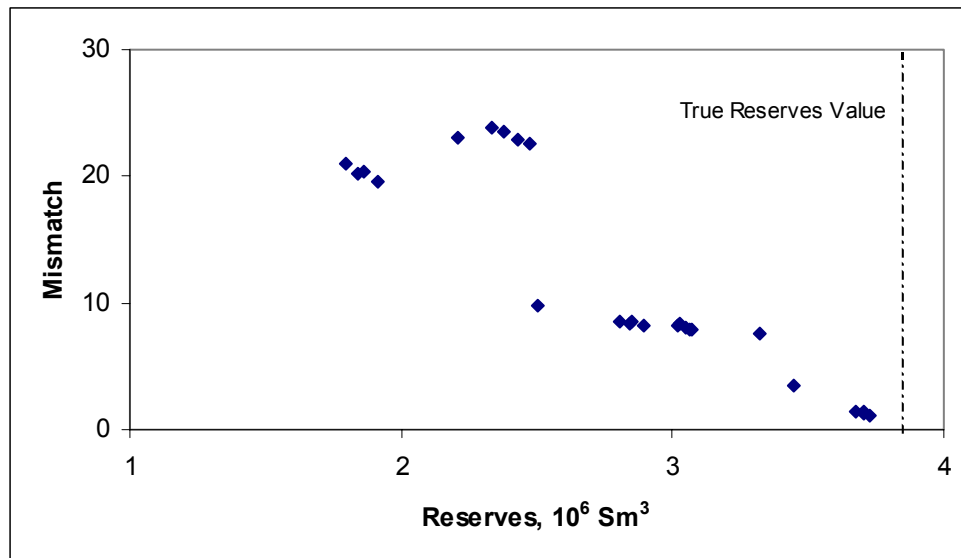


Fig. 5.18—Mismatch-reserves crossplot (Case 3).

Case 4. In Cases 1, 2 and 3, the starting models all underpredicted the reserves value. The application of the integrated mismatch method in Cases 1 and 2 bracketed the true case, but Case 3 did not because neither the permeability nor porosity range in the

experimental design bracketed the true case. Neither of them could compensate each other. As a result, the true case reserves was not bracketed by experiments in the design. In Case 4, I wanted to check whether the integrated mismatch method would still bracket the true case for a starting model that overpredicts the reserves. In this case, I multiplied the porosity and permeability of the five layers by a random number between 0.5 and 1.5 (Table 5.10). This transformation from the true case produced another nonoptimal case to test our proposed method. The cumulative oil production for this starting model is $3.90 \times 10^6 \text{ Sm}^3$, which is slightly greater than the true case. Thus, this starting model overpredicts the true reserves as well.

Table 5.10—Random Permeability and Porosity Multipliers for Case 4.

Multiplier	Layer 1	Layer 2	Layer 3	Layer 4	Layer 5
Porosity	1.06	0.98	0.78	0.86	1.16
Permeability	0.92	1.06	0.96	1.18	0.88

I used the same experimental design (Table 5.11) as all the other cases. After conducting 25 reservoir simulation runs with Eclipse, I recorded the reserves and calculated the mismatches with Eq. 3-1.

After regressions, the response surfaces for reserves and mismatch take the same form as Eq. 5-1 and Eq. 5-2, but the regression coefficients have changed (Table 5.12 and 5.13). The predicted reserves (also called the regressed reserves) are plotted against the observed values (the values calculated with the reservoir simulator) in Fig. 5.19. We can

clearly see that the regression quality is excellent. All the points fall on the 45° line that passes through the origin. That means that the predicted and the observed values are almost the same. The residuals vs. predicted reserves are plotted in Fig. 5.20.

Table 5.11—Four-Factor Experimental Design, Case 4.

Permeability Layer 1, 3-5	Porosity Layer 1, 3-5	Permeability Layer 2	Porosity Layer 2	Reserves (10^6 Sm^3)	Mismatch (dimensionless)
1.5	1.5	1.5	1.5	4.201	2.777
1.5	1.5	1.5	0.5	4.197	2.547
1.5	1.5	0.5	1.5	4.200	2.785
1.5	1.5	0.5	0.5	4.196	2.557
1.5	0.5	1.5	1.5	3.499	8.299
1.5	0.5	1.5	0.5	3.356	9.350
1.5	0.5	0.5	1.5	3.457	8.620
1.5	0.5	0.5	0.5	3.316	9.709
0.5	1.5	1.5	1.5	3.885	3.411
0.5	1.5	1.5	0.5	3.839	3.552
0.5	1.5	0.5	1.5	3.844	3.477
0.5	1.5	0.5	0.5	3.806	3.645
0.5	0.5	1.5	1.5	2.902	9.286
0.5	0.5	1.5	0.5	2.802	10.181
0.5	0.5	0.5	1.5	2.801	9.999
0.5	0.5	0.5	0.5	2.714	10.896
1.5	1	1	1	4.095	1.740
0.5	1	1	1	3.534	4.518
1	1.5	1	1	4.117	1.550
1	0.5	1	1	3.199	9.216
1	1	1.5	1	3.914	0.878
1	1	0.5	1	3.892	0.901
1	1	1	1.5	3.919	0.844
1	1	1	0.5	3.882	0.964
1	1	1	1	3.904	0.884

We can see from Fig. 5.19 that, although there are two points whose absolute values are a little bit higher than other points, the fit is reasonable.

Table 5.12—Reserves Coefficients (Case 4).

a0	0.096272	a8	-0.001
a1	1.440739	a9	0.165556
a2	2.899187	a10	-0.03446
a3	0.120653	a11	0.020464
a4	0.078946	a12	-0.03278
a5	-0.45085	a13	-0.04875
a6	-0.93003	a14	0.003633
a7	-0.00522		

Table 5.13—Mismatch Coefficients (Case 4).

b0	42.46294	b8	-1.13748
b1	-3.78077	b9	-7.83428
b2	-55.0096	b10	0.273095
b3	1.278239	b11	0.01923
b4	0.851253	b12	0.452353
b5	4.481781	b13	0.899032
b6	23.20655	b14	-0.00734
b7	-1.13665		

The predicted mismatch (also called the regressed mismatch) is plotted against the observed values (the values calculated from the reservoir simulation runs) in Fig. 5.21. The regression model is not excellent this time; some of the points are off the 45° line that passes through the origin. The residuals vs. predicted mismatch are plotted in Fig. 5.22. We can see from this plot that, although four points have larger residuals, overall the residuals seem to be randomly distributed. Thus, we consider the regression model to be acceptable.

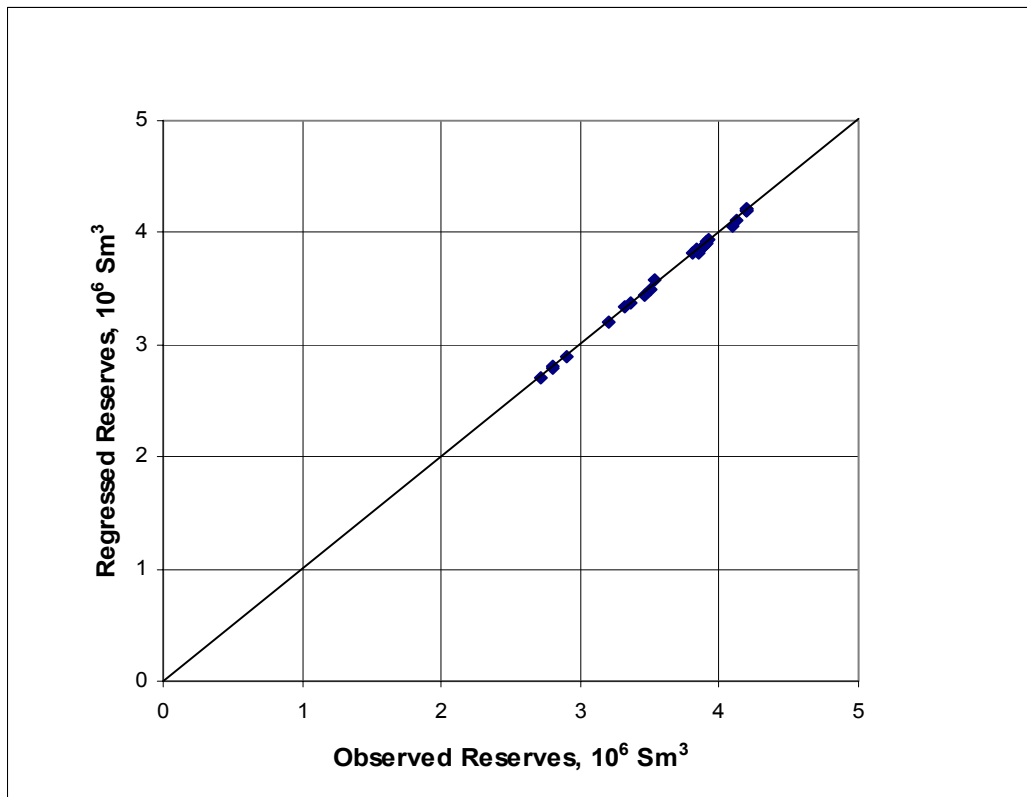


Fig. 5.19—Predicted vs. observed reserves (Case 4).

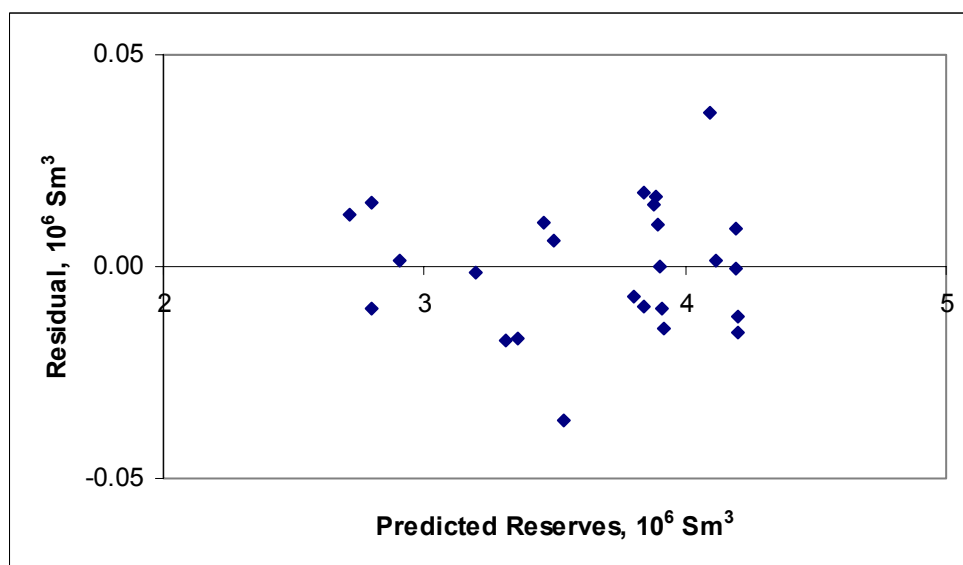


Fig. 5.20—Reserves response surface residual analysis (Case 4).

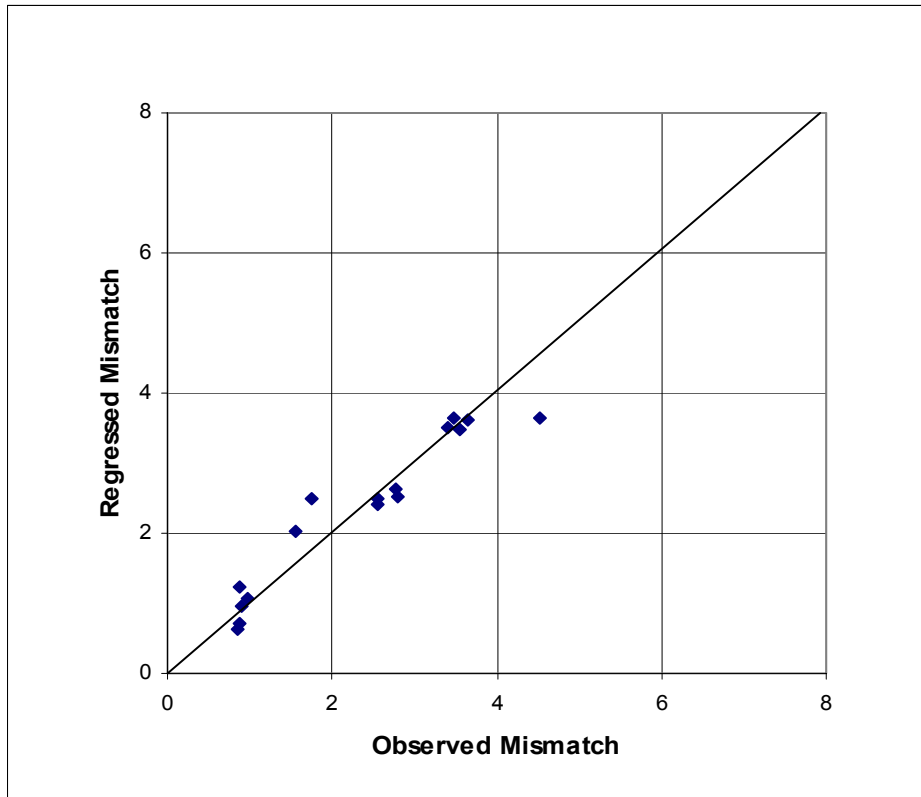


Fig. 5.21—Predicted vs. observed mismatch (Case 4).

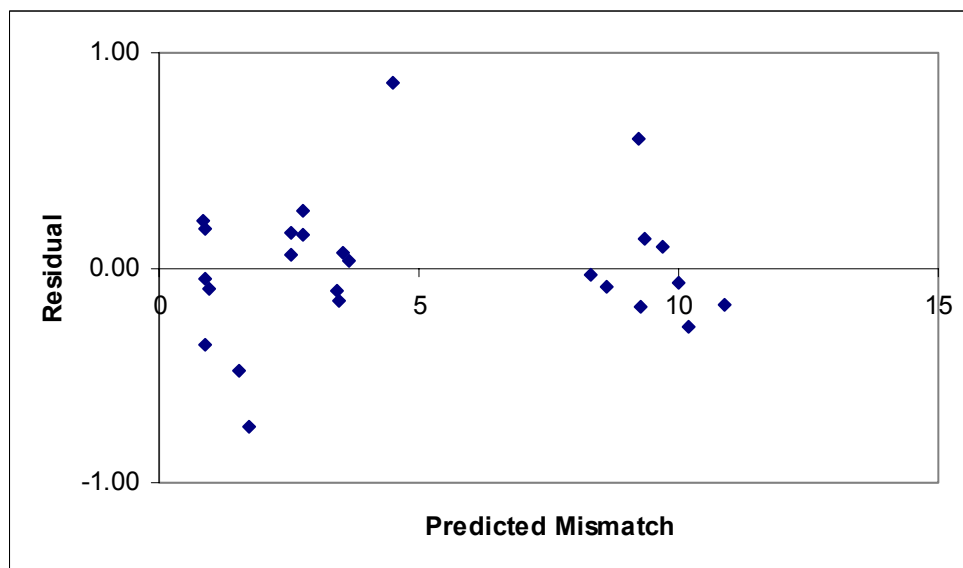


Fig. 5.22—Mismatch response surface residual analysis (Case 4).

Following the same procedure as in other cases produced the following results for the reserves distribution after 16.5 years: 90%= $4.18 \times 10^6 \text{ Sm}^3$, 50%= $4.06 \times 10^6 \text{ Sm}^3$, and 10%= $3.86 \times 10^6 \text{ Sm}^3$. The true case reserves value is $3.87 \times 10^6 \text{ Sm}^3$, which is included within the 90% to 10% range (Fig. 5.23). In this case, our starting model slightly overpredicts the true reserves value, but with the integrated mismatch method it covers the true case. This again illustrates that although the integrated mismatch method starts from a nonoptimal case, it still gives a range for the reserves prediction that brackets the correct result—the true case.

Case 5. In this case, I multiplied the porosity and permeability for each of the layers by 2.1. Because $2.1 \times 0.5 = 1.05 > 1$, the parameter ranges do not bracket the true case for either porosity or permeability. The cumulative oil production for this starting model is $4.20 \times 10^6 \text{ Sm}^3$, which is significantly greater than the true case ($3.87 \times 10^6 \text{ Sm}^3$). The experimental design, the reserves and the mismatch values are listed in Table 5.14.

The table shows that 23 of the 25 reserves values are $4.20 \times 10^6 \text{ Sm}^3$, which is the largest value. This means that the reserves values are not very sensitive to the key variables. Experimental design will not work well in this kind of situation. The minimum reserves value is $3.93 \times 10^6 \text{ Sm}^3$, which is greater than the true reserves ($3.87 \times 10^6 \text{ Sm}^3$). We know that the predicted reserves will be within the range of reserves from the experiments, but that range does not include the true reserves value. Following the same procedure as in

Table 5.14—Four-Factor Experimental Design, Case 5.

Permeability Layer 1, 3-5	Porosity Layer 1, 3-5	Permeability Layer 2	Porosity Layer 2	Reserves (10^6 Sm^3)	Mismatch (dimensionless)
1.5	1.5	1.5	1.5	4.202	5.364
1.5	1.5	1.5	0.5	4.202	5.254
1.5	1.5	0.5	1.5	4.202	5.354
1.5	1.5	0.5	0.5	4.202	5.248
1.5	0.5	1.5	1.5	4.202	3.897
1.5	0.5	1.5	0.5	4.202	3.530
1.5	0.5	0.5	1.5	4.202	3.898
1.5	0.5	0.5	0.5	4.202	3.518
0.5	1.5	1.5	1.5	4.202	3.806
0.5	1.5	1.5	0.5	4.202	3.603
0.5	1.5	0.5	1.5	4.202	3.824
0.5	1.5	0.5	0.5	4.202	3.608
0.5	0.5	1.5	1.5	4.025	1.563
0.5	0.5	1.5	0.5	3.963	1.123
0.5	0.5	0.5	1.5	3.991	1.576
0.5	0.5	0.5	0.5	3.931	1.028
1.5	1	1	1	4.202	4.755
0.5	1	1	1	4.202	2.887
1	1.5	1	1	4.202	4.895
1	0.5	1	1	4.202	3.095
1	1	1.5	1	4.202	4.225
1	1	0.5	1	4.202	4.240
1	1	1	1.5	4.202	4.354
1	1	1	0.5	4.202	4.098
1	1	1	1	4.202	4.233

other cases gave the following results for the reserves distribution after 16.5 years:

90%= $4.12 \times 10^6 \text{ Sm}^3$, 50%= $4.05 \times 10^6 \text{ Sm}^3$, and 10%= $4.00 \times 10^6 \text{ Sm}^3$. The true case

reserves value is $3.87 \times 10^6 \text{ Sm}^3$, which is not included in the 90% to 10% range above.

This case again illustrated that the integrated mismatch method will not work if the true case reserves is not covered by its experiments.

Case 6. In Case 6, I started from the true case without changing any of the parameter values. Following the same procedure as in other cases gave the following results for the reserves distribution after 16.5 years: 90%= $4.17 \times 10^6 \text{ Sm}^3$, 50%= $3.98 \times 10^6 \text{ Sm}^3$, and 10%= $3.74 \times 10^6 \text{ Sm}^3$. As we expected, the true reserves value of $3.87 \times 10^6 \text{ Sm}^3$ is bracketed by the predicted reserves range.

5.4.2 Multiple Method Comparisons

The experimental design and response surface method, the relative variation method, and the multiple realization tree method were applied to several of the cases for comparison. The results are shown in Fig. 5.23.

Starting from the true reservoir model (Case 6), all four methods bracket the true reserves value; the relative variation method gives the largest uncertainty range while the integrated mismatch method gives the smallest range. When starting from a nonoptimal reservoir model (Case 1) that cuts the porosity to half of the true case, only the integrated mismatch method brackets the true case while all the other three methods do not. The reason is that the other methods do not incorporate model mismatch (and thus likelihood) into the reserves uncertainty analysis. For Case 2, again the experimental design and response surface method does not bracket the true case while the integrated mismatch method does.

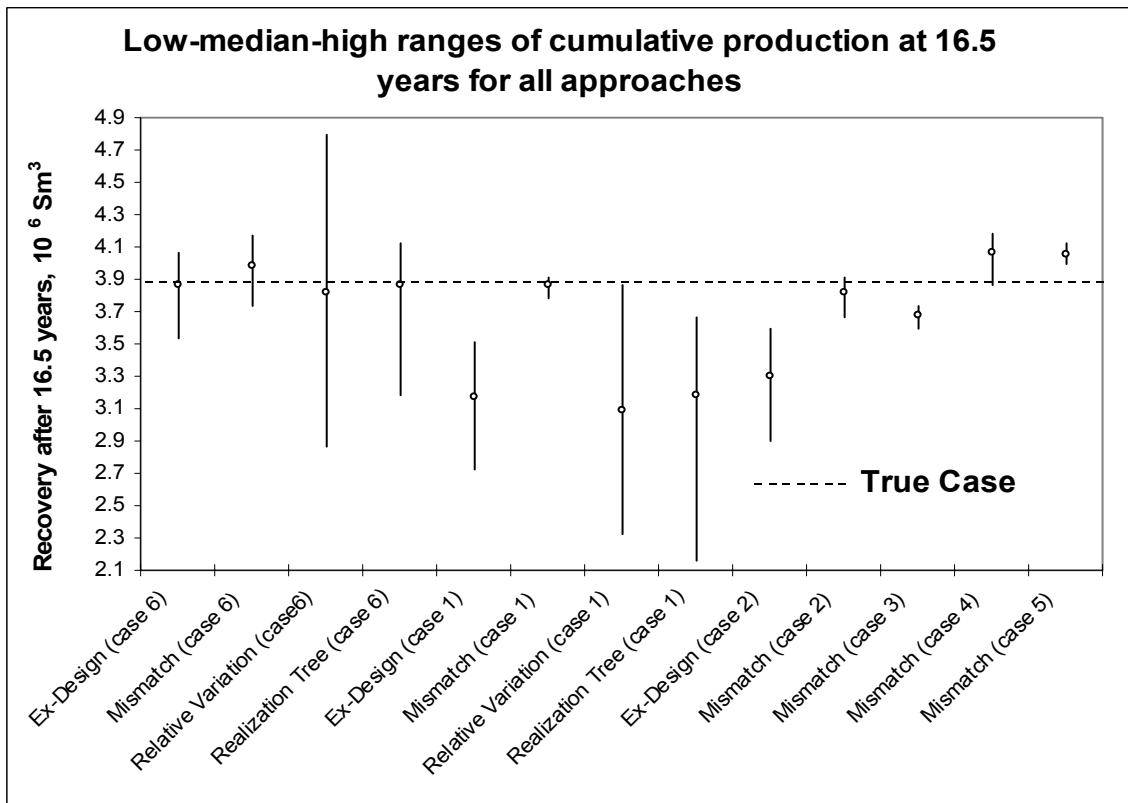


Fig. 5.23—Multiple case comparisons.

Fig. 5.24³⁷ compares our results to results of other methods from various institutions.

Some of the methods bracket the true reserves value, and others do not.

When starting from nonoptimal reservoir models, the integrated mismatch method will bracket the true reserves value if the experimental designs encompass the true case parameters. If the experimental designs do not encompass all the true case parameters, but the true reserves is covered by the experiments, the integrated mismatch method may still bracket the true case. This applies if there is a strong correlation between mismatch

and closeness to the true reserves value. However, a strong correlation is not guaranteed to exist in all reservoir problems.

This method does not need a large number of simulation runs for the uncertainty analysis (25 in this case), while some other methods need hundreds of runs. This is another advantage of the integrated mismatch method.

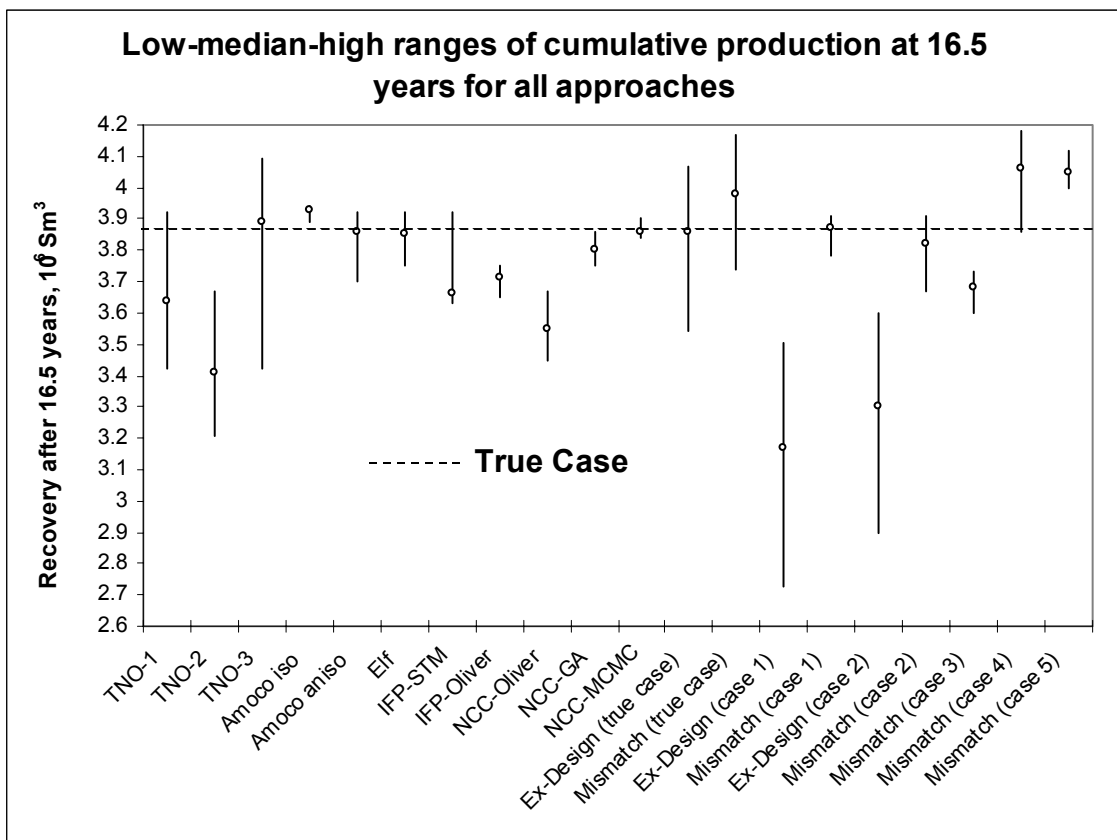


Fig. 5.24—Multiple method comparisons from different participants.

CHAPTER VI

LIMITATIONS AND FUTURE WORK

The integrated mismatch method has the following limitations:

- (1) It depends critically upon the choice of parameters. If key influential parameters are left out, uncertainty may be underestimated significantly, as in the Pabst field. If the user includes too many influential parameters, it will need a large number of reservoir simulation runs that will be time-consuming and expensive. More influential parameters in the model are not necessarily good for the prediction; sometimes more parameters, especially the nonsensitive ones, can deteriorate the prediction. When selecting the parameters, the team should try to select the most influential parameters and not include too many parameters.
- (2) Accuracy of the method is a function of an arbitrary choice of parameter ranges in the experimental design. The integrated reservoir study team decides the ranges of the parameters. If they use narrower ranges, the experiments might not cover the true reservoir model; thus the predicted reserves will not cover the true reserves value. When the team decides the ranges of the parameters, if they are not sure about the range of a parameter, choosing a larger range will be better than a small one.
- (3) Like most methods for estimating uncertainty, it is impossible to verify the accuracy of only one prediction from the integrated mismatch method. It is only by calibrating uncertainty estimates over many trials that we can determine their reliabilities.⁸

On the basis of the above limitations of the integrated mismatch method, we recommend the following be investigated in future work:

- (1) Choice of parameter ranges should be investigated further.
- (2) Future studies should apply the integrated mismatch method to more field examples.
- (3) We also note that the integrated mismatch method appears to yield smaller ranges than for other methods. This may appear to be desirable at first glance. However, it is our impression that the general feeling within the industry is that most uncertainty estimates are too narrow (the certainty is overestimated). Thus, methods that result in smaller uncertainty estimates may not be better even if they are more precise. We expect this has to do more with the choice of parameterization than the method itself. This warrants further investigation along with the other limitations mentioned.
- (4) Calibration of uncertainty estimates should be investigated as a means of improving uncertainty estimation methods.

CHAPTER VII

CONCLUSIONS

On the basis of this research on uncertainty analysis methods, we have reached the following conclusions:

- (1) The integrated mismatch method tends to generate smaller uncertainty ranges than the other methods investigated in this study. When starting from nonoptimal reservoir models, in some cases the integrated mismatch method is able to bracket the true reserves value while methods fail to bracket it.
- (2) The integrated mismatch method incorporates the quality of the history match into the reserves prediction. Although starting from nonoptimal reservoir models that underpredict or overpredict the reserves, as long as the experimental designs encompass the true case parameters, the method predicts ranges that bracket the true reserves value.
- (3) When none of the parameters for the true case is bracketed in the experimental design, the integrated mismatch method does not predict a range that brackets the true reserves value. This would suggest that larger parameter ranges are better than smaller ranges when applying the integrated mismatch method.
- (4) When only some of the parameters for the true case are bracketed in the experimental design, the integrated mismatch method may still be able to bracket the true reserves value. This appears to apply when results of the experiments bracket the true reserves value and there is a correlation between mismatch and closeness to the true reserves value.

- (5) The experimental design and response surface method does not take the quality of the history match into account; thus, it will likely give poor uncertainty quantification when the starting models are not close to the true case.
- (6) The experimental design and response surface method requires input parameter probability distributions, such as triangular distributions, which are subjective. The integrated mismatch method does not have this requirement; parameter probabilities are derived from the mismatch between model results and observed performance data.

NOMENCLATURE

Variables

ϕ	=	porosity
AH	=	reservoir volume.ft ³
S_w	=	water saturation
x	=	random variable
S	=	response surface function
$P(x)$	=	probability density function of x
\bar{x}	=	reservoir parameter vector
ε	=	model error
M	=	mismatch, dimensionless
N_s	=	number of observed production data time series
N_{ij}	=	number of observations in j^{th} time series
w	=	weighting factor, dimensionless
y^{cal}	=	calculated production data
y^{obs}	=	observed production data
σ	=	standard deviation of measure error
c	=	normalization constant
L	=	weighting function
N	=	original hydrocarbon in place, bbl
N_{REF}	=	reference hydrocarbon in place, bbl

Δ	=	relative variation around the reference value ³
RF	=	recovery factor
RF_{REF}	=	reference recovery factor
R	=	reserves, STB.
a	=	low boundary of a triangular distribution
b	=	high boundary of a triangular distribution
p	=	mode of triangular distribution
U	=	standard uniform random number generator
T	=	random variate
x_1	=	permeability multiplier of Layers 1, 3-5
x_2	=	porosity multiplier of Layers 1, 3-5
x_3	=	permeability multiplier of Layer 2
x_4	=	porosity multiplier of Layer 2

REFERENCES

1. Diego, J., Lopez, Y., Ferreira, H. and Carnes, A.C.: “An Integrated Reservoir Study To Improve Field Performance,” paper SPE 39843 presented at the 1998 SPE International Petroleum Conference and Exhibition, Villahermosa, Mexico 3 –5 March.
2. Lopez, D., Munoz, R., Gonzalez, J.E., Gou, Y., Pascual, J.C. *et al.*: “Large Scale Integrated Reservoir Study: The Bachaquero Intercampos Experience,” paper SPE 53996 presented at the 1999 SPE Latin American and Caribbean Petroleum Engineering Conference, Caracas, 21 – 23 April.
3. Sharma, R., Bondarev, A., Sharry, J. Shelepov, V., Greensmith, M. *et al.*: “Integrated Study of Vatyogan Oil Field, West-Siberian Region of Russia,” paper SPE 62900 presented at the 2000 SPE Annual Technical Conference and Exhibition, Dallas, 1 – 4 October.
4. Bouman, L., Koopman, A. and Ibrahim, N.S.: “The Obaiyed Gas Recovery Project – A Fully Integrated Study,” paper SPE 68182 presented at the 2001 SPE Middle East Oil Show, Bahrain, 17 – 20 March.
5. Cosentino, L., Coury, Y., Daniel, J.M., Manceau, E., Ravenne, C. *et al.*: “Integrated Study of a Fractured Middle East Reservoir With Stratiform Super-K Intervals – Part 2: Upscaling and Dual Media Simulation,” paper SPE 68184 presented at the 2001 SPE Middle East Oil Show, Bahrain, 17 – 20 March.
6. Caldwell, R.H. and Heather, D.I.: “Characterizing Uncertainty in Oil and Gas Evaluations,” paper SPE 68592 presented at the 2001 SPE Hydrocarbon Economics and Evaluation Symposium, Dallas, 2 – 3 April.
7. Salomao, M.C. and Grell, A.P.: “Uncertainty in Production Profiles on the Basis of Geostatistic Characterization and Flow Simulation,” paper SPE 69477 presented at the 2001 SPE Latin American and Caribbean Petroleum Engineering Conference, Buenos Aires, Argentina, 25 – 28 March.

8. Capen, E.C.: "The Difficulty of Assessing Uncertainty," paper SPE 5579 presented at the 1975 SPE-AIME Annual Technical Conference and Exhibition, Dallas, 28 September – 1 October.
9. Garb, F.A.: "Assessing Risk and Uncertainty in Evaluation Hydrocarbon Producing Properties," paper 1986 SPE 15921 presented at the SPE Eastern Regional Meeting, Columbus, Ohio, 12 – 14 November.
10. Baldwin, D.E.: "A Monte Carlo Model for Pressure Transient Analysis," paper SPE 2568 presented at 1969 SPE Annual Meeting, Denver, 28 September – 1 October.
11. Huffman, C.H. and Thompson, R.S.: "Probability Ranges for Reserves Estimates From Decline Curve Analysis," paper SPE 28333 presented at the 1994 SPE Annual Technical Conference and Exhibition, New Orleans, 25 – 28 September.
12. Murtha, J.A.: "Infill Drilling in the Clinton: Monte Carlo Techniques Applied to the Material Balance Equation," paper SPE 17068 presented at the 1987 SPE Eastern Regional Meeting, Pittsburgh, 21 – 23 October.
13. Wiggins, M.L. and Zhang, X.: "Using PC's and Monte Carlo Simulation To Assess Risks in Workover Evaluations," paper SPE 26243 presented at the 1993 SPE Petroleum Computer Conference, New Orleans, 11 – 14 July.
14. Gilman, J.R., Brickey, R.T. and Redd, M.M.: "Monte Carlo Techniques for Evaluating Producing Properties," paper SPE 39925 presented at the 1998 SPE Rocky Mountain Regional Low Permeability Reservoirs Symposium, Denver, 5 – 8 April.
15. Murtha, J.A.: "Monte Carlo Simulation: Its Status and Future," paper SPE 37932 presented at the 1997 SPE Annual Technical Conference and Exhibition, San Antonio, 5 – 8 October.
16. Murtha, J.A.: "Incorporating Historical Data in Monte Carlo Simulation," paper SPE 26245 presented at the 1993 SPE Petroleum Computer Conference, New Orleans, 11 – 14 July.

17. Jensen, J.L., Lake, L.W., Corbett, P.W.M., and Goggin, D.J.: *Statistics for Petroleum Engineers and Geoscientists*. second edition. Elsevier Science B.V., The Netherlands, 2000.
18. Peterson, S.K., Murtha, J.A. and Schneider, F.F.: "Brief: Risk Analysis and Monte Carlo Simulation Applied to the Generation of Drilling AFE Estimates," *JPT* (June 1995) P504.
19. Komlosi, Z.P.: "Application: Monte Carlo Simulation in Risk Evaluation of E & P Projects," paper SPE 68578 present at the 2001 SPE Hydrocarbon Economics and Evaluation Symposium, Dallas, 2-3 April.
20. Galli, A., Armstrong, M. and Jehl, B.: "Comparing Three Methods for Evaluating Oil Projects: Option Pricing, Decision Trees, and Monte Carlo Simulations," paper SPE 52949 presented at the 1999 Hydrocarbon Economics and Evaluation Symposium, Dallas, 20-23 March.
21. Kokolis, G.P., Litvak, B.L., Rapp, W.J. and Wang, B.: "Scenario Selection for Valuation of Multiple Prospect Opportunities: A Monte Carlo Play Simulation Approach," paper SPE 52977 presented at the 1999 Hydrocarbon Economics and Evaluation Symposium, Dallas, 20-23 March.
22. Han, C., Kang, J.M, and Choe, J.: "Monte Carlo Simulation on the Effect of Fracture Characteristics on Reduction of Permeability by In-Situ Bacteria Growth," paper SPE 72166 presented at the 2001 Asia Pacific Improve Oil Recovery Conference, Kuala Lumpur, 8 – 9 October.
23. Portella, R.C.M., Salomao, M.C., Blauth, M. and Duarte, R.L.B.: "Uncertainty Quantification to Evaluate the Value of Information in a Deepwater Reservoir," paper SPE 79707 presented at the 2003 SPE Reservoir Simulation Symposium, Houston, 3-5 February.
24. White, C.D. and Royer, S.A.: "Experimental Design as a Framework for Reservoir Studies," paper SPE 79676 presented at the 2003 SPE Reservoir Simulation Symposium, Houston, 3-5 February.

25. White, C.D., Willis, B.J., Narayanan, K. and Dutton, S.P.: “Identifying and Estimating Significant Geologic Parameters With Experimental Design,” *SPEJ* (September 2001) 311.
26. Friedmann, F., Chawathe, A. and Larue, D.K.: “Assessing Uncertainty in Channelized Reservoirs Using Experimental Designs,” paper SPE 71622 presented at the 2001 Annual Technical Conference and Exhibition, New Orleans, 30 September – 3 October.
27. Manceau, E., Mezghani, M., Zabala-Mezghani, I. and Roggero, F.: “Combination of Experimental Design and Joint Modeling Methods for Quantifying the Risk Associated with Deterministic and Stochastic Uncertainties – An Integrated Test Study,” paper SPE 71620 presented at the 2001 SPE Annual Technical Conference and Exhibition, New Orleans, 30 September – 3 October.
28. Charles, T., Guemeue, J.M., Corre, B, Vincent, G., and Dubrule, O.: “Experience with the Quantification of Subsurface Uncertainties,” paper SPE 68703 presented at the 2001 SPE Asia Pacific Oil and Gas Conference and Exhibition held in Jakarta, Indonesia, 17 – 19 April.
29. Corre, B., Thore, P., Feraudy, V. and Vincent, G.: “Integrated Uncertainty Assessment For Project Evaluation and Risk Analysis,” paper SPE 65205 presented at the 2000 SPE European Petroleum Conference, Paris, 24 – 25 October.
30. van Elk, J.F., Guerrero, L., Vijayan, K. and Gupta, R.: “Improved Uncertainty Management in Field Development Studies through the Application of the Experimental Design Method to the Multiple Realizations Approach,” paper SPE 64462 presented at the 2000 SPE Annual Technical Conference and Exhibition, Dallas, 1 – 4 October.
31. Venkataraman, R.: “Application of the Method of Experimental Design to Quantify Uncertainty in Production Profiles,” paper SPE 59422 presented at the 2000 SPE Asia Pacific Conference on Integrated Modeling for Asset Management, Yokohama, Japan, 25 – 26 April 2000.

32. Dejean, J.P. and Blanc, G.: “Managing Uncertainties on Production Predictions Using Integrated Statistical Methods,” paper SPE 56696 presented at the 1999 SPE Annual Technical Conference and Exhibition, Houston, 3 – 6 October.
33. Narayanan, K, White, C.D., Lake, L.W. and Willis, B.J.: “Response Surface Methods for Upscaling Heterogeneous Geologic Models,” paper SPE 51923 present at the SPE Reservoir Simulation Symposium, Houston, 14 – 17 February 1999.
34. Faidi, S.A., Ponting, D.K. and Eagling, T.L.: “Experimental Design in Interactive Reservoir Simulation,” paper SPE 36005 presented at the 1996 Petroleum Conference, Dallas, 2-5 June.
35. Steagall, D.E. and Schiozer, D.J.: “Uncertainty Analysis in Reservoir Production Forecasts During Appraisal And Pilot Production Phases,” paper SPE 66399 presented at the 2001 SPE Reservoir Simulation Symposium, Houston, 11 – 14 February.
36. Twartz, S.K., Gorjy, F. and Milne, I.G.: “A Multiple Realisation Approach to Managing Uncertainty in the North Rankin Gas Condensate Field, Western Australia,” paper SPE 50078 presented at the 1998 SPE Asia Pacific Oil & Gas Conference and Exhibition, Perth, Australia, 12 – 14 October.
37. Floris, F.J.T., Bush, M.D., Cuypers, M., Roggero, F. and Syversveen, A-R.: “Methods For Quantifying the Uncertainty of Production Forecasts: A Comparative Study,” *Petroleum Geoscience*, (2001), 7. S87.
38. Barker, W.J., Cuypers, M and Holden, L.: “Quantifying Uncertainty in Production Forecasts: Another Look at the PUNQ-S3 Problem,” SPEJ (December 2001) 433.
39. PUNQ-S3 Project: Production Forecasting with Uncertainty Quantification. <http://www.nitg.tno.nl/punq/>.

APPENDIX A

PUNQ-S3 ECLIPSE DATA FILE

```

-- *-----*
-- *
-- * base grid model with input parameters *
-- *
-- *-----*
RUNSPEC
PUNQ-S3 MODEL
= NDIVIX NDIVY NDIVZ
  19 28 5 /
= OIL WAT GAS DISGAS VAPOIL QAPITR QWATTR QGASTR NOTRAC NWTRAC NGTRAC
  T T T T F F F F 0 0 0 /
= UNIT CONVENTION
  'METRIC' /
= NRPVT NPPVT NTPVT NTROCC QROCKC QRCREV
  30 30 1 1 F F /
= NSSFUN NTSFUN QDIRK QREVK QVEOP QHYST QSCAL QSDIR QSREV NSEND NTEND
  35 1 F T F F F F T 1 1 /
= NDRXVD NTEQUL NDPRVD QUIESC QTHPRS QREVTH QMOBIL NTTRVD NSTRVD
  5 1 100 T F T F 1 1 /
= NTFIP QGRAID QPAIR QTDISP NTFRG QTDSK NRFRG NMFPR NETRC MHISTM NMHISTR
  5 F F F 0 F 0 0 0 /
= NWMAXZ NCWMAX NGMAXZ NWGMAX NLGRMAX NMAXCL
  20 40 2 20 0 0 /
= QIMCOL NWCOLC NUPCOL
  F 0 3 /
= MXMFLO MXMTHP MXMWFR MXMGFR MXMALQ NMMVFT
  10 10 10 10 1 1 /
= MXSFLO MXSTHP NMSVFT
  10 10 1 /
= NANAQU NCAMAX NIFTBL NRIFTB
  2 120 0 0 /
= DAY MONTH YEAR
  01 'JAN' 1967 /
= QSOLVE NSTACK QFMTOU QFMTIN QUNOUT QUNINP NGDISK IDYNAM
  T 25 F F T T /

MESSAGES
8* 10000 /

NOECHO

GRID
INIT

-- put in your PORO, PERMX and PERMZ
INCLUDE
  'PUNQS3.PRP'
/

```

```

COPY
'PERMX' 'PERMY' /
/

```

```

-- get corner point geometry
INCLUDE
'PUNQS3.GEO'
/

```

```

PROPS =====

```

```

-- RELATIVE PERMEABILITY AND CAPPILARY PRESSURE CURVES

```

```

SWFN
0.2 0.0 0.0
0.3 0.00024 0.0
0.4 0.0039 0.0
0.5 0.02 0.0
0.6 0.062 0.0
0.7 0.152 0.0
0.8 0.316 0.0
0.9 0.585 0.0
1.0 1.0 0.0
/

```

```

SOF3
0.1 0.0 0.0
0.2 0.018 0.0
0.3 0.073 0.025
0.4 0.165 0.1
0.5 0.294 0.225
0.6 0.459 0.4
0.7 0.661 0.625
0.8 0.9 0.9
/

```

```

SGFN
0.0 0.0 0.0
0.1 0.00000077 0.0
0.2 0.000049 0.0
0.3 0.00056 0.0
0.4 0.0032 0.0
0.5 0.012 0.0
0.6 0.036 0.0
0.7 0.091 0.0
0.8 0.2 0.0
/

```

```

-- PVT DATA

```

```

PVTO
11.460 40.000 1.064 4.338 /
17.890 60.000 1.078 3.878 /
24.320 80.000 1.092 3.467 /

```

30.760	100.000	1.106	3.100	/
37.190	120.000	1.120	2.771	/
43.620	140.000	1.134	2.478	/
46.840	150.000	1.141	2.343	/
50.050	160.000	1.148	2.215	/
53.270	170.000	1.155	2.095	/
56.490	180.000	1.162	1.981	/
59.700	190.000	1.169	1.873	/
62.920	200.000	1.176	1.771	/
66.130	210.000	1.183	1.674	/
69.350	220.000	1.190	1.583	/
72.570	230.000	1.197	1.497	/
74.000	234.460	1.200	1.460	
	250.000	1.198	1.541	
	300.000	1.194	1.787	/
80.000	245.000	1.220	1.400	
	300.000	1.215	1.700	/

/

PVDG

40.00	0.02908	0.00880	
60.00	0.01886	0.00920	
80.00	0.01387	0.00960	
100.00	0.01093	0.01000	
120.00	0.00899	0.01040	
140.00	0.00763	0.01090	
150.00	0.00709	0.01110	
160.00	0.00662	0.01140	
170.00	0.00620	0.01160	
180.00	0.00583	0.01190	
190.00	0.00551	0.01210	
200.00	0.00521	0.01240	
210.00	0.00495	0.01260	
220.00	0.00471	0.01290	
230.00	0.00449	0.01320	
234.46	0.00440	0.01330	

/

DENSITY

912.0 1000.0 0.8266

/

PVTW

234.46 1.0042 5.43E-05 0.5 1.11E-04 /

-- ROCK COMPRESSIBILITY

--

-- REF. PRES COMPRESSIBILITY

ROCK

235 0.00045 /

-- SWITCH OFF OUTPUT OF ALL PROPS DATA

STONE1

REGIONS =====

ENDBOX

SOLUTION =====

AQUCT

1 2355 234 137.5 0.2125 3.5E-05 3000 19.6 95 1 1 /
 2 2355 234 137.5 0.2125 3.5E-05 3200 6.0 95 1 1 /

AQUANCON

1 14 14 4 4 5 5 'I-' 1180.7 /
 1 15 15 4 4 5 5 'J-' 1186.7 /
 1 16 16 4 4 5 5 'J-' 1189.7 /
 1 17 17 4 4 5 5 'J-' 1197.7 /
 1 18 18 4 4 5 5 'I-' 1204.3 /
 1 12 12 5 5 5 5 'I+' 1094.6 /
 1 13 13 5 5 5 5 'I-' 1115.7 /
 1 11 11 6 6 5 5 'J-' 1031.0 /
 1 10 10 7 7 5 5 'I-' 999.6 /
 1 9 9 8 8 5 5 'I-' 983.6 /
 1 8 8 9 9 5 5 'I-' 987.8 /
 1 7 7 10 10 5 5 'I-' 1001.5 /
 1 6 6 11 11 5 5 'I-' 1005.3 /
 1 6 6 12 12 5 5 'I-' 966.6 /
 1 5 5 13 13 5 5 'I-' 911.7 /
 1 5 5 14 14 5 5 'I-' 877.4 /
 1 4 4 15 15 5 5 'I-' 835.6 /
 1 4 4 16 16 5 5 'I-' 819.1 /
 1 3 3 17 17 5 5 'I-' 755.5 /
 1 3 3 18 18 5 5 'I-' 720.2 /
 1 3 3 19 19 5 5 'I-' 673.3 /
 1 3 3 20 20 5 5 'I-' 633.9 /
 1 3 3 21 21 5 5 'I-' 596.0 /
 1 3 3 22 22 5 5 'I-' 607.8 /
 1 3 3 23 23 5 5 'I-' 614.3 /
 1 3 3 24 24 5 5 'I-' 598.3 /
 1 3 3 25 25 5 5 'I-' 460.6 /
 1 4 4 26 26 5 5 'I-' 153.2 /
 1 5 5 26 26 5 5 'J+' 256.8 /
 1 6 6 27 27 5 5 'I-' 251.4 /
 1 7 7 27 27 5 5 'J+' 255.2 /
 1 8 8 27 27 5 5 'J+' 247.2 /
 1 9 9 27 27 5 5 'J+' 232.8 /
 1 10 10 27 27 5 5 'J+' 227.4 /
 1 11 11 27 27 5 5 'J+' 222.8 /
 1 12 12 27 27 5 5 'I+' 223.2 /

 1 14 14 4 4 4 4 'I-' 1180.7 /
 1 15 15 4 4 4 4 'J-' 1186.7 /
 1 16 16 4 4 4 4 'J-' 1189.7 /
 1 17 17 4 4 4 4 'J-' 1197.7 /
 1 18 18 4 4 4 4 'I-' 1204.3 /

1 12 12 5 5 4 4 'I+' 1094.6 /
 1 13 13 5 5 4 4 'I-' 1115.7 /
 1 11 11 6 6 4 4 'J-' 1031.0 /
 1 10 10 7 7 4 4 'I-' 999.6 /
 1 9 9 8 8 4 4 'I-' 983.6 /
 1 8 8 9 9 4 4 'I-' 987.8 /
 1 7 7 10 10 4 4 'I-' 1001.5 /
 1 6 6 11 11 4 4 'I-' 1005.3 /
 1 6 6 12 12 4 4 'I-' 966.6 /
 1 5 5 13 13 4 4 'I-' 911.7 /
 1 5 5 14 14 4 4 'I-' 877.4 /
 1 4 4 15 15 4 4 'I-' 835.6 /
 1 4 4 16 16 4 4 'I-' 819.1 /
 1 3 3 17 17 4 4 'I-' 755.5 /
 1 3 3 18 18 4 4 'I-' 720.2 /
 1 3 3 19 19 4 4 'I-' 673.3 /
 1 3 3 20 20 4 4 'I-' 633.9 /
 1 3 3 21 21 4 4 'I-' 596.0 /
 1 3 3 22 22 4 4 'I-' 607.8 /
 1 3 3 23 23 4 4 'I-' 614.3 /
 1 3 3 24 24 4 4 'I-' 598.3 /
 1 3 3 25 25 4 4 'I-' 733.9 /
 1 4 4 26 26 4 4 'I-' 303.9 /
 1 5 5 26 26 4 4 'J+' 256.8 /
 1 6 6 27 27 4 4 'I-' 251.4 /
 1 7 7 27 27 4 4 'J+' 255.2 /
 1 8 8 27 27 4 4 'J+' 247.2 /
 1 9 9 27 27 4 4 'J+' 232.8 /
 1 10 10 27 27 4 4 'J+' 227.4 /
 1 11 11 27 27 4 4 'J+' 222.8 /
 1 12 12 27 27 4 4 'I+' 223.2 /

 1 14 14 4 4 3 3 'I-' 1180.7 /
 1 15 15 4 4 3 3 'J-' 1186.7 /
 1 16 16 4 4 3 3 'J-' 1189.7 /
 1 17 17 4 4 3 3 'J-' 1197.7 /
 1 18 18 4 4 3 3 'I-' 1204.3 /
 1 12 12 5 5 3 3 'I+' 1094.6 /
 1 13 13 5 5 3 3 'I-' 1115.7 /
 1 11 11 6 6 3 3 'J-' 1031.0 /
 1 10 10 7 7 3 3 'I-' 999.6 /
 1 9 9 8 8 3 3 'I-' 983.6 /
 1 8 8 9 9 3 3 'I-' 987.8 /
 1 7 7 10 10 3 3 'I-' 1001.5 /
 1 6 6 11 11 3 3 'I-' 1005.3 /
 1 6 6 12 12 3 3 'I-' 966.6 /
 1 5 5 13 13 3 3 'I-' 911.7 /
 1 5 5 14 14 3 3 'I-' 877.4 /
 1 4 4 15 15 3 3 'I-' 835.6 /
 1 4 4 16 16 3 3 'I-' 819.1 /
 1 3 3 17 17 3 3 'I-' 755.5 /
 1 3 3 18 18 3 3 'I-' 720.2 /
 1 3 3 19 19 3 3 'I-' 673.3 /

1	3	3	20	20	3	3	'I-'	633.9	/
1	3	3	21	21	3	3	'I-'	596.0	/
1	3	3	22	22	3	3	'I-'	607.8	/
1	3	3	23	23	3	3	'I-'	614.3	/
1	3	3	24	24	3	3	'I-'	598.3	/
1	3	3	25	25	3	3	'I-'	733.9	/
1	4	4	26	26	3	3	'I-'	303.9	/
1	5	5	26	26	3	3	'J+'	256.8	/
1	6	6	27	27	3	3	'I-'	251.4	/
1	7	7	27	27	3	3	'J+'	255.2	/
1	8	8	27	27	3	3	'J+'	247.2	/
1	9	9	27	27	3	3	'J+'	232.8	/
1	10	10	27	27	3	3	'J+'	227.4	/
1	11	11	27	27	3	3	'J+'	222.8	/
1	12	12	27	27	3	3	'I+'	223.2	/
2	15	15	1	1	2	2	'I-'	979.0	/
2	16	16	1	1	2	2	'J-'	963.7	/
2	17	17	1	1	2	2	'J-'	940.0	/
2	18	18	1	1	2	2	'I+'	904.5	/
2	14	14	2	2	2	2	'I-'	860.9	/
2	11	11	3	3	2	2	'I-'	665.4	/
2	12	12	3	3	2	2	'J-'	657.5	/
2	13	13	3	3	2	2	'J-'	652.0	/
2	10	10	4	4	2	2	'I-'	586.0	/
2	9	9	5	5	2	2	'I-'	620.4	/
2	8	8	6	6	2	2	'I-'	743.0	/
2	7	7	7	7	2	2	'I-'	213.5	/
2	6	6	8	8	2	2	'I-'	284.7	/
2	6	6	9	9	2	2	'I-'	366.6	/
2	5	5	10	10	2	2	'I-'	395.4	/
2	5	5	11	11	2	2	'I-'	464.4	/
2	5	5	12	12	2	2	'I-'	504.3	/
2	4	4	13	13	2	2	'I-'	553.3	/
2	4	4	14	14	2	2	'I-'	595.7	/
2	3	3	15	15	2	2	'I-'	716.9	/
2	2	2	16	16	2	2	'I-'	583.6	/
2	2	2	17	17	2	2	'I-'	576.6	/
2	2	2	18	18	2	2	'I-'	518.7	/
2	1	1	23	23	2	2	'I-'	750.1	/
2	1	1	24	24	2	2	'I-'	767.4	/
2	1	1	25	25	2	2	'I-'	698.9	/
2	2	2	26	26	2	2	'I-'	721.1	/
2	3	3	27	27	2	2	'I-'	666.0	/
2	4	4	28	28	2	2	'I-'	644.2	/
2	5	5	28	28	2	2	'J+'	743.7	/
2	15	15	1	1	1	1	'I-'	1958.0	/
2	16	16	1	1	1	1	'J-'	1927.4	/
2	17	17	1	1	1	1	'J-'	1880.5	/
2	18	18	1	1	1	1	'I+'	1809.0	/
2	14	14	2	2	1	1	'I-'	1721.9	/
2	11	11	3	3	1	1	'I-'	1330.8	/

2 12 12 3 3 1 1 'J-' 1315.0 /
 2 13 13 3 3 1 1 'J-' 1303.9 /
 2 10 10 4 4 1 1 'I-' 1172.1 /
 2 9 9 5 5 1 1 'I-' 1240.8 /
 2 8 8 6 6 1 1 'I-' 1486.0 /
 2 7 7 7 7 1 1 'I-' 1222.1 /
 2 6 6 8 8 1 1 'I-' 1242.7 /
 2 6 6 9 9 1 1 'I-' 1171.9 /
 2 5 5 10 10 1 1 'I-' 988.7 /
 2 5 5 11 11 1 1 'I-' 961.8 /
 2 5 5 12 12 1 1 'I-' 1022.0 /
 2 4 4 13 13 1 1 'I-' 1110.6 /
 2 4 4 14 14 1 1 'I-' 1189.5 /
 2 3 3 15 15 1 1 'I-' 1131.3 /
 2 2 2 16 16 1 1 'I-' 1350.2 /
 2 2 2 17 17 1 1 'I-' 1491.5 /
 2 2 2 18 18 1 1 'I-' 1442.2 /
 2 1 1 23 23 1 1 'I-' 1167.1 /
 2 1 1 24 24 1 1 'I-' 1253.7 /
 2 1 1 25 25 1 1 'I-' 1306.9 /
 2 2 2 26 26 1 1 'I-' 1183.3 /
 2 3 3 27 27 1 1 'I-' 1070.9 /
 2 4 4 28 28 1 1 'I-' 1179.4 /
 2 5 5 28 28 1 1 'J+' 1260.5 /
 /

-- DATUM DATUM OWC OWC GOC GOC RSVD RVVD SOLN
 -- DEPTH PRESS DEPTH PCOW DEPTH PCOG TABLE TABLE METH
 EQUIL

2355.00 234.46 2395.0 0.00 2355.0 0.000 1 1* 0 /

RSVD
 2175 74.00
 2496 74.00 /

SUMMARY =====

RUNSUM
 SEPARATE

RPTONLY

FOPT
 FGPT
 FWPT

WOPR
 'PRO-1'
 'PRO-4'
 'PRO-5'
 'PRO-11'
 'PRO-12'

```
'PRO-15'
'PRO-23'
-- 'PRO-24'
-- 'PRO-29'
-- 'PRO-50'
/
```

```
WBHP
'PRO-1'
'PRO-4'
'PRO-5'
'PRO-11'
'PRO-12'
'PRO-15'
-- 'PRO-23'
-- 'PRO-24'
-- 'PRO-29'
-- 'PRO-50'
/
```

```
WGOR
'PRO-1'
'PRO-4'
'PRO-5'
'PRO-11'
'PRO-12'
'PRO-15'
-- 'PRO-23'
-- 'PRO-24'
-- 'PRO-29'
-- 'PRO-50'
/
```

```
WWCT
'PRO-1'
'PRO-4'
'PRO-5'
'PRO-11'
'PRO-12'
'PRO-15'
-- 'PRO-23'
-- 'PRO-24'
-- 'PRO-29'
-- 'PRO-50'
/
```

SCHEDULE

```
--RPTSCHED
-- 'SGAS' 'SWAT' 'RESTART' /
```

```
-- 1 1 1 1 1 0 2 3 5 0 0 0 1 1 0 0 0
-- 0 0 0 0 0 0 0 0 0 0 0 0 0 0 0 0 0
```

-- 0 0 0 0 0 0 0 0 0 0 0 0 0 0 0 /

-- SET 'NO RESOLUTION' OPTION
DRSDT
0 /

----- WELL SPECIFICATION DATA -----

WELSPECS

'PRO-1' 'G1' 10 22 2362.2 'OIL' 1* 'STD' 3* 'SEG' /
'PRO-4' 'G1' 9 17 2373.0 'OIL' 1* 'STD' 3* 'SEG' /
'PRO-5' 'G1' 17 11 2381.7 'OIL' 1* 'STD' 3* 'SEG' /
'PRO-11' 'G1' 11 24 2386.0 'OIL' 1* 'STD' 3* 'SEG' /
'PRO-12' 'G1' 15 12 2380.5 'OIL' 1* 'STD' 3* 'SEG' /
'PRO-15' 'G1' 17 22 2381.0 'OIL' 1* 'STD' 3* 'SEG' /
--'PRO-23' 'G1' 5 23 2380.7 'OIL' 1* 'STD' 3* 'SEG' /
--'PRO-24' 'G1' 7 14 2382.5 'OIL' 1* 'STD' 3* 'SEG' /
--'PRO-29' 'G1' 15 7 2376.7 'OIL' 1* 'STD' 3* 'SEG' /
--'PRO-50' 'G1' 12 12 2362.2 'OIL' 1* 'STD' 3* 'SEG' /

/

COMPDAT

--
 RADIUS SKIN
'PRO-1' 10 22 5 5 'OPEN' 2* 0.15 1* 5.0 /
'PRO-1' 10 22 4 4 'OPEN' 2* 0.15 1* 5.0 /
'PRO-4' 9 17 5 5 'OPEN' 2* 0.15 1* 5.0 /
'PRO-4' 9 17 4 4 'OPEN' 2* 0.15 1* 5.0 /
'PRO-5' 17 11 4 4 'OPEN' 2* 0.15 1* 5.0 /
'PRO-5' 17 11 3 3 'OPEN' 2* 0.15 1* 5.0 /
'PRO-11' 11 24 4 4 'OPEN' 2* 0.15 1* 5.0 /
'PRO-11' 11 24 3 3 'OPEN' 2* 0.15 1* 5.0 /
'PRO-12' 15 12 5 5 'OPEN' 2* 0.15 1* 5.0 /
'PRO-12' 15 12 4 4 'OPEN' 2* 0.15 1* 5.0 /
'PRO-15' 17 22 4 4 'OPEN' 2* 0.15 1* 5.0 /
--'PRO-23' 5 23 2 2 'OPEN' 2* 0.15 1* 5.0 /
--'PRO-23' 5 23 1 1 'OPEN' 2* 0.15 1* 5.0 /
--'PRO-24' 7 14 2 2 'OPEN' 2* 0.15 1* 5.0 /
--'PRO-24' 7 14 1 1 'OPEN' 2* 0.15 1* 5.0 /
--'PRO-29' 15 7 2 2 'OPEN' 2* 0.15 1* 5.0 /
--'PRO-29' 15 7 1 1 'OPEN' 2* 0.15 1* 5.0 /
--'PRO-50' 12 12 3 3 'OPEN' 2* 0.15 1* 5.0 /
--'PRO-50' 12 12 2 2 'OPEN' 2* 0.15 1* 5.0 /

/

WCONPROD

'PRO*' 'SHUT' 6* 120.0 /
/

WCUTBACK

'PRO*' 1* 200.0 2* 0.75 'OIL' 120.0 /
/

----- PRODUCTION SCHEDULE -----

TSTEP

0.01

/

WELOPEN

'PRO-1' 'OPEN' /

'PRO-4' 'OPEN' /

'PRO-5' 'OPEN' /

'PRO-11' 'OPEN' /

'PRO-12' 'OPEN' /

'PRO-15' 'OPEN' /

/

WELTARG

'PRO-1' 'ORAT' 100.0 /

'PRO-4' 'ORAT' 100.0 /

'PRO-5' 'ORAT' 100.0 /

'PRO-11' 'ORAT' 100.0 /

'PRO-12' 'ORAT' 100.0 /

'PRO-15' 'ORAT' 100.0 /

/

TSTEP

1 /

DATES

1 'FEB' 1967 /

/

DATES

1 'MAR' 1967 /

/

DATES

1 'APR' 1967 /

/

WELTARG

'PRO-1' 'ORAT' 200.0 /

'PRO-4' 'ORAT' 200.0 /

'PRO-5' 'ORAT' 200.0 /

'PRO-11' 'ORAT' 200.0 /

'PRO-12' 'ORAT' 200.0 /

'PRO-15' 'ORAT' 200.0 /

/

TSTEP

1 /

DATES

1 'MAY' 1967 /

/

DATES

1 'JUN' 1967 /

/

DATES
1 'JUL' 1967 /
/

WELTARG
'PRO-1' 'ORAT' 100.0 /
'PRO-4' 'ORAT' 100.0 /
'PRO-5' 'ORAT' 100.0 /
'PRO-11' 'ORAT' 100.0 /
'PRO-12' 'ORAT' 100.0 /
'PRO-15' 'ORAT' 100.0 /
/

TSTEP
1 /

DATES
1 'AUG' 1967 /
/

DATES
1 'SEP' 1967 /
/

DATES
1 'OCT' 1967 /
/

WELTARG
'PRO-1' 'ORAT' 50.0 /
'PRO-4' 'ORAT' 50.0 /
'PRO-5' 'ORAT' 50.0 /
'PRO-11' 'ORAT' 50.0 /
'PRO-12' 'ORAT' 50.0 /
'PRO-15' 'ORAT' 50.0 /
/

TSTEP
1 /

DATES
1 'NOV' 1967 /
/

DATES
1 'DEC' 1967 /
/

DATES
1 'JAN' 1968 /
/

-- End for test purposes

WELTARG

'PRO-1' 'ORAT' 0.0 /
 'PRO-4' 'ORAT' 0.0 /
 'PRO-5' 'ORAT' 0.0 /
 'PRO-11' 'ORAT' 0.0 /
 'PRO-12' 'ORAT' 0.0 /
 'PRO-15' 'ORAT' 0.0 /

/

TSTEP

1 /

-- Just to include shut-in

DATES

1 'JAN' 1969 /

/

DATES

1 'JAN' 1970 /

/

DATES

1 'JAN' 1971 /

/

-- End for buildup-test purposes

WELTARG

'PRO-1' 'ORAT' 150.0 /
 'PRO-4' 'ORAT' 150.0 /
 'PRO-5' 'ORAT' 150.0 /
 'PRO-11' 'ORAT' 150.0 /
 'PRO-12' 'ORAT' 150.0 /
 'PRO-15' 'ORAT' 150.0 /

/

TSTEP

1 /

DATES

1 'JUL' 1971 /

/

-- work over --

DATES

1 'JAN' 1972 /

/

WELTARG

'PRO-1' 'ORAT' 0.0 /
 'PRO-4' 'ORAT' 0.0 /

'PRO-5' 'ORAT' 0.0 /
'PRO-11' 'ORAT' 0.0 /
'PRO-12' 'ORAT' 0.0 /
'PRO-15' 'ORAT' 0.0 /
/

TSTEP
1 /

DATES
15 'JAN' 1972 /
/

WELTARG
'PRO-1' 'ORAT' 150.0 /
'PRO-4' 'ORAT' 150.0 /
'PRO-5' 'ORAT' 150.0 /
'PRO-11' 'ORAT' 150.0 /
'PRO-12' 'ORAT' 150.0 /
'PRO-15' 'ORAT' 150.0 /
/

TSTEP
1 /

DATES
1 'JUL' 1972 /
/

DATES
1 'JAN' 1973 /
/

WELTARG
'PRO-1' 'ORAT' 0.0 /
'PRO-4' 'ORAT' 0.0 /
'PRO-5' 'ORAT' 0.0 /
'PRO-11' 'ORAT' 0.0 /
'PRO-12' 'ORAT' 0.0 /
'PRO-15' 'ORAT' 0.0 /
/

TSTEP
1 /

DATES
15 'JAN' 1973 /
/

WELTARG
'PRO-1' 'ORAT' 150.0 /
'PRO-4' 'ORAT' 150.0 /
'PRO-5' 'ORAT' 150.0 /
'PRO-11' 'ORAT' 150.0 /

'PRO-12' 'ORAT' 150.0 /
'PRO-15' 'ORAT' 150.0 /
/

TSTEP
1 /

DATES
1 'JUL' 1973 /
/

DATES
1 'JAN' 1974 /
/

WELTARG
'PRO-1' 'ORAT' 0.0 /
'PRO-4' 'ORAT' 0.0 /
'PRO-5' 'ORAT' 0.0 /
'PRO-11' 'ORAT' 0.0 /
'PRO-12' 'ORAT' 0.0 /
'PRO-15' 'ORAT' 0.0 /
/

TSTEP
1 /

DATES
15 'JAN' 1974 /
/

WELTARG
'PRO-1' 'ORAT' 150.0 /
'PRO-4' 'ORAT' 150.0 /
'PRO-5' 'ORAT' 150.0 /
'PRO-11' 'ORAT' 150.0 /
'PRO-12' 'ORAT' 150.0 /
'PRO-15' 'ORAT' 150.0 /
/

TSTEP
1 /

DATES
1 'JUL' 1974 /
/

DATES
1 'JAN' 1975 /
/

WELTARG
'PRO-1' 'ORAT' 0.0 /
'PRO-4' 'ORAT' 0.0 /
'PRO-5' 'ORAT' 0.0 /

'PRO-11' 'ORAT' 0.0 /
'PRO-12' 'ORAT' 0.0 /
'PRO-15' 'ORAT' 0.0 /
/

TSTEP
1 /

DATES
15 'JAN' 1975 /
/

WELTARG
'PRO-1' 'ORAT' 150.0 /
'PRO-4' 'ORAT' 150.0 /
'PRO-5' 'ORAT' 150.0 /
'PRO-11' 'ORAT' 150.0 /
'PRO-12' 'ORAT' 150.0 /
'PRO-15' 'ORAT' 150.0 /
/

TSTEP
1 /

DATES
1 'JUL' 1975 /
/

DATES
1 'JAN' 1976 /
/

WELTARG
'PRO-1' 'ORAT' 0.0 /
'PRO-4' 'ORAT' 0.0 /
'PRO-5' 'ORAT' 0.0 /
'PRO-11' 'ORAT' 0.0 /
'PRO-12' 'ORAT' 0.0 /
'PRO-15' 'ORAT' 0.0 /
/

TSTEP
1 /

DATES
15 'JAN' 1976 /
/

WELTARG
'PRO-1' 'ORAT' 150.0 /
'PRO-4' 'ORAT' 150.0 /
'PRO-5' 'ORAT' 150.0 /
'PRO-11' 'ORAT' 150.0 /
'PRO-12' 'ORAT' 150.0 /

'PRO-15' 'ORAT' 150.0 /
/

TSTEP
1 /

DATES
1 'JUL' 1976 /
/

DATES
1 'JAN' 1977 /
/

WELTARG
'PRO-1' 'ORAT' 0.0 /
'PRO-4' 'ORAT' 0.0 /
'PRO-5' 'ORAT' 0.0 /
'PRO-11' 'ORAT' 0.0 /
'PRO-12' 'ORAT' 0.0 /
'PRO-15' 'ORAT' 0.0 /
/

TSTEP
1 /

DATES
15 'JAN' 1977 /
/

WELTARG
'PRO-1' 'ORAT' 150.0 /
'PRO-4' 'ORAT' 150.0 /
'PRO-5' 'ORAT' 150.0 /
'PRO-11' 'ORAT' 150.0 /
'PRO-12' 'ORAT' 150.0 /
'PRO-15' 'ORAT' 150.0 /
/

TSTEP
1 /

DATES
1 'JUL' 1977 /
/

DATES
1 'JAN' 1978 /
/

WELTARG
'PRO-1' 'ORAT' 0.0 /
'PRO-4' 'ORAT' 0.0 /
'PRO-5' 'ORAT' 0.0 /
'PRO-11' 'ORAT' 0.0 /

'PRO-12' 'ORAT' 0.0 /
'PRO-15' 'ORAT' 0.0 /
/

TSTEP
1 /

DATES
15 'JAN' 1978 /
/

WELTARG
'PRO-1' 'ORAT' 150.0 /
'PRO-4' 'ORAT' 150.0 /
'PRO-5' 'ORAT' 150.0 /
'PRO-11' 'ORAT' 150.0 /
'PRO-12' 'ORAT' 150.0 /
'PRO-15' 'ORAT' 150.0 /
/

TSTEP
1 /

DATES
1 'JUL' 1978 /
/

DATES
1 'JAN' 1979 /
/

WELTARG
'PRO-1' 'ORAT' 0.0 /
'PRO-4' 'ORAT' 0.0 /
'PRO-5' 'ORAT' 0.0 /
'PRO-11' 'ORAT' 0.0 /
'PRO-12' 'ORAT' 0.0 /
'PRO-15' 'ORAT' 0.0 /
/

TSTEP
1 /

DATES
15 'JAN' 1979 /
/

WELTARG
'PRO-1' 'ORAT' 150.0 /
'PRO-4' 'ORAT' 150.0 /
'PRO-5' 'ORAT' 150.0 /
'PRO-11' 'ORAT' 150.0 /
'PRO-12' 'ORAT' 150.0 /
'PRO-15' 'ORAT' 150.0 /

/

TSTEP

1 /

DATES

1 'JUL' 1979 /

/

DATES

1 'JAN' 1980 /

/

WELTARG

'PRO-1' 'ORAT' 0.0 /

'PRO-4' 'ORAT' 0.0 /

'PRO-5' 'ORAT' 0.0 /

'PRO-11' 'ORAT' 0.0 /

'PRO-12' 'ORAT' 0.0 /

'PRO-15' 'ORAT' 0.0 /

/

TSTEP

1 /

DATES

15 'JAN' 1980 /

/

WELTARG

'PRO-1' 'ORAT' 150.0 /

'PRO-4' 'ORAT' 150.0 /

'PRO-5' 'ORAT' 150.0 /

'PRO-11' 'ORAT' 150.0 /

'PRO-12' 'ORAT' 150.0 /

'PRO-15' 'ORAT' 150.0 /

/

TSTEP

1 /

DATES

1 'JUL' 1980 /

/

DATES

1 'JAN' 1981 /

/

WELTARG

'PRO-1' 'ORAT' 0.0 /

'PRO-4' 'ORAT' 0.0 /

'PRO-5' 'ORAT' 0.0 /

'PRO-11' 'ORAT' 0.0 /

'PRO-12' 'ORAT' 0.0 /

'PRO-15' 'ORAT' 0.0 /
/

TSTEP
1 /

DATES
15 'JAN' 1981 /
/

WELTARG
'PRO-1' 'ORAT' 150.0 /
'PRO-4' 'ORAT' 150.0 /
'PRO-5' 'ORAT' 150.0 /
'PRO-11' 'ORAT' 150.0 /
'PRO-12' 'ORAT' 150.0 /
'PRO-15' 'ORAT' 150.0 /
/

TSTEP
1 /

DATES
1 'JUL' 1981 /
/

DATES
1 'JAN' 1982 /
/

WELTARG
'PRO-1' 'ORAT' 0.0 /
'PRO-4' 'ORAT' 0.0 /
'PRO-5' 'ORAT' 0.0 /
'PRO-11' 'ORAT' 0.0 /
'PRO-12' 'ORAT' 0.0 /
'PRO-15' 'ORAT' 0.0 /
/

TSTEP
1 /

DATES
15 'JAN' 1982 /
/

WELTARG
'PRO-1' 'ORAT' 150.0 /
'PRO-4' 'ORAT' 150.0 /
'PRO-5' 'ORAT' 150.0 /
'PRO-11' 'ORAT' 150.0 /
'PRO-12' 'ORAT' 150.0 /
'PRO-15' 'ORAT' 150.0 /
/

TSTEP

1 /

DATES

1 'JUL' 1982 /

/

DATES

1 'JAN' 1983 /

/

WELTARG

'PRO-1' 'ORAT' 0.0 /

'PRO-4' 'ORAT' 0.0 /

'PRO-5' 'ORAT' 0.0 /

'PRO-11' 'ORAT' 0.0 /

'PRO-12' 'ORAT' 0.0 /

'PRO-15' 'ORAT' 0.0 /

/

TSTEP

1 /

DATES

15 'JAN' 1983 /

/

WELTARG

'PRO-1' 'ORAT' 150.0 /

'PRO-4' 'ORAT' 150.0 /

'PRO-5' 'ORAT' 150.0 /

'PRO-11' 'ORAT' 150.0 /

'PRO-12' 'ORAT' 150.0 /

'PRO-15' 'ORAT' 150.0 /

/

TSTEP

1 /

DATES

1 'JUL' 1983 /

/

END

VITA

Name: Guohong Zhang

Permanent Address: c/o Harold Vance Department of Petroleum Engineering
Texas A&M University
College Station, Texas 77843-3116

Education: Ph.D., Petroleum Engineering
Texas A&M University, December 2003

M.S., Petroleum Engineering
Research Institute of Petroleum E&D, July 1995

B.S., Petroleum Engineering
Jiangnan Petroleum Institute, July 1992